GEOTRACK

Bridgewater Bay-1 well
Otway Basin, Victoria

AFTA® Apatite Fission Track Analysis and (U-Th)/He apatite dating

DATA REPORT

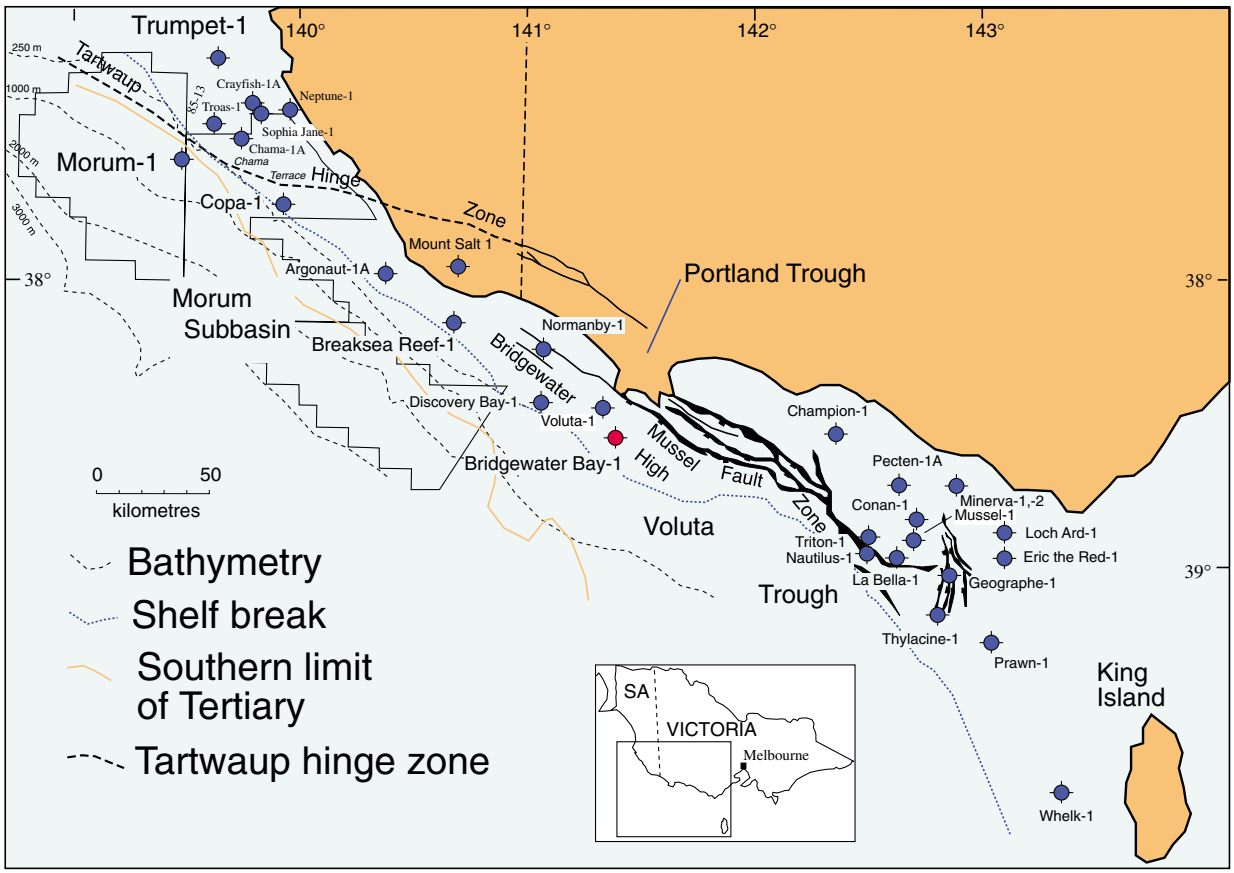

A report prepared for

Petroleum Division, DPI, Melbourne, Victoria

Report prepared by:	I. R. Duddy
Data reduction by:	R.A. Mooney
AFTA determinations by:	C.E. O'Brien
Microprobe determinations by:	P.G.F. Watson
(U-Th)/He apatite dating:	Dr. Peter Crowhurst, CSIRO

August 2003

Geotrack International Pty Ltd ABN 16 006 821 209
37 Melville Road, Brunswick West, Victoria 3055, Australia Ph +613 9380 1077 facsimile +61 3 9380 1477
email mail@geotrack.com.au

Otway Basin, Victoria

AFTA® Apatite Fission Track Analysis and (U-Th)/He apatite dating

Data Report for the Bridgewater Bay-1 well

GEOTRACK REPORT #876

1. Thermal history reconstruction

1.1 Introduction

This report presents AFTA® apatite fission track analysis and (U-Th)/He apatite dating data from the **Bridgewater Bay-1 well** collected from the DPI core repository, Werribee. The location of the Bridgewater Bay-1 well is shown in Figure 1.1.

In all, six cuttings samples from Bridgewater Bay-1 well were processed. Yields of detrital apatite, as summarised in Table A.1, varied from none to excellent, with sufficient apatite recovered enabling AFTA to be performed on 3 samples and (U-Th)/He apatite dating on three samples. The suitable yields and the generally high quality of the apatite grains recovered has provided highly reliable data which will form the basis of sound thermal history interpretations.

Details of all AFTA samples, including sample depths, stratigraphic ages and estimates of present temperature for each sample, are summarised in Table A.1, with similar information for the (U-Th)/He apatite dating sample given in Table E.1 (Appendix E). Details of present temperature estimation are summarised in Section A.3 (below).

New vitrinite reflectance (VR) results by Keiraville Konsultants were attempted on eleven, as summarised in Table D.2. (Appendix D). In addition, open-file VR data (some from Keiraville Konsultants) are available from the Bridgewater Bay-1 well (Table D.3. Appendix D).

1.2 Report structure

Sample details are discussed in Appendix A, together with the yields of detrital apatite obtained after mineral separation. Sample preparation and analytical details are

described in Appendix B, and are followed by presentation of all AFTA data, including raw track counts and fission track ages for individual grains. The presentation of data in the form of Tables and Figures throughout the report is discussed in detail in Appendix B. Appendix C outlines the principles employed in interpreting the AFTA data in terms of thermal history. Appendix D discusses the principles involved in integrating AFTA and VR data to provide a rigorous thermal history reconstruction. Appendix E outlines the principles involved in determining (U-Th)/He ages and their use in thermal history reconstruction with sample details presented in Table E.1 and detailed results in Tables E.2 and E.3.

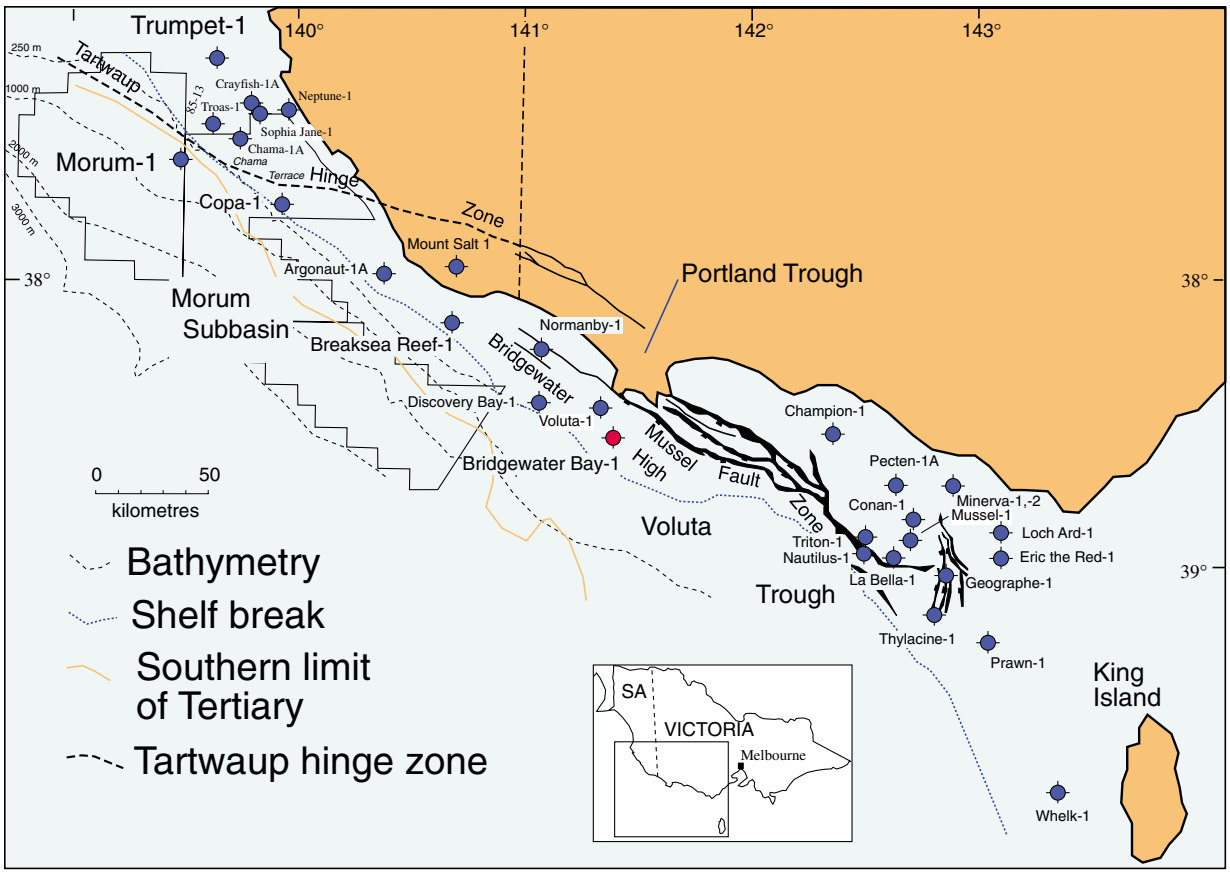

Figure 1.1: Location of the **Bridgewater Bay-1 well** (red symbol), Otway Basin, offshore Victoria.

APPENDIX A

Sample Details, Geological Data and Apatite Compositions

A.1 Sample details

Six cuttings samples from the **Bridgewater Bay-1 well**, offshore **Otway Basin of Victoria,** (Figure 1.1), were processed through the mineral separation procedures to recover apatite for AFTA® and (U-Th)/He apatite dating. Yields of detrital apatite, as summarised in Table A.1, varied from none to excellent, with sufficient apatite recovered enabling AFTA to be performed on 3 samples and (U-Th)/He apatite dating on three samples.

Details of all AFTA samples, including sample depths, stratigraphic ages and estimates of present temperature for each sample, are summarised in Table A.1, with similar information for the (U-Th)/He apatite dating sample given in Table E.1 (Appendix E). Details of present temperature estimation are summarised in Section A.3 (below).

New vitrinite reflectance (VR) results by Keiraville Konsultants were attempted on eleven samples from Bridgewater Bay-1, as summarised in Table D.2. (Appendix D). In addition, open-file VR data (some from Keiraville Konsultants) are available (Table D.3. Appendix D).

A.2 Stratigraphic details

Depths to the formation tops in the preserved section in the **Bridgewater Bay-1 well** were provided by Geoscience Australia (GA) whereas the biostratigraphy was obtained from Partridge (1996). The formation tops were assigned chronostratic ages using the Young and Laurie (1996) time-scale for Australia.

The formation top depths provided by GA and the stratigraphic age information from Partridge (1996) are summarised for each well in Table A.2, in the form of depths (TVD bKB) and ages of major units in the well. The stratigraphic age of each AFTA sample, derived from this information, is summarised in Table A.1, while similar information for the VR samples is summarised in Tables D.2 and D.3 (Appendix D) and for the (U-Th)/He apatite dating samples in Table E.1 (Appendix E).

A.3 Present temperatures

In application of any technique involving estimation of paleotemperatures, it is critical to control the present temperature profile, since estimation of maximum paleotemperatures proceeds from trying to determine how much of the observed effect can be explained by the magnitude of present temperatures.

Recorded temperature data are often not reported in sufficient detail to allow rigorous analysis (typically consisting of single BHT measurements at a given depth for a single time since circulation). In order to have a consistent methodology for this well with other Geotrack studies in the region, all BHT data are treated in the same way. Measured BHT data obtained from log headers in the relevant well completion report (WCR) are adjusted by a simplified correction procedure adapted from the literature (Oxburgh and Andrews-Speed, 1981; Andrews-Speed et al., 1984). While no doubt simplistic, this procedure has the advantage of allowing a common approach in all wells, and appears to give roughly consistent results. Furthermore, the thermal history tools applied in this study are calibrated in studies using this same approach, and therefore use of this correction method provides a high degree of internal consistency.

Using a sea-bed temperature of 15°C, quoted BHT data are corrected by increasing the difference between the surface temperature and the uncorrected BHT by 20% for uncorrected temperatures below 150°F (66°C), and by 25% above 150°F. Where multiple temperature measurements were available at a given depth, the earliest recorded BHT value is used. (Corrected BHT data derived from the above method are usually in good agreement with uncorrected DST data if these data are available). Where appropriate, a linear geothermal gradient, constrained to the surface temperature, is fitted to the BHT data corrected in this way.

Raw and corrected BHT values and the resulting geothermal gradients for **Bridgewater Bay-1 well** derived from the above procedure using a sea-bed temperature of 15°C are listed in Table A.3 and are plotted against depth in Figure A.1. Inspection of Figure A.1 shows that there is some scatter in the available BHT measurements with depth, although a linear gradient of 30.6°C/km is reasonably well-defined. Initially, present-day temperature values used for interpreting the thermal history results in each AFTA, (U-Th)/He apatite dating and VR sample were interpolated from this average linear gradient, but kinetic modelling of the AFTA data in key deeper samples showed that this gradient is too high, predicting greater fission track annealing than observed. On this basis, the present-day gradient was revised lower in order to match the deeper AFTA results, giving a gradient of 26.6°C/km. This lower gradient is used in the final thermal history interpretation of all of the shallower AFTA and (U-Th)/He apatite dating samples.

A.4 Apatite Grain morphologies

The majority of grains analysed from all samples (dominantly of Late Cretaceous depositional age) from these three wells were euhedral and sub-rounded euhedral in shape and there are no obvious trends that can be related to the stratigraphy or possible provenance differences.

A.5 Apatite compositions

The annealing kinetics of fission tracks in apatite are affected by chemical composition, specifically the Cl content, as explained in more detail in Appendix C. In all samples collected for this study, Cl contents were measured in all apatite grains analysed (i.e. for both fission track age determination and track length measurement), and the measured compositions in individual grains have been employed in interpreting the AFTA data, using methods outlined in Appendix C.

Chlorine contents were measured using a fully automated Jeol JXA-5A electron microprobe equipped with a computer controlled X-Y-Z stage and three computer controlled wavelength dispersive crystal spectrometers, with an accelerating voltage of 15kV and beam current of 25nA. The beam was defocussed to 20 µm diameter to avoid problems associated with apatite decomposition, which occur under a fully focussed 1 µm - 2 µm beam. The X-Y co-ordinates of dated grains within the grain mount were transferred from the Autoscan Fission Track Stage to a file suitable for direct input into the electron microprobe. The identification of each grain was verified optically prior to analysis. Cl count rates from the analysed grains were converted to wt% Cl by reference to those from a Durango apatite standard (Melbourne University Standard APT151) analysed at regular intervals. This approach implicitly takes into account atomic number absorption and fluorescence matrix effects, which are normally calculated explicitly when analysing for all elements. A value of 0.43 wt% Cl was used for the Durango standard, based on repeated measurements on the same single fragment using pure rock salt (NaCl) as a standard for chlorine. This approach gives essentially identical results to Cl contents determined from full compositional measurements, but has the advantage of reducing analytical time by a factor of ten or more.

Cl contents in individual grains are listed in the fission track Age Data Sheets in Appendix B, together with histograms of Cl contents in individual samples and plots of fission track age against Cl content. Table B.3 (Appendix B) contains fission track age and length data grouped into 0.1 wt% Cl intervals on the basis of chlorine contents of the grains from which the data are derived.

Lower limits of detection for chlorine content have been calculated for typical analytical conditions (beam current, counting time, etc.) and are listed in Table A.4. Errors in wt% composition are given as a percentage and quoted at 1σ for chlorine determinations. A generalised summary of errors for various wt% chlorine values is presented in Table A.5.

Bridgewater Bay-1: Samples GC876-7 and -8 from the Paaratte Formation both gave poor apatite yields but show spreads up to ~1 wt% Cl; the more Cl-rich grains are younger, close to the stratigraphic and are consistent with a mixed volcanogenic source (c.f. Figure C.4c, Appendix C), probably reworking of the Early Cretaceous Eumeralla Formation. On the other hand, the Cl-poor grains tend to be older suggesting an original Paleozoic source terrain (see age data sheet, Appendix B).

Similarly, GC876-12 from the Waarre Formation gave a good apatite yield and these show a range in chlorine from 0 to 1.9wt% (see age data sheet, Appendix B), characteristic of apatites derived from a mixed volcanogenic provenance (c.f. Figure C.4c, Appendix C). The fission track ages are severely reduced by annealing at elevated paleotemperatures and provide no data on the age of the provenance, whether reworking of the Early Cretaceous Eumeralla Formation, or possibly a Triassic-Jurassic volcanogenic provenance as seen in other Otway Basin Late Cretaceous samples.

References

Andrews-Speed, C.P., Oxburgh, E.R. and Cooper, B.A. (1984). Temperatures and depth-dependent heat flow in Western North Sea, *AAPG Bulletin*, 11, 1764 - 1784.

Dickinson, J.A., Wallace, M.W., Holdgate, G.R., Daniels, J., Gallagher, S.J. and Thomas, L., 2001. Neogene Tectonics in SE Australia: implications for petroleum systems. The APPEA Journal, 41, 37-52.

Geary, G.C. and Reid, I.S.A., 1998. Geology and prospectivity of the Offshore Eastern Otway Basin, Victoria - for the 1998 Acreage Release. *Victorian Initiative for Minerals and Petroleum Report* 55. Department of Natural Resources and Environment.

Oxburgh, E.R. and Andrews-Speed, C.P. (1981). Temperature, Thermal gradients and heat flow in the Southwestern North Sea. In: Illing, L. V. and Hobson, G.D. (eds.) The petroleum geology of the continental shelf of NW Europe, Heyden, 141 - 151.

Partridge, A.D., 1996. A review of palaeontology data for preparation of STRATDAT datums for selected Otway Basin wells. Biostrata Report 1996/5 (unpublished).

Young, G.R., and Laurie, G.C. (eds), 1996. An Australian Phanerozoic Timescale. Oxford University Press, Melbourne, 279p.

Table A.1: Details of fission track samples and apatite yields - samples from Otway Basin (Geotrack Report #876)

Sample number	Depth (m)	Sample type	Stratigraphic Subdivision	Stratigraphic age (Ma)	Present temperature *1 (°C)	Raw weight (g)	Washed weight (g)	Apatite yield *2
Bridgewater Bay-1								
GC876-5	1600-1750	cuttings	Paaratte Fm	83-77	62	280	80	excellent
GC876-6	1890-2020	cuttings	Paaratte Fm	83-77	71	360	160	excellent
GC876-7	2115-2215	cuttings	Paaratte Fm	83-77	77	410	180	excellent
GC876-8	2590-2720	cuttings	Belfast Mdst - Paaratte Fm	89-77	92	300	80	poor
GC876-10	3495-3615	cuttings	Belfast Mdst	89-84	120	170	50	none
GC876-12	4100-4200	cuttings	Waare Fm	92-90	138	70	30	good

*1 See Appendix A for discussion of present temperature data.

*2 Yield based on quantity of mineral suitable for age determination. Excellent: >20 grains; Good: 15-19 grains; Fair: 10-14 grains; Poor: 5-9 grains; Very Poor: <5 grains.

Table A.2: Summary of stratigraphy - Otway Basin (Geotrack Report #876)

	KB elevation (mAMSL)	Water Depth (m)	Stratigraphic Interval	Depth of Top TVD rKB (m)	Age of Top (Ma)
Bridgewater Bay-1					
	22	109	Whalers Bluff Fm	131	0
			Unconformity	825	5
			Pt Campbell lst	825	10
			Unconformity	861	15
			Narrawaturk Marl	861	38
			Mepunga Fm	883	40
			Unconformity	901	42
			Dilwyn Fm	901	50
			Pember Mdst	1168	54
			Pebble Pt Fm	1201	56
			Unconformity	1244	62
			Timboon Sst	1244	64.5
			Paaratte Fm	1600	77
			Nullawaarre Greensand	2640	83
			Belfast Mdst	2715	84
			Flaxmans Fm	4005	89
			Waare Fm	4100	90
			TD	4200	92

All depths quoted are with respect to KB, except where otherwise stated.

Table A.3: Summary of temperature data - Otway Basin (Geotrack Report #876)

KB elevation (mAMSL)	Water Depth (m)	Depth (ft)	BHT (°F)	BHT (°C)	T.S.C (hrs)	Depth (m)	Corrected BHT (°C)	Geothermal gradient (°C/km)
Bridgewater Bay-1								
22	109							30.6
		5256	118.9	48.3	4.5	1602.0	55.0	
		11594	194.0	90.0	9.5	3534.0	108.8	
		13781	253.9	123.3	10.2	4200.5	150.4	

Quoted BHT values have been corrected by increasing the difference between surface temperature and measured BHT by 20% for measured temperatures <150°F (<66°C) and by 25% for temperatures >150°F (>66°C). A sea-bed temperature of 15°C has been assumed.

All depths quoted are with respect to KB, except where otherwise stated.

*Measurements not used in calculation of geothermal gradient.

Table A.4: Lower Limits of Detection for Apatite Analyses (Geotrack Report #876)

Element	LLD (95% c.l.)		LLD (99% c.l.)	
	(wt%)	(ppm)	(wt%)	(ppm)
Cl	0.01	126	0.02	182

Table A.5: Per cent errors in chlorine content (Geotrack Report #876)

Chlorine content (wt%)	Error (%)
0.01	9.3
0.02	8.7
0.05	7.3
0.10	6.1
0.20	4.7
0.50	3.2
1.00	2.3
1.50	1.9
2.00	1.7
2.50	1.5
3.00	1.4

Errors quoted are at 1σ. See Appendix A for more details.

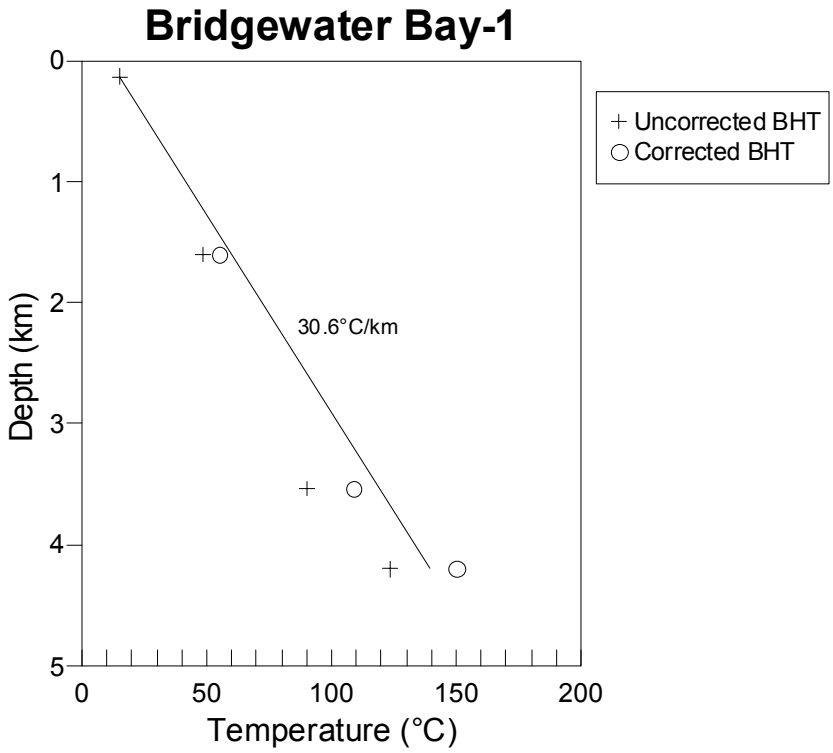

Figure A.1: Present temperature profile calculated for **well Bridgewater Bay-1, Otway Basin.** See Table A.3 and Appendix A for more detail.

APPENDIX B

Sample Preparation, Analytical Details and Data Presentation

B.1 Sample Preparation

Core and outcrop samples are crushed in a jaw crusher and then ground to sand grade in a rotary disc mill. Cuttings samples are washed and dried before grinding to sand grade. The ground material is then washed to remove dust, dried and processed by conventional heavy liquid and magnetic separation techniques to recover heavy minerals. Apatite grains are mounted in epoxy resin on glass slides, polished and etched for 20 sec in 5M HNO_3 at 20°C to reveal the fossil fission tracks.

After etching, all mounts are cut down to 1.5 x 1 cm, and cleaned in detergent, alcohol and distilled water. The mounts are then sealed in intimate contact with low-uranium muscovite detectors within heat-shrink plastic film. Each batch of mounts is stacked between two pieces of uranium standard glass, which has been prepared in similar fashion. The stack is then inserted into an aluminium can for irradiation.

After irradiation, the mica detectors are removed from the grain mounts and standard glasses and etched in hydrofluoric acid to reveal the fission tracks produced by induced fission of ^{235}U in the apatite and standard glass.

B.2 Analytical Details

Fission track ages

Fission track ages are calculated using the standard fission track age equation using the zeta calibration method (equation five of Hurford and Green, 1983), viz:

$$\text{F.T. AGE} = \frac{1}{\lambda_D} \ln \left[1 + \left(\frac{\zeta \lambda_D \rho_s g \rho_D}{\rho_i} \right) \right] \qquad \text{B.1}$$

where:
- λ_D = Total decay constant of ^{238}U (= 1.55125 x 10^{-10})
- ζ = Zeta calibration factor
- ρ_s = Spontaneous track density
- ρ_i = Induced track density
- ρ_D = Track density from uranium standard glass
- g = A geometry factor (= 0.5)

Fission track ages are determined by the external detector method or EDM (Gleadow, 1981). The EDM has the advantage of allowing fission track ages to be determined on single grains. In apatite, tracks are counted in 20 grains from each mount wherever possible. In those samples where the desired number is not present, all available grains are counted, the actual number depending on the availability of suitably etched and oriented grains. Only grains oriented with surfaces parallel to the crystallographic c-axis are analysed. Such grains can be identified on the basis of the etching characteristics, as well as from morphological evidence in euhedral grains. The grain mount is scanned sequentially, and the first 20 suitably oriented grains identified are analysed.

Tracks are counted within an eyepiece graticule divided into 100 grid squares. In each grain, the number of spontaneous tracks (N_s) within a certain number of grid squares (N_a) is recorded. The number of induced tracks (N_i) in the corresponding location within the mica external detector is then counted. Spontaneous and induced track densities (ρ_s and ρ_i, respectively) are calculated by dividing the track counts by the total area counted, given by the product of Na and the area or each grid square (determined by calibration against a ruled stage graticule or diffraction grating). Fission track ages may be calculated by substituting track counts (N_s and N_i) for track densities (ρ_s and ρ_i) in equation B.1, since the areas cancel in the ratio.

Translation between apatite grains in the grain mount and external detector locations corresponding to each grain is carried out using Autoscan™ microcomputer-controlled automatic stages (Smith and Leigh Jones, 1985). This system allows repeated movement between grain and detector, and all grain locations are stored for later reference if required.

Neutron irradiations are carried out in a well-thermalised flux (X-7 facility; Cd ratio for Au ~98) in the Australian Atomic Energy Commission's HIFAR research reactor. Total neutron fluence is monitored by counting tracks in mica external detectors attached to two pieces of Corning Glass Works standard glass CN5 (containing ~11 ppm Uranium) included in the irradiation canister at each end of the sample stack. In determining track densities in external detectors irradiated adjacent to uranium standard glasses, 25 fields are normally counted in each detector. The total track count (N_D) is divided by the total area counted to obtain the track density (ρ_D). The positions of the counted fields are arranged in a 5 X 5 grid covering the whole area of the detector. For typical track densities of between ~5 X 10^5 and 5 X 10^6, this is a convenient arrangement to sample across the detector while gathering sufficient counts to achieve a precision of ~±2% in a reasonable time.

A small flux gradient is often present in the irradiation facility over the length of the sample package. If a detectable gradient is present, the track count in the external detector adjacent to each standard glass is converted to a track density (ρ_D) and a value for each mount in the stack is calculated by linear interpolation. When no detectable gradient is present, the track counts in the two external detectors are pooled to give a single value of ρ_D, which is used to calculate fission track ages for each sample.

A Zeta calibration factor (ζ) has been determined empirically for each observer by analysing a set of carefully chosen age standards with independently known K-Ar ages, following the methods outlined by Hurford and Green (1983) and Green (1985).

All track counting is carried out using Zeiss(R) Axioplan microscopes, with an overall linear magnification of 1068 x using dry objectives.

For further details and background information on practical aspects of fission track age determination, see e.g. Fleischer, Price and Walker (1975), Naeser (1979) and Hurford (1986).

Track length measurements

For track length studies in apatite, the full lengths of "confined" fission tracks are measured. Confined tracks are those which do not intersect the polished surface but have been etched from other tracks or fractures, so that the whole length of the track is etched. Confined track lengths are measured using a digitising tablet connected to a microcomputer, superimposed on the microscope field of view via a projection tube. With this system, calibrated against a stage graticule ruled in 2 μm divisions, individual tracks can be measured to a precision of ± 0.2 μm. Tracks are measured only in prismatic grains, characterised by sharp polishing scratches with well-etched tracks of narrow cone angle in all orientations, because of the anisotropy of annealing of fission tracks in apatite (as discussed by Green et al. 1986). Tracks are also measured following the recommendations of Laslett et al. (1982), the most important of which is that only horizontal tracks should be measured. One hundred tracks are measured whenever possible. In apatite samples with low track density, or in those samples in which only a small number of apatite grains are obtained, fewer confined tracks may be available. In such cases, the whole mount is scanned to measure as many confined tracks as possible.

Integrated fission track age and length measurement

Fission track age determination and length measurement are now made in a single pass of the grain mount, in an integrated approach. The location of each grain in which

tracks are either counted or measured is recorded for future reference. Thus, track length measurements can be tied to age determination in individual grains. As a routine procedure we do not measure the age of every grain in which lengths are determined, as this would be much too time-consuming. Likewise we do not only measure ages in grain in which lengths are measured, as this would bias the age data against low track density grains. Nevertheless, the ability to determine the fission track age of certain grains from which length data originate can be a particularly useful aid to interpretation in some cases. Grain location data are not provided in this report, but are available on request.

B.3 Data Presentation

Fission track age data

Data sheets summarising the apatite fission track age data, including full details of fission track age data for individual apatite grains in each sample, together with the primary counting results and statistical data, are given in the following pages. Individual grain fission track ages are calculated from the ratio of spontaneous to induced fission track counts for each grain using equation B.1, and errors in the single grain ages are calculated using Poissonian statistics, as explained in more detail by Galbraith (1981) and Green (1981). All errors are quoted as $\pm 1\sigma$ throughout this report, unless otherwise stated.

The variability of fission track ages between individual apatite grains within each sample can be assessed using a chi-squared (χ^2) statistic (Galbraith, 1981), the results of which are summarised for each sample in the data sheets. If all the grains counted belong to a single age population, the probability of obtaining the observed χ^2 value, for ν degrees of freedom (where ν = number of crystals -1), is listed in the data sheets as $P(\chi^2)$ or P(chi squared).

A $P(\chi^2)$ value greater than 5% can be taken as evidence that all grains are consistent with a single population of fission track age. In this case, the best estimate of the fission track age of the sample is given by the "pooled age", calculated from the ratio of the total spontaneous and induced track counts in all grains analysed. Errors for the pooled age are calculated using the "conventional" technique outlined by Green (1981), based on the total number of tracks counted for each track density measurement (see also Galbraith, 1981).

A $P(\chi^2)$ value of less than 5% denotes a significant spread of single grain ages, suggesting real differences exist between the fission track ages of individual apatite

grains. A significant spread in grain ages can result either from inheritance of detrital grains from mixed source areas (in sedimentary rocks), or from differential annealing in apatite grains of different composition, within a narrow range of temperature.

Calculation of the pooled age inherently assumes that only a single population of ages is present, and is thus not appropriate to samples containing a significant spread of fission track ages. In such cases Galbraith, has recently devised a means of estimating the modal age of a distribution of single grain fission track ages which is referred to as the "central age". Calculation of the central age assumes that all single grain ages belong to a Normal distribution of ages, with a standard deviation (σ) known as the "age dispersion". An iterative algorithm (Galbraith and Laslett, 1993) is used to provide estimates of the central age with its associated error, and the age dispersion, which are all quoted in the data sheets. Note that this treatment replaces use of the "mean age", which has used been in the past for those samples in which $P(\chi^2)<5\%$. For samples in which $P(\chi^2)>5\%$, the central age and the pooled age should be equal, and the age dispersion should be less than ~10%.

Table B.1 summarises the fission track age data in apatite from each sample analysed.

Construction of radial plots of single grain age data

Single grain age data are best represented in the form of radial plot diagrams (Galbraith, 1988, 1990). As illustrated in Figure B.1, these plots display the variation of individual grain ages in a plot of y against x, where:

$$y = (z_j - z_o) / \sigma_i \qquad x = 1/\sigma_j \qquad \text{B.2}$$

and; z_j = Fission track age of grain j
z_o = A reference age
σ_j = Error in age for grain j

In this plot, all points on a straight line from the origin define a single value of fission track age, and, at any point, the value of x is a measure of the precision of each individual grain age. Therefore, precise individual grain ages fall to the right of the plot (small error, high x), which is useful, for example, in enabling precise, young grains to be identified. The age scale is shown radially around the perimeter of the plot (in Ma). If all grains belong to a single age population, all data should scatter between y = +2 and y = -2, equivalent to scatter within $\pm 2\sigma$. Scatter outside these boundaries shows a significant spread of individual grain ages, as also reflected in the values of $P(\chi^2)$ and age dispersion.

In detail, rather than using the fission track age for each grain as in equation B.2, we use:

$$z_j = \frac{N_{sj}}{N_{ij}} \qquad \sigma_j = \{1/N_{sj} + 1/N_{ij}\} \qquad \text{B.3}$$

as we are interested in displaying the scatter within the data from each sample in comparison with that allowed by the Poissonian uncertainty in track counts, without the additional terms which are involved in determination of the fission track age (ρ_D, ζ, etc).

Zero ages cannot be displayed in such a plot. This can be achieved using a modified plot, (Galbraith, 1990) with:

$$z_j = \text{arc sin}\sqrt{\left\{\frac{N_{sj}+3/8}{N_{sj}+N_{ij}+3/4}\right\}} \qquad \sigma_j = \frac{1}{2}\sqrt{\left\{\frac{1}{N_{sj}+N_{ij}}\right\}} \qquad \text{B.4}$$

Note that the numerical terms in the equation for z_j are standard terms, introduced for statistical reasons. Using this arc-sin transformation, zero ages plot on a diagonal line which slopes from upper left to lower right. Note that this line does not go through the origin. Figure B.2 illustrates this difference between conventional and arc-sin radial plots, and also provides a simple guide to the structure of radial plots.

Use of arc-sin radial plots is particularly useful in assessing the relative importance of zero ages. For instance, grains with $N_s = 0$, $N_i = 1$ are compatible with ages up to ~900 Ma (at the 95% confidence level), whereas grains with $N_s = 0$, $N_i = 50$ are only compatible with ages up to ~14 Ma. The two data would readily be distinguishable on the radial plot as the 0,50 datum would plot well to the right (high x) compared to the 0,1 datum.

In this report the value of z corresponding to the stratigraphic age of each sample (or the midpoint of the range where appropriate) is adopted as the reference value, z_o. This allows rapid assessment of the fission track age of individual grains in relation to the stratigraphic age, which is a key component in the interpretation of AFTA data, as explained in more detail in Appendix C.

Note that the x axis of the radial plot is normally not labelled, as this would obscure the age scale around the plot. In general labelling is not considered necessary, as we are concerned only with relative variation within the data, rather than absolute values of precision.

Radial plots of the single grain age data in apatite from each sample analysed in this report are shown on the fission track age data summary sheets at the end of this Appendix. Use of radial plots to provide thermal history information is explained in Appendix C and Figure C.7.

Track length data

Distributions of confined track lengths in apatite from each sample are shown as simple histograms on the fission track age data summary sheets at the end of this Appendix. For every track length measurement, the length is recorded to the nearest 0.1 μm, but the measurements have been grouped into 1 μm intervals for construction of these histograms. Each distribution has been normalised to 100 tracks for each sample to facilitate comparison. A summary of the length distribution in each sample is presented in Table B.2, which also shows the mean track length in each sample and its associated error, the standard deviation of each distribution and the number of tracks (N) measured in each sample. The angle which each confined track makes with the crystallographic c-axis is also routinely recorded, as is the width of each fracture within which tracks are revealed. These data are not provided in this report, but can be supplied on request.

Breakdown of data into compositional groups

In Table B.3, AFTA data are grouped into compositional intervals of 0.1 wt% Cl width. Parameters for each interval represent the data from all grains with Cl contents within each interval. Also shown are the parameters for each compositional interval predicted from the Default Thermal History (see Section 2.1). These data form the basis of interpretation of the AFTA data, which takes full account of the influence of Cl content on annealing kinetics, as described in Appendix C. Distributions of Cl contents in all apatites analysed from each sample (i.e. for both age and length determinations) are shown on the fission track age data summary sheets at the end of this Appendix.

Plots of fission track age against Cl content for individual apatite grains

Fission track ages of single apatite grains within individual samples are plotted against the Cl content of each grain on the fission track age data summary sheets at the end of this Appendix. These plots are useful in assessing the degree of annealing, as expressed by the fission track age data. For example, if grains with a range of Cl contents from zero to some upper limit all give similar fission track ages which are significantly less than the stratigraphic age, then grains with these compositions must have been totally annealed. Alternatively, if fission track age falls rapidly with decreasing Cl content, the sample displays a high degree of partial annealing.

B.4 A note on terminology

Note that throughout this report, the term "fission track age" is understood to denote the parameter calculated from the fission track age equation, using the observed spontaneous and induced track counts (either pooled for all grains or for individual grains). The resulting number (with units of Ma) should not be taken as possessing any significance in terms of events taking place at the time indicated by the measured fission track age, but should rather be regarded as a measure of the integrated thermal history of the sample, and should be interpreted in that light using the principles outlined in Appendix C. Use of the term "apparent age" is not considered to be useful in this regard, as almost every fission track age should be regarded as an apparent age, in the classic sense, and repeated use becomes cumbersome.

References

Fleischer, R. L., Price, P. B., and Walker, R. M. (1975) Nuclear tracks in solids, University of California Press, Berkeley.

Galbraith, R. F. (1981) On statistical models for fission-track counts. *Mathematical Geology*, 13, 471-488.

Galbraith, R. F. (1988) Graphical display of estimates having differing standard errors. *Technometrics*, 30, 271-281.

Galbraith, R. F. (1990) The radial plot: graphical assessment of spread in ages. *Nuclear Tracks*, 17, 207-214.

Galbraith R.F. & Laslett G.M. (1993) Statistical methods for mixed fission track ages. *Nuclear Tracks* 21, 459-470.

Gleadow, A. J. W. (1981) Fission track dating methods; what are the real alternatives? *Nuclear Tracks*, 5, 3-14.

Green, P. F. (1981) A new look at statistics in fission track dating. *Nuclear Tracks 5*, 77-86.

Green, P. F. (1985) A comparison of zeta calibration baselines in zircon, sphene and apatite. *Chem. Geol. (Isot. Geol. Sect.)*, 58, 1-22.

Green, P. F., Duddy, I. R., Gleadow, A. J. W., Tingate, P. R. and Laslett, G. M. (1986) Thermal annealing of fission tracks in apatite 1. A qualitative description. *Chem. Geol. (Isot. Geosci. Sect.)*, 59, 237-253.

Hurford, A. J. (1986) Application of the fission track dating method to young sediments: Principles, methodology and Examples. *In:* Hurford, A. J., Jäger, E. and Ten Cate, J. A. M. (*eds*), Dating young sediments, CCOP Technical Publication 16, CCOP Technical Secretariat, Bangkok, Thailand.

Hurford, A. J. and Green, P. F. (1982) A user's guide to fission track dating calibration. *Earth. Planet. Sci Lett.* 59, 343-354.

Hurford, A. J. and Green, P. F. (1983) The zeta age calibration of fission track dating. *Isotope Geoscience* 1, 285-317.

Laslett, G. M., Kendall, W. S., Gleadow, A. J. W. and Duddy, I. R. (1982) Bias in measurement of fission track length distributions. *Nuclear Tracks*, 6, 79-85.

Naeser, C. W. (1979) Fission track dating and geologic annealing of fission tracks. *In:* Jäger, E. and Hunziker, J. C. (*eds*), Lectures in Isotope Geology, Springer Verlag, Berlin.

Smith, M. J. and Leigh-Jones, P. (1985) An automated microscope scanning stage for fission-track dating. *Nuclear Tracks*, 10, 395-400.

Table B.1: Apatite fission track analytical results - samples from Otway Basin (Geotrack Report #876)

Sample number	Number of grains	ρ_D (N_D) x10^6/cm²	ρ_s (Ns) x10^6/cm²	ρ_i (Ni) x10^6/cm²	Uranium content (ppm)	$P(\chi^2)$ (%)	Age dispersion (%)	Fission track age (Ma)
Bridgewater Bay-1								
GC876-7	6	1.023 (1783)	0.639 (39)	0.934 (57)	10	1	71	131.8 ± 27.6
								*122.6 ± 43.9**
GC876-8	9	1.038 (1783)	0.483 (59)	0.893 (109)	10	92	<1	106.0 ± 17.4
GC876-10			No apatite					
GC876-12	19	1.053 (1783)	0.123 (47)	0.970 (371)	11	9	63	25.3 ± 4.0

ρ_s = spontaneous track density; ρ_i = induced track density; ρ_D = track density in glass standard external detector. Brackets show number of tracks counted. ρ_D and ρ_i measured in mica external detectors; ρ_s measured in internal surfaces.
*Central age, used where sample contains a significant spread of single grain ages ($P(\chi^2)$<5%). Errors quoted at 1σ.
Ages calculated using dosimeter glass CN5, with a zeta of 380.4 ± 5.7 (Analyst: C. O'Brien)

Table B.2: Length distribution summary data - samples from Otway Basin (Geotrack Report #876)

Sample number	Mean track length (µm)	Standard deviation (µm)	Number of tracks (N)	Number of tracks in Length Intervals (µm)																			
				1	2	3	4	5	6	7	8	9	10	11	12	13	14	15	16	17	18	19	20
Bridgewater Bay-1																							
GC876-7	11.44	-	1	-	-	-	-	-	-	-	-	-	-	-	1	-	-	-	-	-	-	-	-
GC876-8	13.08	-	1	-	-	-	-	-	-	-	-	-	-	-	-	-	1	-	-	-	-	-	-
GC876-10	No apatite	-	-	-	-	-	-	-	-	-	-	-	-	-	-	-	-	-	-	-	-	-	-
GC876-12	No confined	tracks	-	-	-	-	-	-	-	-	-	-	-	-	-	-	-	-	-	-	-	-	-

Track length measurements by: C. O'Brien

Table B.3: AFTA Data in Compositional Groups - (Geotrack Report #876)

Cl Wt %	Default fission track age* (Ma)	Measured fission track age (Ma)	Error in age (Ma)	P (χ^2)	Number of grains	Default fission track length* (µm)	Mean Track length (µm)	Error in length (µm)	Std deviation (µm)	Number of lengths	Number of grains	Number of tracks in length interval (µm) 1	2	3	4	5	6	7	8	9	10	11	12	13	14	15	16	17	18	19	20
Bridgewater Bay-1																															
876-7†	**70**	**122.6**	**43.9**	**0.8**	**6**	**12.4**	**11.4**	**0.0**	**0.0**	**1**	**1**	**0**	**0**	**0**	**0**	**0**	**0**	**0**	**0**	**0**	**0**	**0**	**1**	**0**	**0**	**0**	**0**	**0**	**0**	**0**	**0**
0.0 - 0.1	68	135.2	91.5	1.1	2	12.4	11.4	0.0	0.0	1	1	0	0	0	0	0	0	0	0	0	0	0	1	0	0	0	0	0	0	0	0
0.1 - 0.2	68	347.3	176.5	100.0	1	12.6	0.0	0.0	0.0	0	0	0	0	0	0	0	0	0	0	0	0	0	0	0	0	0	0	0	0	0	0
0.2 - 0.3	-	-	-	-		-	-	-	-	-	-	-	-	-	-	-	-	-	-	-	-	-	-	-	-	-	-	-	-	-	-
0.3 - 0.4	-	-	-	-		-	-	-	-	-	-	-	-	-	-	-	-	-	-	-	-	-	-	-	-	-	-	-	-	-	-
0.4 - 0.5	-	-	-	-		-	-	-	-	-	-	-	-	-	-	-	-	-	-	-	-	-	-	-	-	-	-	-	-	-	-
0.5 - 0.6	71	115.7	84.6	100.0	1	13.1	0.0	0.0	0.0	0	0	0	0	0	0	0	0	0	0	0	0	0	0	0	0	0	0	0	0	0	0
0.6 - 0.7	-	-	-	-		-	-	-	-	-	-	-	-	-	-	-	-	-	-	-	-	-	-	-	-	-	-	-	-	-	-
0.7 - 0.8	-	-	-	-		-	-	-	-	-	-	-	-	-	-	-	-	-	-	-	-	-	-	-	-	-	-	-	-	-	-
0.8 - 0.9	73	21.6	22.8	100.0	1	13.4	0.0	0.0	0.0	0	0	0	0	0	0	0	0	0	0	0	0	0	0	0	0	0	0	0	0	0	0
0.9 - 1.0	73	96.6	37.5	100.0	1	13.4	0.0	0.0	0.0	0	0	0	0	0	0	0	0	0	0	0	0	0	0	0	0	0	0	0	0	0	0
876-8†	**66**	**106.0**	**17.4**	**92.1**	**9**	**11.0**	**13.1**	**0.0**	**0.0**	**1**	**1**	**0**	**0**	**0**	**0**	**0**	**0**	**0**	**0**	**0**	**0**	**0**	**0**	**0**	**1**	**0**	**0**	**0**	**0**	**0**	**0**
0.0 - 0.1	62	140.6	43.6	77.1	2	11.0	13.1	0.0	0.0	1	1	0	0	0	0	0	0	0	0	0	0	0	0	0	1	0	0	0	0	0	0
0.1 - 0.2	63	0.0	1478.3	0.0	1	11.2	0.0	0.0	0.0	0	0	0	0	0	0	0	0	0	0	0	0	0	0	0	0	0	0	0	0	0	0
0.2 - 0.3	65	118.6	33.8	92.0	2	11.5	0.0	0.0	0.0	0	0	0	0	0	0	0	0	0	0	0	0	0	0	0	0	0	0	0	0	0	0
0.3 - 0.4	66	49.2	55.0	100.0	1	11.8	0.0	0.0	0.0	0	0	0	0	0	0	0	0	0	0	0	0	0	0	0	0	0	0	0	0	0	0
0.4 - 0.5	-	-	-	-		-	-	-	-	-	-	-	-	-	-	-	-	-	-	-	-	-	-	-	-	-	-	-	-	-	-
0.5 - 0.6	68	91.5	42.0	100.0	1	12.1	0.0	0.0	0.0	0	0	0	0	0	0	0	0	0	0	0	0	0	0	0	0	0	0	0	0	0	0
0.6 - 0.7	-	-	-	-		-	-	-	-	-	-	-	-	-	-	-	-	-	-	-	-	-	-	-	-	-	-	-	-	-	-
0.7 - 0.8	70	71.4	29.5	100.0	1	12.4	0.0	0.0	0.0	0	0	0	0	0	0	0	0	0	0	0	0	0	0	0	0	0	0	0	0	0	0
0.8 - 0.9	-	-	-	-		-	-	-	-	-	-	-	-	-	-	-	-	-	-	-	-	-	-	-	-	-	-	-	-	-	-
0.9 - 1.0	-	-	-	-		-	-	-	-	-	-	-	-	-	-	-	-	-	-	-	-	-	-	-	-	-	-	-	-	-	-
1.0 - 1.1	71	108.8	60.7	100.0	1	12.6	0.0	0.0	0.0	0	0	0	0	0	0	0	0	0	0	0	0	0	0	0	0	0	0	0	0	0	0

*Fission Track Age and Mean Track Length predicted from the Default Thermal History (i.e. if the sample has not been hotter in the past)
†Combined data for all compositional groups

Table B.3: Continued - (Geotrack Report #876)

Cl Wt %	Default fission track age* (Ma)	Measured fission track age (Ma)	Error in age (Ma)	P (χ^2)	Number of grains	Default fission track length* (µm)	Mean Track length (µm)	Error in length (µm)	Std deviation (µm)	Number of lengths	Number of grains	Number of tracks in length interval (µm) 1	2	3	4	5	6	7	8	9	10	11	12	13	14	15	16	17	18	19	20
876-12†	**2**	**25.3**	**4.0**	**8.6**	**19**	**8.1**	**0.0**	**0.0**	**0.0**	**0**	**0**	**0**	**0**	**0**	**0**	**0**	**0**	**0**	**0**	**0**	**0**	**0**	**0**	**0**	**0**	**0**	**0**	**0**	**0**	**0**	**0**
0.0 - 0.1	0	6.2	6.9	1.3	2	0.0	0.0	0.0	0.0	0	0	0	0	0	0	0	0	0	0	0	0	0	0	0	0	0	0	0	0	0	0
0.1 - 0.2	0	0.0	64.2	0.0	1	0.0	0.0	0.0	0.0	0	0	0	0	0	0	0	0	0	0	0	0	0	0	0	0	0	0	0	0	0	0
0.2 - 0.3	0	0.0	53.0	0.0	1	0.0	0.0	0.0	0.0	0	0	0	0	0	0	0	0	0	0	0	0	0	0	0	0	0	0	0	0	0	0
0.3 - 0.4	0	18.2	13.4	100.0	1	0.0	0.0	0.0	0.0	0	0	0	0	0	0	0	0	0	0	0	0	0	0	0	0	0	0	0	0	0	0
0.4 - 0.5	0	14.5	6.7	60.0	5	0.0	0.0	0.0	0.0	0	0	0	0	0	0	0	0	0	0	0	0	0	0	0	0	0	0	0	0	0	0
0.5 - 0.6	0	44.3	24.5	23.0	2	0.0	0.0	0.0	0.0	0	0	0	0	0	0	0	0	0	0	0	0	0	0	0	0	0	0	0	0	0	0
0.6 - 0.7	0	0.0	18.1	0.0	3	7.3	0.0	0.0	0.0	0	0	0	0	0	0	0	0	0	0	0	0	0	0	0	0	0	0	0	0	0	0
0.7 - 0.8	-	-	-	-		-	-	-	-	-	-	-	-	-	-	-	-	-	-	-	-	-	-	-	-	-	-	-	-	-	-
0.8 - 0.9	-	-	-	-		-	-	-	-	-	-	-	-	-	-	-	-	-	-	-	-	-	-	-	-	-	-	-	-	-	-
0.9 - 1.0	-	-	-	-		-	-	-	-	-	-	-	-	-	-	-	-	-	-	-	-	-	-	-	-	-	-	-	-	-	-
1.0 - 1.1	3	59.8	39.4	100.0	1	7.9	0.0	0.0	0.0	0	0	0	0	0	0	0	0	0	0	0	0	0	0	0	0	0	0	0	0	0	0
1.1 - 1.2	-	-	-	-		-	-	-	-	-	-	-	-	-	-	-	-	-	-	-	-	-	-	-	-	-	-	-	-	-	-
1.2 - 1.3	6	21.3	10.0	100.0	1	7.9	0.0	0.0	0.0	0	0	0	0	0	0	0	0	0	0	0	0	0	0	0	0	0	0	0	0	0	0
1.3 - 1.4	8	45.5	11.9	100.0	1	7.9	0.0	0.0	0.0	0	0	0	0	0	0	0	0	0	0	0	0	0	0	0	0	0	0	0	0	0	0
1.4 - 1.5	-	-	-	-		-	-	-	-	-	-	-	-	-	-	-	-	-	-	-	-	-	-	-	-	-	-	-	-	-	-
1.5 - 1.6	-	-	-	-		-	-	-	-	-	-	-	-	-	-	-	-	-	-	-	-	-	-	-	-	-	-	-	-	-	-
1.6 - 1.7	-	-	-	-		-	-	-	-	-	-	-	-	-	-	-	-	-	-	-	-	-	-	-	-	-	-	-	-	-	-
1.7 - 1.8	-	-	-	-		-	-	-	-	-	-	-	-	-	-	-	-	-	-	-	-	-	-	-	-	-	-	-	-	-	-
1.8 - 1.9	20	46.0	17.1	100.0	1	8.3	0.0	0.0	0.0	0	0	0	0	0	0	0	0	0	0	0	0	0	0	0	0	0	0	0	0	0	0

*Fission Track Age and Mean Track Length predicted from the Default Thermal History (i.e. if the sample has not been hotter in the past)
†Combined data for all compositional groups

Estimates	z_i
Standard errors	σ_i
Reference value	z_o
Standardised estimates	$y_i = (z_i - z_o) / \sigma_i$
Precision	$x_i = 1 / \sigma_i$

PLOT y_i against x_i

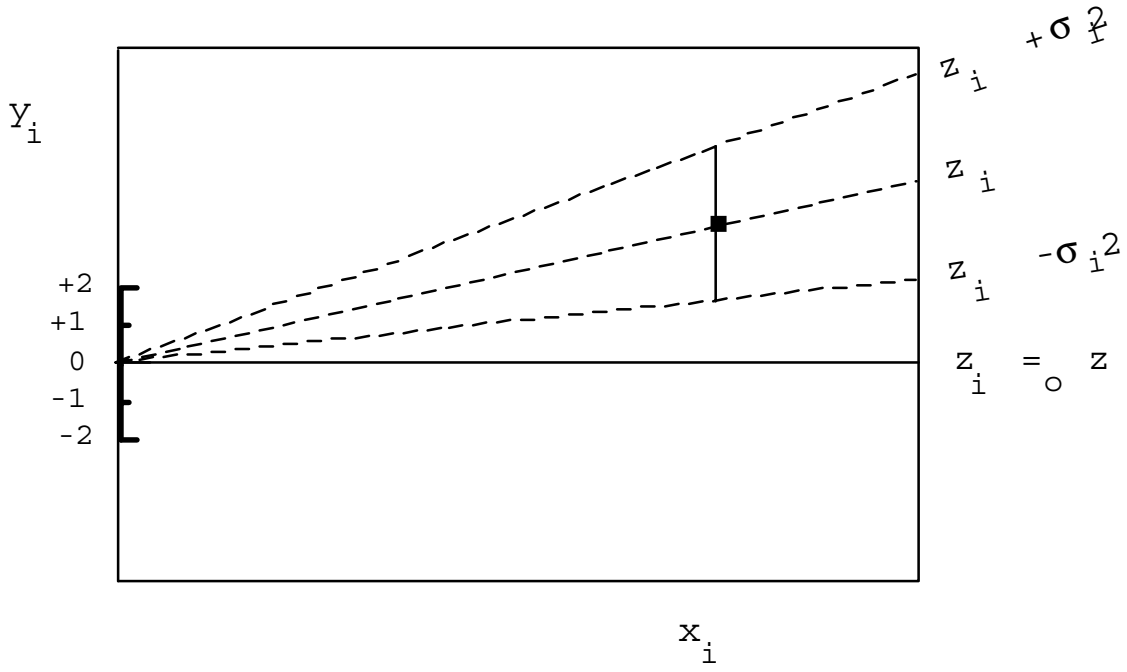

Slope of line from origin through data point $= y_i / x_i$

$= \{(z_i - z_o)/\sigma_i\} / \{1/\sigma_i\}$

$= z_i - z_o$

Key Points:

Radial lines emanating from the origin correspond to fixed values of z

Data points with higher values of x_i have greater precision.

Error bars on all points are the same size in this plot.

Figure B.1 Basic construction of a radial plot. In AFTA, the estimates z_i correspond to the fission track age values for individual apatite grains. Any convenient value of age can be chosen as the reference value corresponding to the horizontal in the radial plot. Radial lines emanating from the origin with positive slopes correspond to fission track ages greater than the reference value. Lines with negative slopes correspond to fission track ages less than the reference value.

Normal radial plot (equations B.2 and B.3)

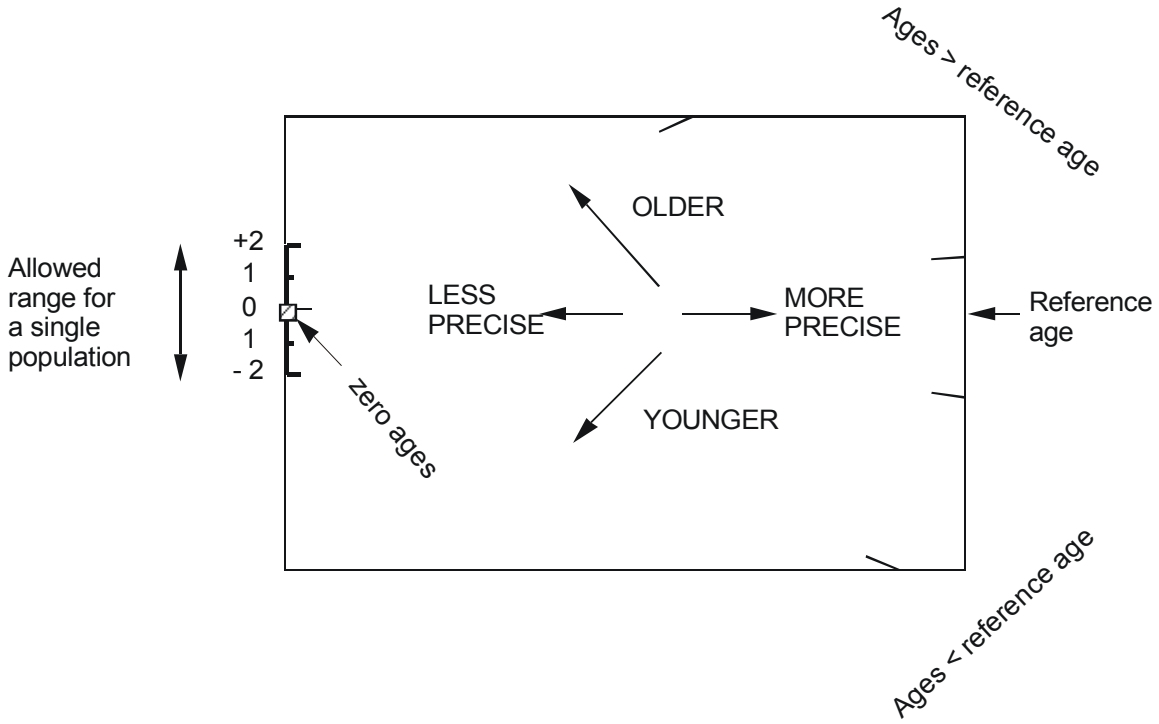

Arc-sin radial plot (equations B.2 and B.4)

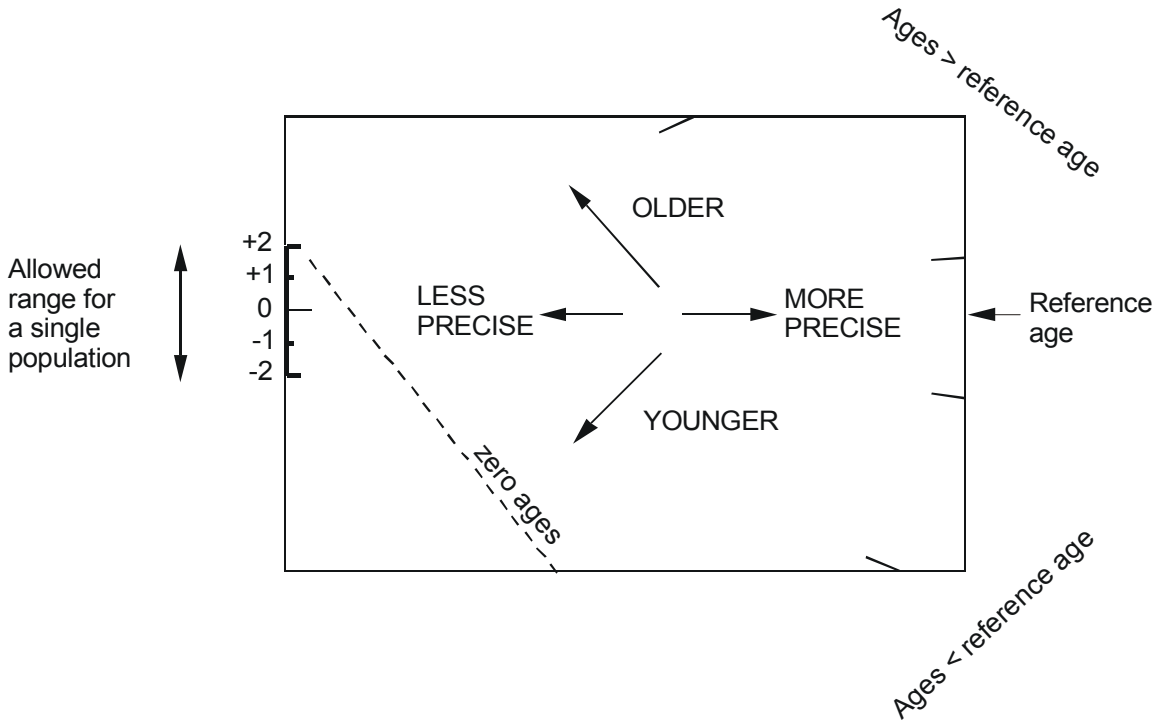

Figure B.2 Simplified structure of Normal and Arc-sin radial plots.

Fission Track Age Data Sheets - Glossary

N_s	=	Number of spontaneous tracks in N_a grid squares
N_i	=	Number of induced tracks in N_a grid squares
N_a	=	Number of grid squares counted in each grain
RATIO	=	N_S/N_i
U (ppm)	=	Uranium content of each grain (= U content of standard glass * ρ_i/ρ_D)
Cl (wt%)	=	Weight percent chlorine content of each grain
ρ_s	=	Spontaneous track density (ρ_s) = N_s/ (N_a*area of basic unit)
ρ_i	=	Induced track density (ρ_i) = N_i/(N_a*area of basic unit)
F.T. AGE	=	Fission track age, calculated using equation B.1
Area of basic unit	=	Area of one grid square
Chi squared	=	χ^2 parameter, used to assess variation of single grain ages within the sample
P(chi squared)	=	Probability of obtaining observed χ^2 value for the relevant number of degrees of freedom, if all grains belong to a single population
Age Dispersion	=	% variation in single grain ages - see discussion in text re "Central age"
N_s/N_i	=	Pooled ratio, total spontaneous tracks divided by total induced tracks for all grains
Mean ratio	=	Mean of (N_s/N_i) for individual grains
Zeta	=	Calibration constant, determined empirically for each observer
ρ_D	=	Track density (ρ_D) from uranium standard glass (interpolated from values at each end of stack)
ND	=	Total number of tracks counted for determining ρ_D
POOLED AGE	=	Fission track age calculated from pooled ratio N_s/N_i. Valid only when P(χ2) > 5%
CENTRAL AGE	=	Alternative to pooled age when P(χ2)< 5%

Key to Figures:

A: Radial plot of single grain ages *(See Figures B.1 and B.2 for details of radial plot construction)*	B: Distribution of Cl contents in apatite grains
C: Single grain age vs weight % Cl for individual apatite grains.	D: Distribution of confined track lengths

GC876-7 Apatite
Counted by: COB

Bridgewater Bay-1 2115-2215m

Slide ref	Current grain no	N_s	N_i	N_a	ρ_s	ρ_i	RATIO	U (ppm)	Cl (wt%)	F.T. AGE (Ma)
G933-1	4	2	10	12	2.648E+05	1.324E+06	0.200	14.8	0.00	38.8 ± 30.1
G933-1	5	11	6	21	8.324E+05	4.540E+05	1.833	5.1	0.12	347.3 ± 176.5
G933-1	6	3	5	9	5.297E+05	8.828E+05	0.600	9.8	0.50	115.7 ± 84.6
G933-1	7	12	7	9	2.119E+06	1.236E+06	1.714	13.8	0.03	325.3 ± 155.0
G933-1	8	10	20	10	1.589E+06	3.178E+06	0.500	35.4	0.97	96.6 ± 37.5
G933-1	9	1	9	36	4.414E+04	3.973E+05	0.111	4.4	0.84	21.6 ± 22.8
		39	57		6.389E+05	9.338E+05		10.4		

Area of basic unit = 6.293E-07 cm^{-2}
χ^2 = 15.524 with 5 degrees of freedom
P(χ^2) = 0.8%
Age Dispersion = 70.888%

Ns / Ni = 0.684 ± 0.142
Mean Ratio = 0.826 ± 0.309

Ages calculated using a zeta of 380.4 ± 5.7 for CN5 glass
ρ_D = 1.023E+06cm^{-2} ND = 1783
ρ_D interpolated between top of can; ρ_D = 1.023E+06cm^{-2} ND = 805
bottom of can; ρ_D = 1.243E+06cm^{-2} ND = 978

POOLED AGE = 131.8 ± 27.6 Ma
CENTRAL AGE = 122.6 ± 43.9 Ma

A:

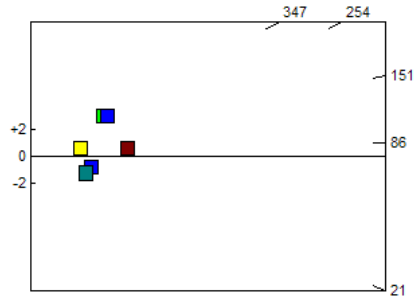

B:

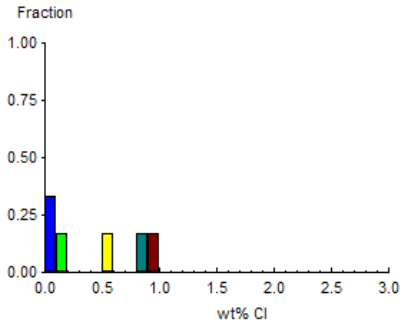

C:

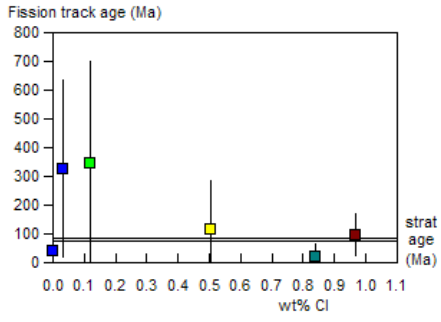

D:

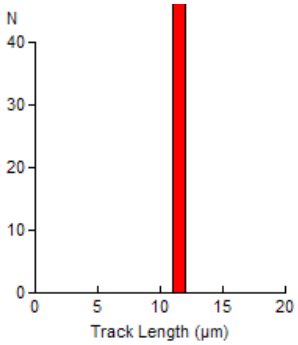

Mean track length 11.44 ± 0.00 µm Std. Dev. µm 1 tracks

GC876-8 Apatite
Counted by: COB

Bridgewater Bay-1 2590-2720m

Slide ref	Current grain no	N_s	N_i	N_a	ρ_s	ρ_i	RATIO	U (ppm)	Cl (wt%)	F.T. AGE (Ma)
G933-2	3	8	22	48	2.648E+05	7.283E+05	0.364	8.0	0.70	71.4 ± 29.5
G933-2	4	0	1	12	0.000E+00	1.324E+05	0.000	1.5	0.13	0.0 ± 1478.3
G933-2	5	10	15	8	1.986E+06	2.980E+06	0.667	32.7	0.00	130.3 ± 53.3
G933-2	6	7	12	36	3.090E+05	5.297E+05	0.583	5.8	0.20	114.2 ± 54.4
G933-2	7	7	15	24	4.635E+05	9.932E+05	0.467	10.9	0.52	91.5 ± 42.0
G933-2	8	5	9	24	3.311E+05	5.959E+05	0.556	6.5	1.07	108.8 ± 60.7
G933-2	9	8	10	12	1.059E+06	1.324E+06	0.800	14.5	0.00	156.0 ± 74.1
G933-2	10	13	21	15	1.377E+06	2.225E+06	0.619	24.4	0.24	121.1 ± 42.9
G933-2	11	1	4	15	1.059E+05	4.238E+05	0.250	4.7	0.36	49.2 ± 55.0
		59	109		4.833E+05	8.928E+05		9.8		

Area of basic unit = 6.293E-07 cm^{-2}
χ^2 = 3.209 with 8 degrees of freedom
P(χ^2) = 92.1%
Age Dispersion = 0.001% (did not converge)

Ns / Ni = 0.541 ± 0.087
Mean Ratio = 0.478 ± 0.081

Ages calculated using a zeta of 380.4 ± 5.7 for CN5 glass
ρ_D = 1.038E+06cm^{-2} ND = 1783
ρ_D interpolated between top of can; ρ_D = 1.023E+06cm^{-2} ND = 805
bottom of can; ρ_D = 1.243E+06cm^{-2} ND = 978

POOLED AGE = 106.0 ± 17.4 Ma
CENTRAL AGE = 106.0 ± 17.4 Ma

A:

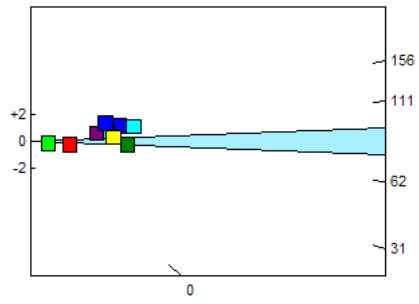

B:

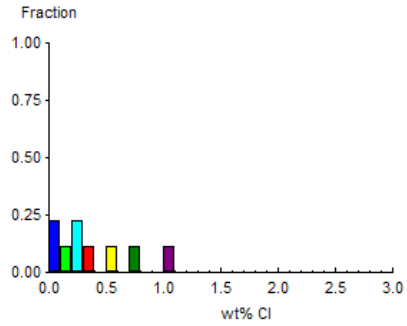

C:

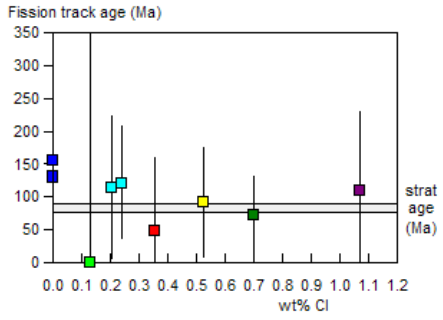

D:

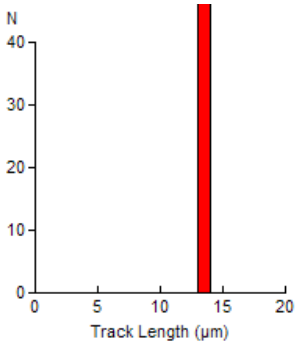

Mean track length 13.08 ± 0.00 µm Std. Dev. µm 1 tracks

GC876-12 Apatite
Counted by: COB

Bridgewater Bay-1 4100-4200m

Slide ref	Current grain no	N_s	N_i	N_a	ρ_s	ρ_i	RATIO	U (ppm)	Cl (wt%)	F.T. AGE (Ma)
G933-3	3	1	7	40	3.973E+04	2.781E+05	0.143	3.0	0.02	28.5 ± 30.5
G933-3	4	5	47	40	1.986E+05	1.867E+06	0.106	20.2	1.23	21.3 ± 10.0
G933-3	5	18	79	100	2.860E+05	1.255E+06	0.228	13.6	1.31	45.5 ± 11.9
G933-3	6	2	22	35	9.080E+04	9.988E+05	0.091	10.8	0.40	18.2 ± 13.4
G933-3	7	0	6	32	0.000E+00	2.980E+05	0.000	3.2	0.40	0.0 ± 64.2
G933-3	8	4	13	24	2.648E+05	8.607E+05	0.308	9.3	0.53	61.3 ± 35.1
G933-3	11	4	36	90	7.063E+04	6.356E+05	0.111	6.9	0.41	22.2 ± 11.7
G933-3	12	9	39	18	7.945E+05	3.443E+06	0.231	37.3	1.83	46.0 ± 17.1
G933-3	13	0	5	20	0.000E+00	3.973E+05	0.000	4.3	0.55	0.0 ± 81.1
G933-3	14	0	6	15	0.000E+00	6.356E+05	0.000	6.9	0.11	0.0 ± 64.2
G933-3	15	3	10	15	3.178E+05	1.059E+06	0.300	11.5	1.01	59.8 ± 39.4
G933-3	16	1	8	16	9.932E+04	7.945E+05	0.125	8.6	0.43	25.0 ± 26.5
G933-3	17	0	5	12	0.000E+00	6.621E+05	0.000	7.2	0.64	0.0 ± 81.1
G933-3	18	0	49	20	0.000E+00	3.893E+06	0.000	42.2	0.08	0.0 ± 6.3
G933-3	19	0	7	15	0.000E+00	7.416E+05	0.000	8.0	0.66	0.0 ± 53.0
G933-3	20	0	7	20	0.000E+00	5.562E+05	0.000	6.0	0.25	0.0 ± 53.0
G933-3	21	0	10	30	0.000E+00	5.297E+05	0.000	5.7	0.43	0.0 ± 34.8
G933-3	23	0	6	24	0.000E+00	3.973E+05	0.000	4.3	0.60	0.0 ± 64.2
G933-3	24	0	9	42	0.000E+00	3.405E+05	0.000	3.7	0.43	0.0 ± 39.3
		47	371		1.228E+05	9.696E+05		10.5		

Area of basic unit = 6.293E-07 cm^{-2}
χ^2 = 26.654 with 18 degrees of freedom
P(χ^2) = 8.6%
Age Dispersion = 62.501%

Ns / Ni = 0.127 ± 0.020
Mean Ratio = 0.086 ± 0.025

Ages calculated using a zeta of 380.4 ± 5.7 for CN5 glass
ρ_D = 1.053E+06cm^{-2} ND = 1783
ρ_D interpolated between top of can; ρ_D = 1.023E+06cm^{-2} ND = 805
bottom of can; ρ_D = 1.243E+06cm^{-2} ND = 978

POOLED AGE = 25.3 ± 4.0 Ma
CENTRAL AGE = 21.3 ± 5.2 Ma

A:

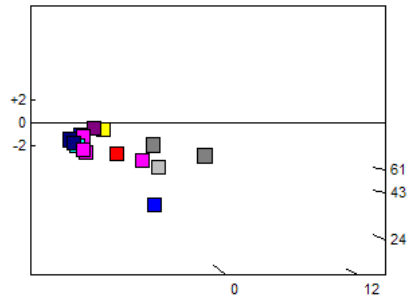

B:

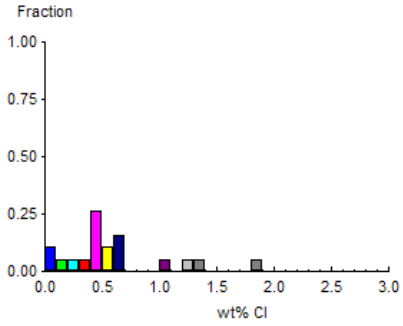

C:

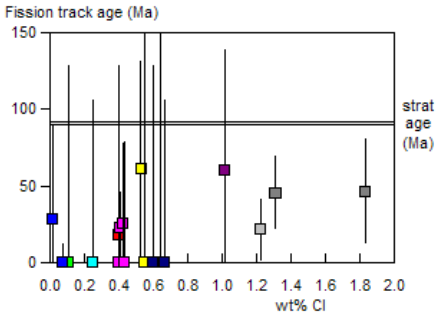

D: No confined tracks

APPENDIX C

Principles of Interpretation of AFTA Data in Sedimentary Basins

C.1 Introduction

Detrital apatite grains are incorporated into sedimentary rocks from three dominant sources - crystalline basement rocks, older sediments and contemporaneous volcanism. Apatites derived from the first two sources will, in general, contain fission tracks when they are deposited, with AFTA parameters characteristic of the source regions. However, apatites derived from contemporaneous volcanism, or from rapidly uplifted basement, will contain no tracks when they are deposited. For now, we will restrict discussion to this situation, and generalise at a later point to cover the case of apatites which contain tracks that have been inherited from source regions.

C.2 Basic principles of Apatite Fission Track Analysis

Fission tracks are trails of radiation damage, which are produced within apatite grains at a more or less constant rate through geological time, as a result of the spontaneous fission of ^{238}U impurity atoms. Therefore, the number of fission events which occur within an apatite grain during a fixed time interval depends on the magnitude of the time interval and the uranium content of the grain. Each fission event leads to the formation of a single fission track, and the proportion of tracks which can intersect a polished surface of an apatite grain depends on the length of the tracks. Therefore, the number of tracks which are etched in unit area of the surface of an apatite grain (the "spontaneous track density") depends on three factors - (i) The time over which tracks have been accumulating; (ii) The uranium content of the apatite grain; and, (iii) The distribution of track lengths in the grain. In sedimentary rocks which have not been subjected to temperatures greater than ~50°C since deposition, spontaneous fission tracks have a characteristic distribution of confined track lengths, with a mean length in the range 14-15 µm and a standard deviation of ~1 µm. In such samples, by measuring the spontaneous track density and the uranium content of a collection of apatite grains, a "fission track age" can be calculated which will be equal to the time over which tracks have been accumulating. The technique is calibrated against other isotopic systems using age standards which also have this type of length distribution (see Appendix B).

In samples which have been subjected to temperatures greater than ~50°C after deposition, fission tracks are shortened because of the gradual repair of the radiation damage which constitutes the unetched tracks. In effect, the tracks shrink from each end, in a process which is known as fission track "annealing". The final length of each individual track is essentially determined by the maximum temperature which that track has experienced. A time difference of an order of magnitude produces a change in fission track parameters which is equivalent to a temperature change of only ~10°C, so temperature is by far the dominant factor in determining the final fission track parameters. As temperature increases, all existing tracks shorten to a length determined by the prevailing temperature, regardless of when they were formed. After the temperature has subsequently decreased, all tracks formed prior to the thermal maximum are "frozen" at the degree of length reduction they attained at that time. Thus, the length of each track can be thought of as a maximum-reading thermometer, recording the maximum temperature to which it has been subjected.

Therefore, in samples for which the present temperature is maximum, all tracks have much the same length, resulting in a narrow, symmetric distribution. The degree of shortening will depend on the temperature, with the mean track length falling progressively from ~14 µm at 50°C, to zero at around 110°-120°C - the precise temperature depending on the timescale of heating and the composition of the apatites present in the sample (see below). Values quoted here relate to times of the order of 10^7 years (heating rates around 1 to 10°C/Ma) and average apatite composition. If the effective timescale of heating is shorter than 10^7 years, the temperature responsible for a given degree of track shortening will be higher, depending in detail on the kinetics of the annealing process (Green et al., 1986; Laslett et al., 1987; Duddy et al., 1988; Green et al., 1989b). Shortening of tracks produces an accompanying reduction in the fission track age, because of the reduced proportion of tracks which can intersect the polished surface. Therefore, the fission track age is also highly temperature dependent, falling to zero at around 120°C due to total erasure of all tracks.

Samples which have been heated to a maximum paleotemperature less than ~120°C at some time in the past and subsequently cooled will contain two populations of tracks, and will show a more complex distribution of lengths and ages. If the maximum paleotemperature was less than ~50°C then the two components will not be resolvable, but for maximum paleotemperatures between ~50° and 120°C the presence of two components can readily be identified. Tracks formed prior to the thermal maximum will all be shortened to approximately the same degree (the precise value depending on the maximum paleotemperature), while those formed during and after cooling will be longer, due to the lower prevailing temperatures. The length distribution in such

samples will be broader than in the simple case, consisting of a shorter and a longer component, and the fission track age will reflect the amount of length reduction shown by the shorter component (determined by the maximum paleotemperature).

If the maximum paleotemperature was sufficient to shorten tracks to between 9 and 11 µm, and cooling to temperatures of ~50°C or less was sufficiently rapid, tracks formed after cooling will have lengths of 14-15 µm and the resulting track length distribution will show a characteristic bimodal form. If the maximum paleotemperature was greater than ~110 to 120°C, all pre-existing tracks will be erased, and all tracks now present will have formed after the onset of cooling. The fission track age in such samples relates directly to the time of cooling.

In thermal history scenarios in which a heating episode is followed by cooling and then temperature increases again, the tracks formed during the second heating phase will undergo progressive shortening. The tracks formed prior to the initial cooling, which were shortened in the first heating episode, will not undergo further shortening until the temperature exceeds the maximum temperature reached in the earlier heating episode. (In practice, differences in timescale of heating can complicate this simple description. In detail, it is the integrated time-temperature effect of the two heating episodes which should be considered.) If the maximum and peak paleotemperatures in the two episodes are sufficiently different (>~10°C), and the later peak paleotemperature is less than the earlier maximum value, then the AFTA parameters allow determination of both episodes. As the peak paleotemperature in the later episode approaches the earlier maximum, the two generations of tracks become increasingly more difficult to resolve, and when the two paleotemperatures are the same, both components are shortened to an identical degree and all information on the earlier heating phase will be lost.

No information is preserved on the approach to maximum paleotemperature because the great majority of tracks formed up to that time have the same mean track length. Only those tracks formed in the last few per cent of the history prior to the onset of cooling are not shortened to the same degree (because temperature dominates over time in the annealing kinetics). These form a very small proportion of the total number of tracks and therefore cannot be resolved within the length distribution because of the inherent spread of several µm in the length distribution.

To summarise, AFTA allows determination of the magnitude of the maximum temperature and the time at which cooling from that maximum began. In some circumstances, determination of a subsequent peak paleotemperature and the time of cooling is also possible.

C.3 Quantitative understanding of fission track annealing in apatite

Annealing kinetics and modelling the development of AFTA parameters

Our understanding of the behaviour of fission tracks in apatite during geological thermal histories is based on study of the response of fission tracks to elevated temperatures in the laboratory (Green et al., 1986; Laslett et al., 1987; Duddy et al., 1988; Green et al., 1989b), in geological situations (Green et al., 1989a), observations of the lengths of spontaneous tracks in apatites from a wide variety of geological environments (Gleadow et al., 1986), and the relationship between track length reduction and reduction in fission track age observed in controlled laboratory experiments (Green, 1988).

These studies resulted in the capability to simulate the development of AFTA parameters resulting from geological thermal histories for an apatite of average composition (Durango apatite, ~0.43 wt% Cl). Full details of this modelling procedure have been explained in Green et al. (1989b). The following discussion presents a brief explanation of the approach.

Geological thermal histories involving temperatures varying through time are broken down into a series of isothermal steps. The progressive shortening of track length through sequential intervals is calculated using the extrapolated predictions of an empirical kinetic model fitted to laboratory annealing data. Contributions from tracks generated throughout the history (remembering that new tracks are continuously generated through time as new fissions occur) are summed to produce the final distribution of track lengths expected to result from the input history. In summing these components, care is taken to allow for various biases which affect revelation of confined tracks (Laslett et al., 1982). The final length reduction of each component of tracks is converted to a contribution of fission track age, using the relationship between track length and density reduction determined by Green (1988). These age contributions are summed to generate the final predicted fission track age.

This approach depends critically on the assumption that extrapolation of the laboratory-based kinetic model to geological timescales, over many orders of magnitude in time, is valid. This was assessed critically by Green et al. (1989b), who showed that predictions from this approach agree well with observed AFTA parameters in apatites of the appropriate composition in samples from a series of reference wells in the Otway Basin of south-east Australia (Gleadow and Duddy, 1981; Gleadow et al., 1983; Green et al., 1989a). This point is illustrated in Figure C.1. Green et al. (1989b) also quantitatively assessed the errors associated with extrapolation of the Laslett et al. (1987) model from

laboratory to geological timescales (i.e. precision, as opposed to accuracy). Typical levels of precision are ~0.5 µm for mean lengths <~10 µm, and ~0.3 µm for lengths >~10 µm. These figures are equivalent to an uncertainty in estimates of maximum paleotemperature derived using this approach of ~10°C. Precision is largely independent of thermal history for any reasonable geological history. Accuracy of prediction from this model is limited principally by the effect of apatite composition on annealing kinetics, as explained in the next section.

Compositional effects

Natural apatites essentially have the composition $Ca_5(PO_4)_3(F,OH,Cl)$. Most common detrital and accessory apatites are predominantly Fluor-apatites, but may contain appreciable amounts of chlorine. The amount of chlorine in the apatite lattice exerts a subtle compositional control on the degree of annealing, with apatites richer in fluorine being more easily annealed than those richer in chlorine. The result of this effect is that in a single sample, individual apatite grains may show a spread in the degree of annealing (i.e. length reduction and fission track age reduction). This effect becomes most pronounced in the temperature range 90 - 120°C (assuming a heating timescale of ~10 Ma), and can be useful in identifying samples exposed to paleotemperatures in this range. At temperatures below ~80°C, the difference in annealing sensitivity is less marked, and compositional effects can largely be ignored.

Our original quantitative understanding of the kinetics of fission track annealing, as described above, relates to a single apatite (Durango apatite) with ~0.43 wt% Cl, on which most of our original experimental studies were carried out. Recently, we have extended this quantitative understanding to apatites with Cl contents up to ~3 wt%. This new, multi-compositional kinetic model is based both on new laboratory annealing studies on a range of apatites with different F-Cl compositions (Figure C.2), and on observations of geological annealing in apatites from a series of samples from exploration wells in which the section is currently at maximum temperature since deposition. A composite model for Durango apatite composition was first created by fitting a common model to the old laboratory data (from Green et al., 1986) and the new geological data for a similar composition. This was then extended to other compositions on the basis of the multi-compositional laboratory and geological data sets. Details of the multi-compositional model are contained in a Technical Note, available from Geotrack in Melbourne.

The multi-compositional model allows prediction of AFTA parameters for any Cl content between 0 and 3 wt%, using a similar approach to that used in our original single composition modelling, as outlined above. Then, for an assumed or measured distribution of Cl contents within a sample, the composite parameters for the sample can be predicted. The range of Cl contents from 0 to 3 wt% spans the range of compositions commonly encountered, as discussed in the next section.

Predictions of the new multi-compositional model are in good agreement with the geological constraints on annealing rates provided by the Otway Basin reference wells, as shown in Figure C.3. However, note that the AFTA data from these Otway Basin wells were among those used in construction of the new model, so this should not be viewed as independent verification, but rather as a demonstration of the overall consistency of the model.

Distributions of Cl content in common AFTA samples

Figure C.4a shows a histogram of Cl contents, measured by electron microprobe, in apatite grains from more than 100 samples of various types. Most grains have Cl contents less than ~0.5 wt%. The majority of grains with Cl contents greater than this come from volcanic sources and basic intrusives, and contain up to ~2 wt% Cl. Figure C.4b shows the distribution of Cl contents measured in randomly selected apatite grains from 61 samples of "typical" quartzo-feldspathic sandstone. This distribution is similar to that in Figure C.4a, except for a more rapid fall-off as Cl content increases. Apatites from most common sandstones give distributions of Cl content which are very similar to that in Figure C.4b. Volcanogenic sandstones typically contain apatites with higher Cl contents, with a much flatter distribution for Cl contents up to ~1.5%, falling to zero at ~2.5 to 3 wt%, as shown in Figure C.4c. Cl contents in granitic basement samples and high-level intrusives are typically much more dominated by compositions close to end-member Fluorapatite, although many exceptions occur to this general rule.

Information about the spread of Cl contents in samples analysed in this report can be found in Appendix A.

Alternative kinetic models

Recently, both Carlson (1990) and Crowley et al. (1991) have published alternative kinetic models for fission track annealing in apatite. Carlson's model is based on our laboratory annealing data for Durango apatite (Green et al., 1986) and other (unpublished) data. In his abstract, Carlson claims that because his model is "based on explicit physical mechanisms, extrapolations of annealing rates to the lower temperatures and longer timescales required for the interpretation of natural fission track

length distributions can be made with greater confidence than is the case for purely empirical relationships fitted to the experimental annealing data". As explained in detail by Green et al. (1993), all aspects of Carlson's model are in fact purely empirical, and his model is inherently no "better" for the interpretation of data than any other. In fact, detailed inspection shows that Carlson's model does not fit the laboratory data set at all well. Therefore, we recommend against use of this model to interpret AFTA data.

The approach taken by Crowley et al. (1991) is very similar to that taken by Laslett et al., (1987). They have fitted models to new annealing data in two apatites of different composition - one close to end-member Fluorapatite (B-5) and one having a relatively high Sr content (113855). The model developed by Crowley et al. (1991) from their own annealing data for the B-5 apatite gives predictions in geological conditions which are consistently higher than measured values, as shown in Figure C.5. Corrigan (1992) reported a similar observation in volcanogenic apatites in samples from a series of West Texas wells. Since the B-5 apatite is close to end-member Fluor-apatite, while the Otway Group apatites contain apatites with Cl contents from zero up to ~3 wt% (and the West Texas apatites have up to 1 wt%), the fluorapatites should have mean lengths rather less than the measured values, which should represent a mean over the range of Cl contents present. Therefore, the predictions of the Crowley et al. (1991) B-5 model appear to be consistently high.

We attribute this to the rather restricted temperature-time conditions covered by the experiments of Crowley et al. (1991), with annealing times between one and 1000 hours, in contrast to times between 20 minutes and 500 days in the experiments of Green et al. (1986). In addition, few of the measured length values in Crowley et al.'s study fall below 11 μm (in only five out of 60 runs in which lengths were measured in apatite B-5) and their model is particularly poorly defined in this region.

Crowley et al. (1991) also fitted a new model to the annealing data for Durango apatite published by Green et al. (1986). Predictions of their fit to our data are not very much different to those from the Laslett et al. (1987) model (Figure C.6). We have not pursued the differences between their model and ours in detail because the advent of our multi-compositional model has rendered the single compositional approach obsolete.

C.4 Evidence for elevated paleotemperatures from AFTA

The basic principle involved in the interpretation of AFTA data in sedimentary basins is to determine whether the degree of annealing shown by tracks in apatite from a particular sample could have been produced if the sample has never been hotter than its present temperature at any time since deposition. To do this, the burial history derived

from the stratigraphy of the preserved sedimentary section is used to calculate a thermal history for each sample using the present geothermal gradient and surface temperature (i.e. assuming these have not changed through time). This is termed the "Default Thermal History". For each sample, the AFTA parameters predicted as a result of the Default Thermal History are then compared to the measured data. If the data show a greater degree of annealing than calculated on the basis of this history, the sample must have been hotter at some time in the past. In this case, the AFTA data are analysed to provide estimates of the magnitude of the maximum paleotemperature in that sample, and the time at which cooling commenced from the thermal maximum.

The degree of annealing is assessed in two ways - from fission track age and track length data. The stratigraphic age provides a basic reference point for the interpretation of fission track age, because reduction of the fission track age below the stratigraphic age unequivocally reveals that appreciable annealing has taken place after deposition of the host sediment. Large degrees of fission track age reduction, with the pooled or central fission track age very much less than the stratigraphic age, indicate severe annealing, which requires paleotemperatures of at least ~100°C for any reasonable geological time-scale of heating (>~1 Ma). Note that this applies even when apatites contain tracks inherited from source areas. More moderate degrees of annealing can be detected by inspection of the single grain age data, as the most sensitive (fluorine-rich) grains will begin to give fission track ages significantly less than the stratigraphic age before the central or pooled age has been reduced sufficiently to give a noticeable signal. Note that this aspect of the single grain age data can also be used for apatites which have tracks inherited from source areas. If signs of moderate annealing (from single grain age reduction) or severe annealing (from the reduction in pooled or central age) are seen in samples in which the Default Thermal History predicts little or no effect, the sample must have been subjected to elevated paleotemperatures at some time in the past. Figure C.7 shows how increasing degrees of annealing are observable in radial plots of the single grain fission track age data.

Similarly, the present temperature from which a sample is taken, and the way in which this has been approached (as inferred from the preserved sedimentary section), forms a basic point of reference for track length data. The observed mean track length is compared with the mean length predicted from the Default Thermal History. If the observed degree of track shortening in a sample is greater than that expected from the Default Thermal History (i.e. the mean length is significantly less than the predicted value), either the sample must have been subjected to higher paleotemperatures at some time after deposition, or the sample contains shorter tracks which were inherited from sediment source areas at the time the sediment was deposited. If shorter tracks were

inherited from source areas, the sample should still contain a component of longer tracks corresponding to the tracks formed after deposition. In general, the fission track age should be greater than the stratigraphic age. This can be assessed quantitatively using the computer models for the development of AFTA parameters described in an earlier section. If the presence of shorter tracks cannot be explained by their inheritance from source areas, the sample must have been hotter in the past.

C.5 Quantitative determination of the magnitude of maximum paleotemperature and the timing of cooling using AFTA

Values of maximum paleotemperature and timing of cooling in each sample are determined using a forward modelling approach based on the quantitative description of fission track annealing described in earlier sections. The Default Thermal History described above is used as the basis for this forward modelling, but with the addition of episodes of elevated paleotemperatures as required to explain the data. AFTA parameters are modelled iteratively through successive thermal history scenarios in order to identify thermal histories that can account for observed parameters. The range of values of maximum paleotemperature and timing of cooling which can account for the measured AFTA parameters (fission track age and track length distribution) are defined using a maximum likelihood-based approach. In this way, best estimates ("maximum likelihood values") can be defined together with ±95% confidence limits.

In samples in which all tracks have been totally annealed at some time in the past, only a minimum estimate of maximum paleotemperature is possible. In such cases, AFTA data provide most control on the time at which the sample cooled to temperatures at which tracks could be retained. The time at which cooling began could be earlier than this time, and therefore the timing also constitutes a minimum estimate.

Comparison of the AFTA parameters predicted by the multi-compositional model with measured values in samples which are currently at their maximum temperatures since deposition shows a good degree of consistency, suggesting the uncertainty in application of the model should be less than ±10°C. This constitutes a significant improvement over earlier approaches, since the kinetic models used are constrained in both laboratory and geological conditions. It should be appreciated that relative differences in maximum paleotemperature can be identified with greater precision than absolute paleotemperatures, and it is only the estimation of absolute paleotemperature values to which the ±10°C uncertainty relates.

Cooling history

If the data are of high quality and provided that cooling from maximum paleotemperatures began sufficiently long ago (so that the history after this time is represented by a significant proportion of the total tracks in the sample), determination of the magnitude of a subsequent peak paleotemperature and the timing of cooling from that peak may also be possible (as explained in Section C.2). A similar approach to that outlined above provides best estimates and corresponding ±95% confidence limits for this episode. Such estimates may simply represent part of a protracted cooling history, and evidence for a later discrete cooling episode can only be accepted if this scenario provides a significantly improved fit to the data. Geological evidence and consistency of estimates between a series of samples can also be used to verify evidence for a second episode.

In practise, most typical AFTA datasets are only sufficient to resolve two discrete episodes of heating and cooling. One notable exception to this is when a sample has been totally annealed in an early episode, and has then undergone two (or more) subsequent episodes with progressively lower peak paleotemperatures in each. But in general, complex cooling histories involving a series of episodes of heating and cooling will allow resolution of only two episodes, and the results will depend on which episodes dominate the data. Typically this will be the earliest and latest episodes, but if multiple cooling episodes occur within a narrow time interval the result will represent an approximation to the actual history.

C.6 Qualitative assessment of AFTA parameters

Various aspects of thermal history can often be assessed by qualitative assessment of AFTA parameters. For example, samples which have reached maximum paleotemperatures sufficient to produce total annealing, and which only contain tracks formed after the onset of cooling, can be identified from a number of lines of evidence. In a vertical sequence of samples showing increasing degrees of annealing, the transition from rapidly decreasing fission track age with increasing depth to more or less the same age over a range of depth denotes the transition from partial to total annealing of all tracks formed prior to the thermal maximum. In samples in which all tracks have been totally annealed, the single grain age data should show that none of the individual grain fission track ages are significantly older than the time of cooling, and grains in all compositional groups should give the same fission track age unless the sample has been further disturbed by a later episode. If the sample cooled rapidly to sufficiently low temperatures, little annealing will have taken place since cooling, and all grains will

give ages which are compatible with a single population around the time of cooling, as shown in Figure C.7.

Inspection of the distribution of single grain ages in partially annealed samples can often yield useful information on the time of cooling, as the most easily annealed grains (those richest in fluorine) may have been totally annealed prior to cooling, while more retentive (Cl-rich) compositions were only partially annealed (as in Figure C.7, centre). The form of the track length distribution can also provide information, from the relative proportions of tracks with different lengths. All of these aspects of the data can be used to reach a preliminary thermal history interpretation.

C.7 Allowing for tracks inherited from source areas

The effect of tracks inherited from source areas, and present at the time the apatite is deposited in the host sediment, is often posed as a potential problem for AFTA. However, this can readily be allowed for in analysing both the fission track age and length data.

In assessing fission track age data to determine the degree of annealing, the only criterion used is the comparison of fission track age with the value expected on the basis of the Default Thermal History. From this point of view, inherited tracks do not affect the conclusion: if a grain or a sample gives a fission track age which is significantly less than expected, the grain or sample has clearly undergone a higher degree of annealing than can be accounted for by the Default Thermal History, and therefore must have been hotter in the past, whether the sample contained tracks when it was deposited or not.

The presence of inherited tracks does impose a limit on our ability to detect post-depositional annealing from age data alone, as in samples which contain a fair proportion of inherited tracks, moderate degrees of annealing may reduce the fission track age from the original value, but not to a value which is significantly less than the stratigraphic age. This is particularly noticeable in the case of Tertiary samples containing apatites derived from Paleozoic basement. In such cases, although fission track age data may show no evidence of post-depositional annealing, track length data may well show such evidence quite clearly.

The influence of track lengths inherited from source areas can be allowed for by comparison of the fission track age with the value predicted by the Default Thermal History combined with inspection of the track length distribution. If the mean length is much less than the length predicted by the Default Thermal History, either the sample has been subjected to elevated paleotemperatures, sufficient to produce the observed degree of length reduction, or else the sample contains a large proportion of shorter

tracks inherited from source areas. However, in the latter case, the sample should give a pooled or central fission track age correspondingly older than the stratigraphic age, while the length distribution should contain a component of longer track lengths corresponding to the value predicted by the Default Thermal History. It is important in this regard that the length of a track depends primarily on the maximum temperature to which it has been subjected, whether in the source regions or after deposition in the sedimentary basin. Thus, any tracks retaining a provenance signature will have lengths towards the shorter end of the distribution where track lengths will not have "equilibrated" with the temperatures attained since deposition.

In general, it is only in extreme cases that inherited tracks render track length data insensitive to post-depositional annealing. For example, if practically all the tracks in a particular sample were formed prior to deposition, perhaps in a Pliocene sediment in which apatites were derived from a stable Paleozoic shield with fission track ages of ~300 Ma or more, the track length distribution will, in general, be dominated by inheritance, as only ~2% of tracks would have formed after deposition. Post-depositional heating will not be detectable as long as the maximum paleotemperature is insufficient to cause greater shortening than that which occurred in the source terrain. Even in such extreme cases, once a sample is exposed to temperatures sufficient to produce greater shortening than that inherited from source areas, the inherited tracks and those formed after deposition will all undergo the same degree of shortening, and the effects of post-depositional annealing can be recognised. In such cases, the presence of tracks inherited from source areas is actually very useful, because the number of tracks formed after deposition is so small that little or no information would be available without the inherited tracks.

C.8 Plots of fission track age and mean track length vs depth and temperature

AFTA data from well sequences are usually plotted as shown in Figure C.8. This figure shows AFTA data for two scenarios: one in which deposition has been essentially continuous from the Carboniferous to the present and all samples are presently at their maximum paleotemperature since deposition (Figure C.8a); and, one in which the section was exposed to elevated paleotemperatures prior to cooling in the Early Tertiary (Figure C.8b).

In both figures, fission track age and mean track length are plotted against depth and present temperature. Presentation of AFTA data in this way often provides insight into the thermal history interpretation, following principles outlined earlier in this Appendix.

In Figure C.8a**,** for samples at temperatures below ~70°C, the fission track age is either greater than or close to the stratigraphic age, and little fission track age reduction has affected these samples. Track lengths in these samples are all greater than ~13 µm. In progressively deeper samples, both the fission track age and mean track length are progressively reduced to zero at a present temperature of around 110°C, with the precise value depending on the spread of apatite compositions present in the sample. Track length distributions in the shallowest samples would be a mixture of tracks retaining information on the thermal history of source regions, while in deeper samples, all tracks would be shortened to a length determined by the prevailing temperature. This pattern of AFTA parameters is characteristic of a sequence which is currently at maximum temperatures.

The data in Figure C.8b show a very different pattern. The fission track age data show a rapid decrease in age, with values significantly less than the stratigraphic age at temperatures of ~40 to 50°C, at which such a degree of age reduction could not be produced in any geological timescale. Below this rapid fall, the fission track ages do not change much over ~1 km (30°C). This transition from rapid fall to consistent ages is diagnostic of the transition from partial to total annealing. Samples above the "break-in slope" contain two generations of tracks: those formed prior to the thermal maximum, which have been partially annealed (shortened) to a degree which depends on the maximum paleotemperature; and, those formed after cooling, which will be longer. Samples below the break-in slope contain only one generation of tracks, formed after cooling to lower temperatures at which tracks can be retained. At greater depths, where temperatures increase to ~90°C and above, the effect of present temperatures begins to reduce the fission track ages towards zero, as in the "maximum temperatures now" case.

The track length data also reflect the changes seen in the fission track age data. At shallow depths, the presence of the partially annealed tracks shortened prior to cooling causes the mean track length to decrease progressively as the fission track age decreases. However, at depths below the break in slope in the age profile, the track length increases again as the shorter component is totally annealed and so does not contribute to the measured distribution of track lengths. At greater depths, the mean track lengths decrease progressively to zero once more due to the effects of the present temperature regime.

Examples of such data have been presented, e.g. by Green (1989) and Kamp and Green (1990).

C.9 Determining paleogeothermal gradients and amount of section removed on unconformities

Estimates of maximum paleotemperatures in samples over a range of depths in a vertical sequence provides the capability of determining the paleogeothermal gradient immediately prior to the onset of cooling from those maximum paleotemperatures. The degree to which the paleogeothermal gradient can be constrained depends on a number of factors, particularly the depth range over which samples are analysed. If samples are only analysed over ~1 km, then the paleotemperature difference over that range may be only ~20 to 30°C. Since maximum paleotemperatures can often only be determined within a ~10°C range, this introduces considerable uncertainty into the final estimate of paleogeothermal gradient (see Figure C.9).

Another important factor is the difference between maximum paleotemperatures and present temperatures ("net cooling"). If this is only ~10°C, which is similar to the uncertainty in absolute paleotemperature determination, only broad limits can be established on the paleogeothermal gradient. In general, the control on the paleogeothermal gradient improves as the amount of net cooling increases. However, if the net cooling becomes so great that many samples were totally annealed prior to the onset of cooling - so that only minimum estimates of maximum paleotemperatures are possible - constraints on the paleogeothermal gradient from AFTA come only from that part of the section in which samples were not totally annealed. In this case, integration of AFTA data with VR measurements can be particularly useful in constraining the paleo-gradient.

Having constrained the paleogeothermal gradient at the time cooling from maximum paleotemperatures began, if we assume a value for surface temperature at that time, the amount of section subsequently removed by uplift and erosion can be calculated as shown in Figure C.10. The *net* amount of section removed is obtained by dividing the difference between the paleo-surface temperature (T_S) and the intercept of the paleotemperature profile at the present ground surface (T_i) by the estimated paleogeothermal gradient. The *total* amount of section removed is obtained by adding the thickness of section subsequently redeposited above the unconformity to the *net* amount estimated as in Figure C.10. If the analysis is performed using depths from the appropriate unconformity, then the analysis will directly yield the *total* amount of section removed.

Geotrack have developed a method of deriving estimates of both the paleogeothermal gradient and the net amount of section removed using estimated paleotemperatures

derived from AFTA and VR. Perhaps more importantly, this method also provides rigorous values for upper and lower 95% confidence limits on each parameter. The method is based on maximum likelihood estimation of the paleogeothermal gradient and the surface intercept, from a table of paleotemperature and depth values. The method is able to accept ranges for paleotemperature estimates (e.g. where the maximum paleotemperature can only be constrained to between, for example, 60 and 90°C), as well as upper and lower limits (e.g. <60°C for samples which show no detectable annealing; >110°C in samples which were totally annealed). Estimates of paleotemperature from AFTA and VR may be combined or analysed separately. Some results from this method have been reported by Bray et al. (1992). Full details of the methods employed are presented in a confidential, in-house, Geotrack research report, copies of which are available on request from the Melbourne office.

Results are presented in two forms. Likelihood profiles, plotting the log-likelihood as a function of either gradient or section removed, portray the probability of a given value of gradient or section removed. The best estimate is given by the value of gradient or section removed for which the log-likelihood is maximised. Ideally, the likelihood profiles should show a quadratic form, and values of gradient or section removed at which the log-likelihood has fallen by two from the maximum value define the upper and lower 95% confidence limits on the estimates. An alternative method of portraying this information is a crossplot of gradient against section removed, in which values which fall within 95% confidence limits (in two dimensions) are contoured. Note that the confidence limits defined by this method are rather tighter than those from the likelihood profiles, as the latter only reflect variation in one parameter, whereas the contoured crossplot takes variation of both parameters into account.

It must be emphasised that this method relies on the assumption that the paleotemperature profile was linear both throughout the section analysed and through the overlying section which has been removed. While the second part of this assumption can never be confirmed independently, visual inspection of the paleotemperature estimates as a function of depth should be sufficient to verify or deny the linearity of the paleotemperature profile through the preserved section.

Results of this procedure are shown in this report if the data allow sufficiently well-defined paleotemperature estimates to justify use of the method. Where the AFTA data suggest that the section is currently at maximum temperature since deposition, or that the paleotemperature profile was non-linear, or where data are of insufficient quality to allow rigorous paleotemperature estimation, the method is not used.

References

Carlson, W.D. (1990) Mechanisms and kinetics of apatite fission-track annealing. *American Mineralogist*, 75, 1120 - 1139.

Corrigan, J. (1992) Annealing models under the microscope, *On Track*, 2, 9-11.

Crowley, K.D., Cameron, M. and Schaefer, R.L. (1991) Experimental studies of annealing of etched fission tracks in apatite. *Geochimica et Cosmochimica Acta*, 55, 1449-1465.

Duddy, I.R., Green, P.F. and Laslett G.M. (1988) Thermal annealing of fission tracks in apatite 3. Variable temperature behaviour. *Chem. Geol. (Isot. Geosci. Sect.)* , 73, 25-38.

Gleadow, A.J.W. and Duddy, I.R. (1981) A natural long-term track annealing experiment for apatite. *Nuclear Tracks*, 5, 169-174.

Gleadow, A.J.W., Duddy, I.R. and Lovering, J.F. (1983) Fission track analysis; a new tool for the evaluation of thermal histories and hydrocarbon potential. *APEA J,* 23, 93-102.

Gleadow, A.J.W., Duddy, I.R., Green, P.F. and Lovering, J.F. (1986) Confined fission track lengths in apatite - a diagnostic tool for thermal history analysis. *Contr. Min. Petr.*, 94, 405-415.

Green, P.F. (1988) The relationship between track shortening and fission track age reduction in apatite: Combined influences of inherent instability, annealing anisotropy, length bias and system calibration. *Earth Planet. Sci. Lett.*, 89, 335-352.

Green, P.F., Duddy, I.R., Gleadow, A.J.W., Tingate, P.R. and Laslett, G.M. (1986) Thermal annealing of fission tracks in apatite 1. A qualitative description. *Chem. Geol. (Isot. Geosci. Sect.)* , 59, 237-253.

Green, P.F., Duddy, I.R., Gleadow, A.J.W. and Lovering, J.F. (1989a) Apatite Fission Track Analysis as a paleotemperature indicator for hydrocarbon exploration. *In:* Naeser, N.D. and McCulloh, T. (eds.) *Thermal history of sedimentary basins - methods and case histories*, Springer-Verlag, New York, 181-195.

Green, P.F., Duddy, I.R., Laslett, G.M., Hegarty, K.A., Gleadow, A.J.W. and Lovering, J.F. (1989b) Thermal annealing of fission tracks in apatite 4. Quantitative modelling techniques and extension to geological timescales. *Chem. Geol. (Isot. Geosci. Sect.)*, 79, 155-182

Green, P.F., Laslett, G.M. and Duddy, I.R. (1993) Mechanisms and kinetics of apatite fission track annealing: Discussion. *American Mineralogist*, 78, 441-445.

Laslett, G.M., Kendall, W.S., Gleadow, A.J.W. and Duddy, I.R. (1982) Bias in measurement of fission track length distributions. *Nuclear Tracks*, 6, 79-85.

Laslett, G.M., Green, P.F., Duddy, I.R. and Gleadow, A.J.W. (1987) Thermal annealing of fission tracks in apatite 2. A quantitative analysis. *Chem. Geol. (Isot. Geosci. Sect.)*, 65, 1-13.

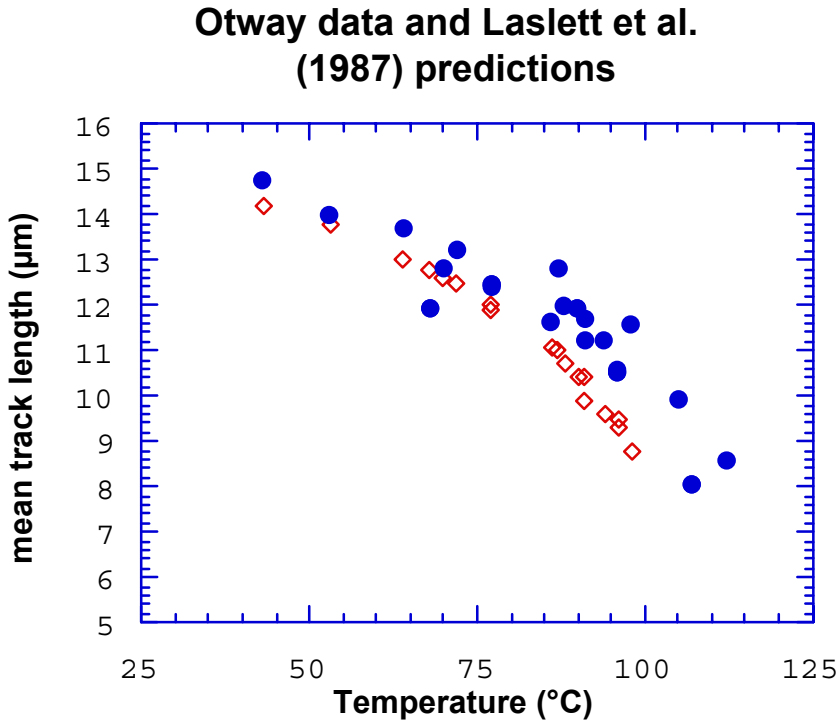

Figure C.1a Comparison of mean track length (solid circles) measured in samples from four Otway Basin reference wells (from Green et al, 1989a) and predicted mean track lengths (open diamonds) from the kinetic model of fission track annealing from Laslett et al. (1987). The predictions underestimate the measured values, but they refer to an apatite composition that is more easily annealed than the majority of apatites in these samples, so this is expected.

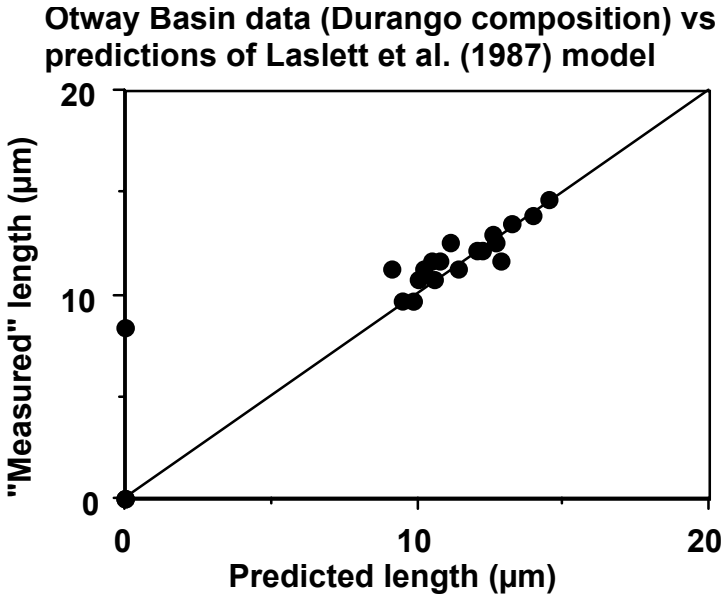

Figure C.1b Comparison of the mean track length in apatites of the same Cl content as Durango apatite from the Otway Group samples illustrated in figure C.1a, with values predicted for apatite of the same composition by the model of Laslett et al. (1987). The agreement is clearly very good except possibly at lengths below ~10 µm.

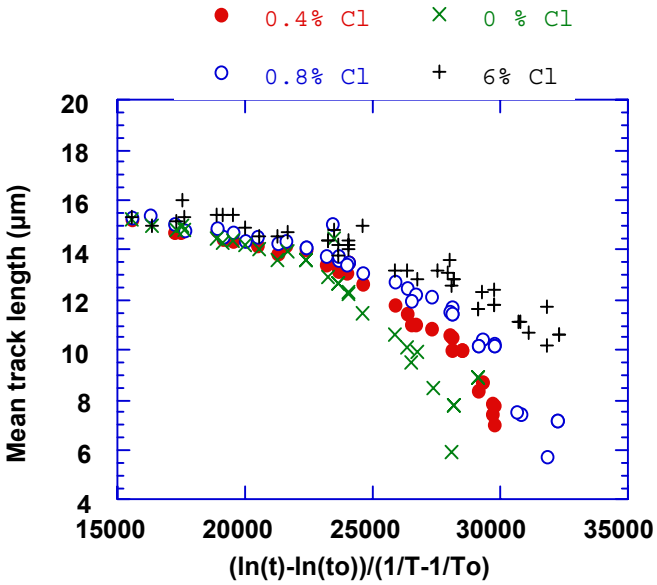

Figure C.2 Mean track length in apatites with four different chlorine contents, as a combined function of temperature and time, to reduce the data to a single scale. Fluorapatites are more easily annealed than chlorapatites, and the annealing kinetics show a progressive change with increasing Cl content.

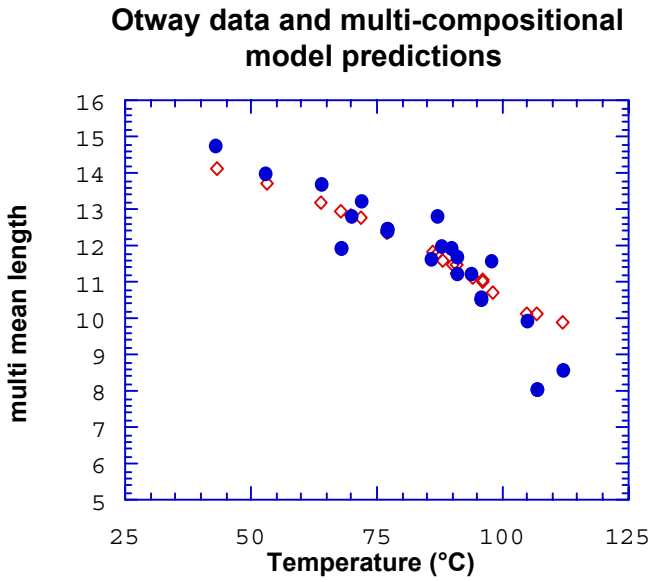

Figure C.3 Comparison of measured mean track length (solid circles) in samples from four Otway Basin reference wells (from Green et al, 1989a) and predicted mean track lengths (open diamonds) from the new multi-compositional kinetic model of fission track annealing described in Section C.3. This model takes into account the spread of Cl contents in apatites from the Otway Group samples and the influence of Cl content on annealing rate. The agreement is clearly very good over the range of the data.

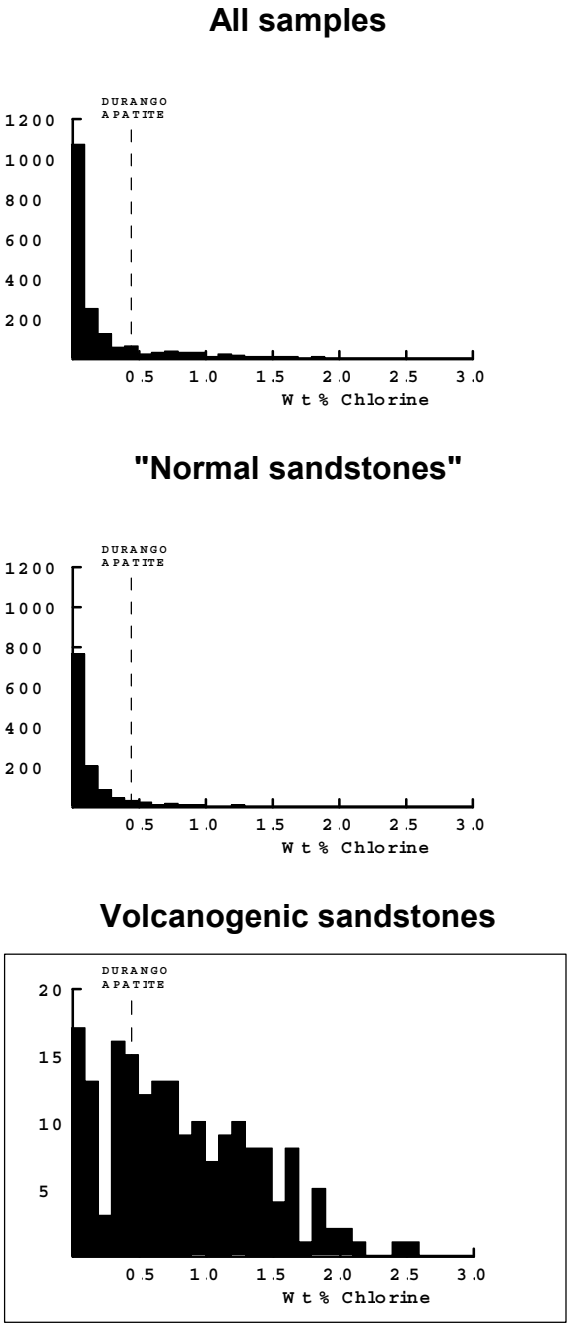

Figure C.4 **a:** Histogram of Cl contents (wt%) in over 1750 apatite grains from over 100 samples of various sedimentary and igneous rocks. Most samples give Cl contents below ~0.5 wt %, while those apatites giving higher Cl contents are characteristic of volcanogenic sandstones and basic igneous sources.

b: Histogram of Cl contents (wt%) in 1168 apatite grains from 61 samples which can loosely be characterised as "normal sandstone". The distribution is similar to that in the upper figure, except for a lower number of grains with Cl contents greater than ~1%.

c: Histogram of Cl contents (wt%) in 188 apatite grains from 15 samples of volcanogenic sandstone. The distribution is much flatter than the other two, with much higher proportion of Cl-rich grains.

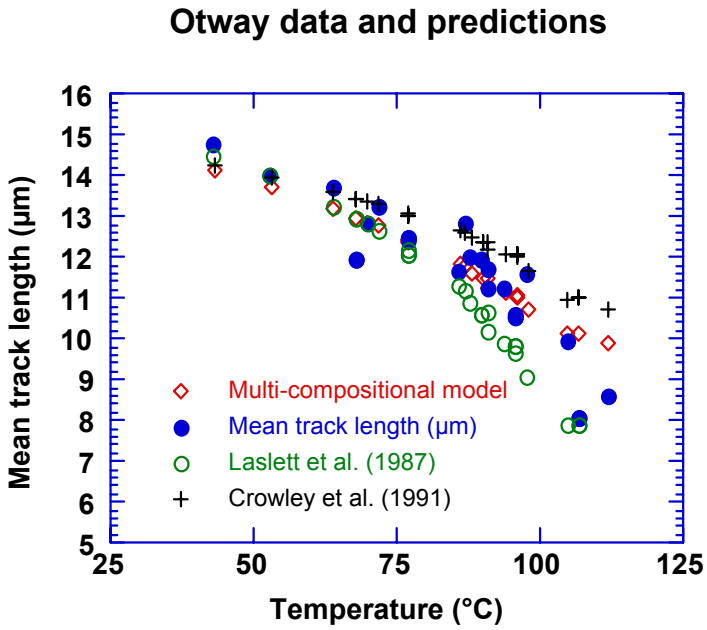

Figure C.5 Comparison of mean track length in samples from four Otway Basin reference wells (from Green et al, 1989a) and predicted mean track lengths from three kinetic models for fission track annealing. The Crowley et al. (1991) model relates to almost pure Fluorapatite (B-5), yet overpredicts mean lengths in the Otway Group samples which are dominated by Cl-rich apatites. The predictions of that model are therefore not reliable.

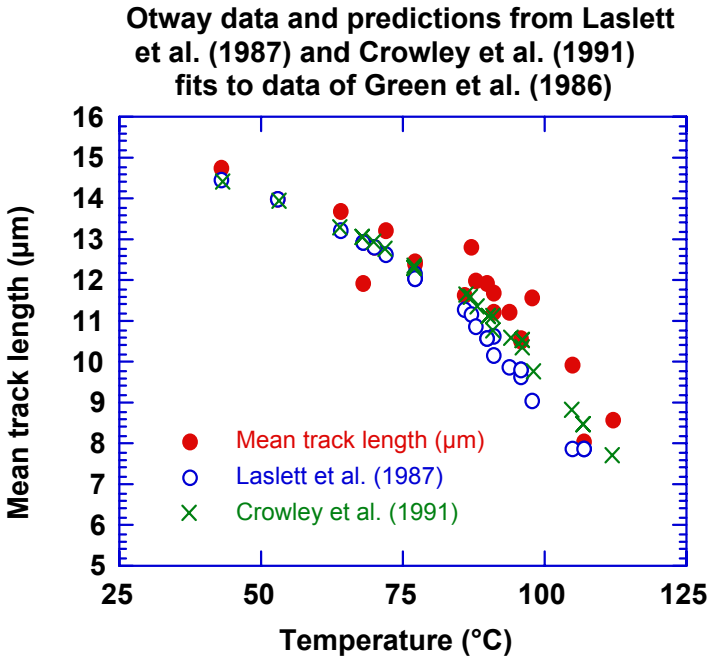

Figure C.6 Comparison of mean track length in samples from four Otway Basin reference wells with values predicted from Laslett et al. (1987) and the model fitted to the annealing data of Green et al. (1986) by Crowley et al. (1991). The predictions of the two models are not very different.

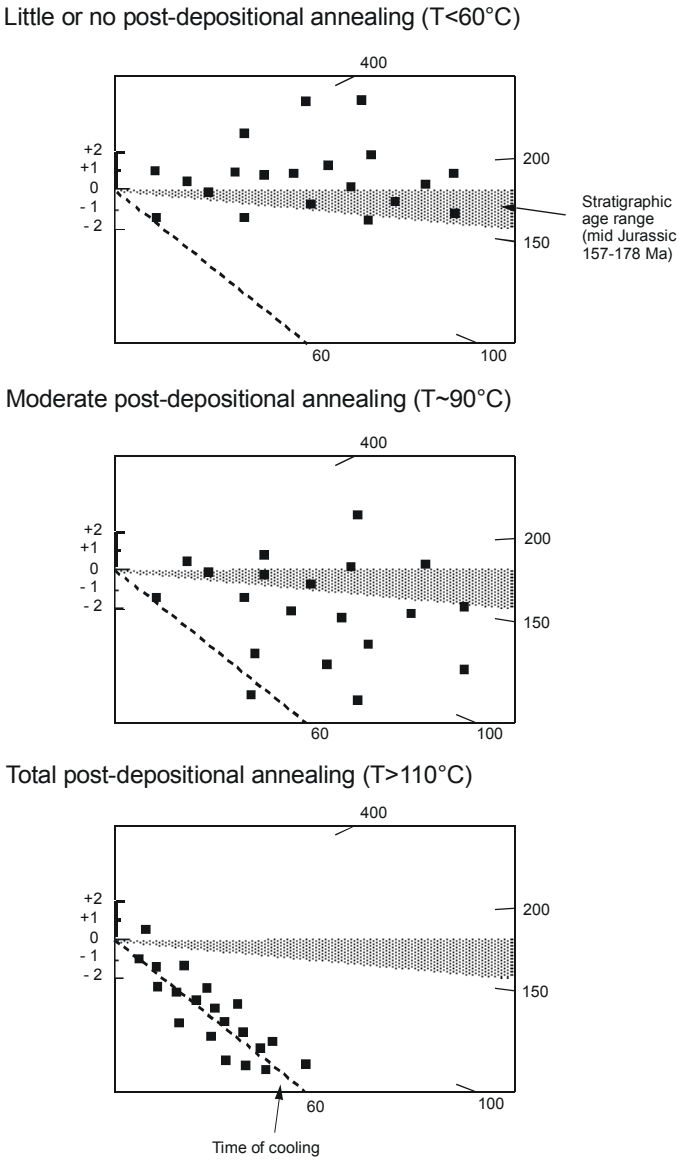

Figure C.7 Radial plots of single grain age data in three samples of mid-Jurassic sandstone that have been subjected to varying degrees of post-depositional annealing prior to cooling at ~60 Ma. The mid-point of the stratigraphic age range has been taken as the reference value (corresponding to the horizontal).

The upper diagram represents a sample which has remained at paleotemperatures less than ~60°C, and has therefore undergone little or no post-depositional annealing. All single grain ages are either compatible with the stratigraphic age (within y = ±2 in the radial plot) or older than the stratigraphic age ($y_i > 2$).

The centre diagram represents a sample which has undergone a moderate degree of post-depositional annealing, having reached a maximum paleotemperature of around ~90°C prior to cooling. While some of the individual grain ages are compatible with the stratigraphic age ($-2 < y_i < +2$) and some may be significantly greater than the stratigraphic age ($y_i > 2$), a number of grains give ages which are significantly less than the stratigraphic age ($y < 2$).

The lower diagram represents a sample in which all apatite grains were totally annealed, at paleotemperatures greater than ~110°C, prior to rapid cooling at ~60 Ma. All grains give fission track ages compatible with a fission track age of ~60 Ma (i.e., all data plot within ±2 of the radial line corresponding to an age of ~60 Ma), and most are significantly younger than the stratigraphic age.

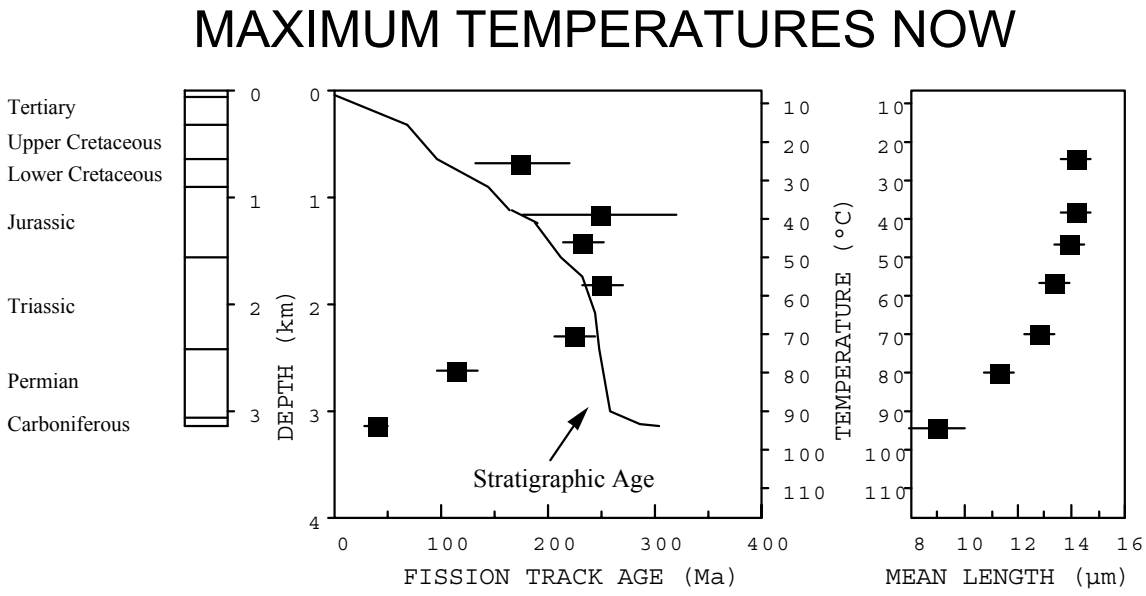

Figure C.8a Typical pattern of AFTA parameters in a well in which samples throughout the entire section are currently at their maximum temperatures since deposition. Both the fission track age and mean track length undergo progressive reduction to zero at temperatures of ~100 - 110°C, the actual value depending on the range of apatite compositions present.

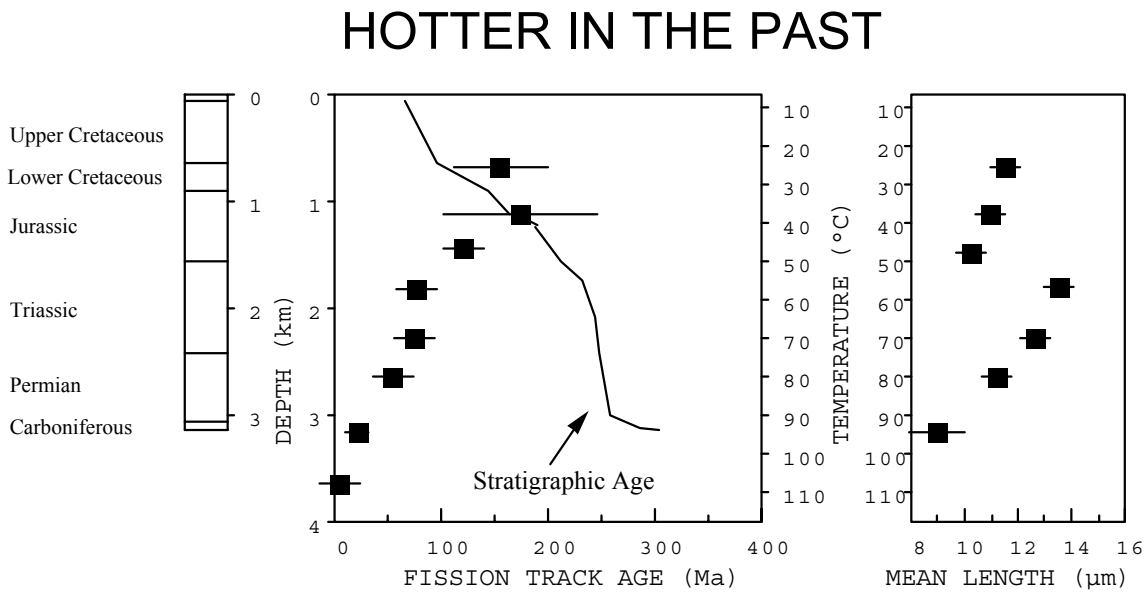

Figure C.8b Typical pattern of AFTA parameters in a well in which samples throughout the section were exposed to elevated paleotemperatures after deposition (prior to cooling in the Early Tertiary, in this case). Both the fission track age and mean track length show more reduction at temperatures of ~40 to 50°C than would be expected at such temperatures. At greater depths (higher temperatures), the constancy of fission track age and the increase in track length are both diagnostic of exposure to elevated paleotemperatures. See Appendix C for further discussion

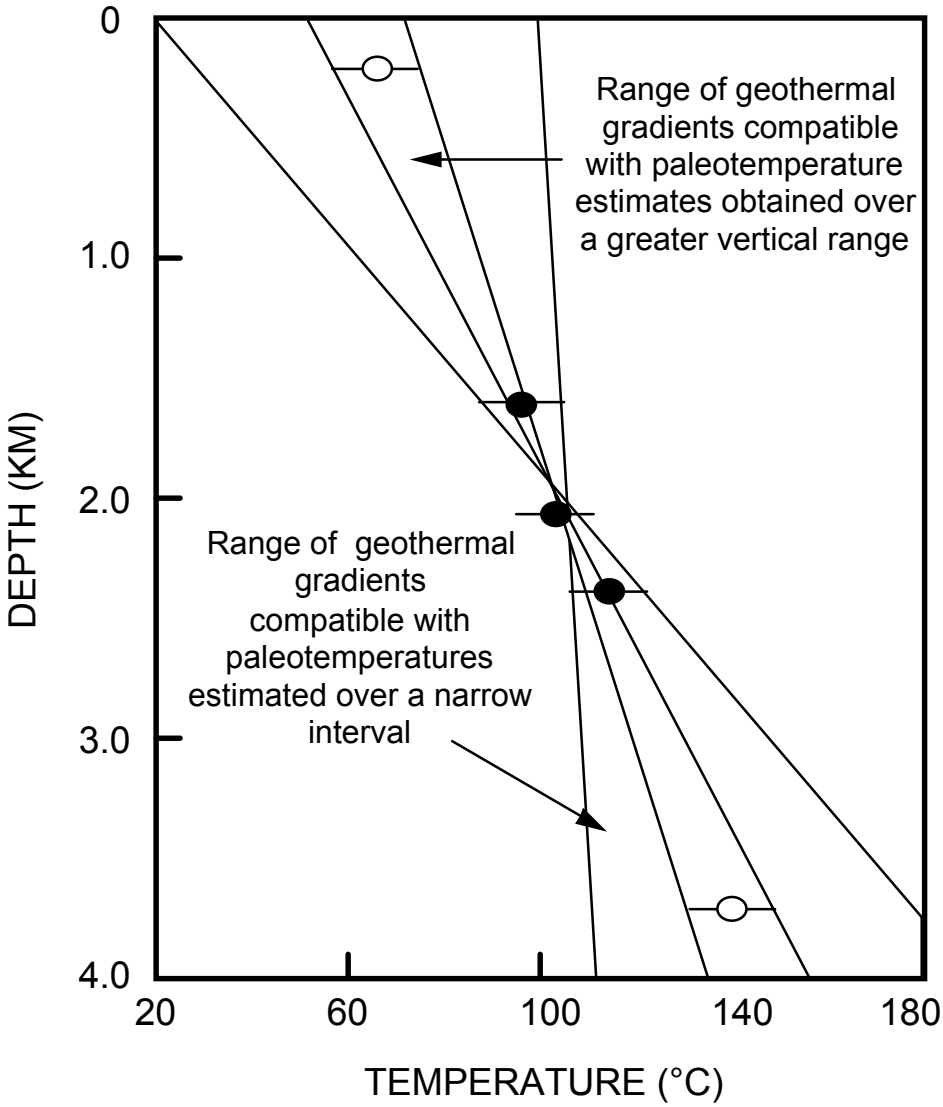

Figure C.9 It is important to obtain paleotemperature constraints over as great a range of depths as possible in order to provide a reliable estimate of paleogeothermal gradient. If paleotemperatures are only available over a narrow depth range, then the paleogeothermal gradient can only be very loosely constrained.

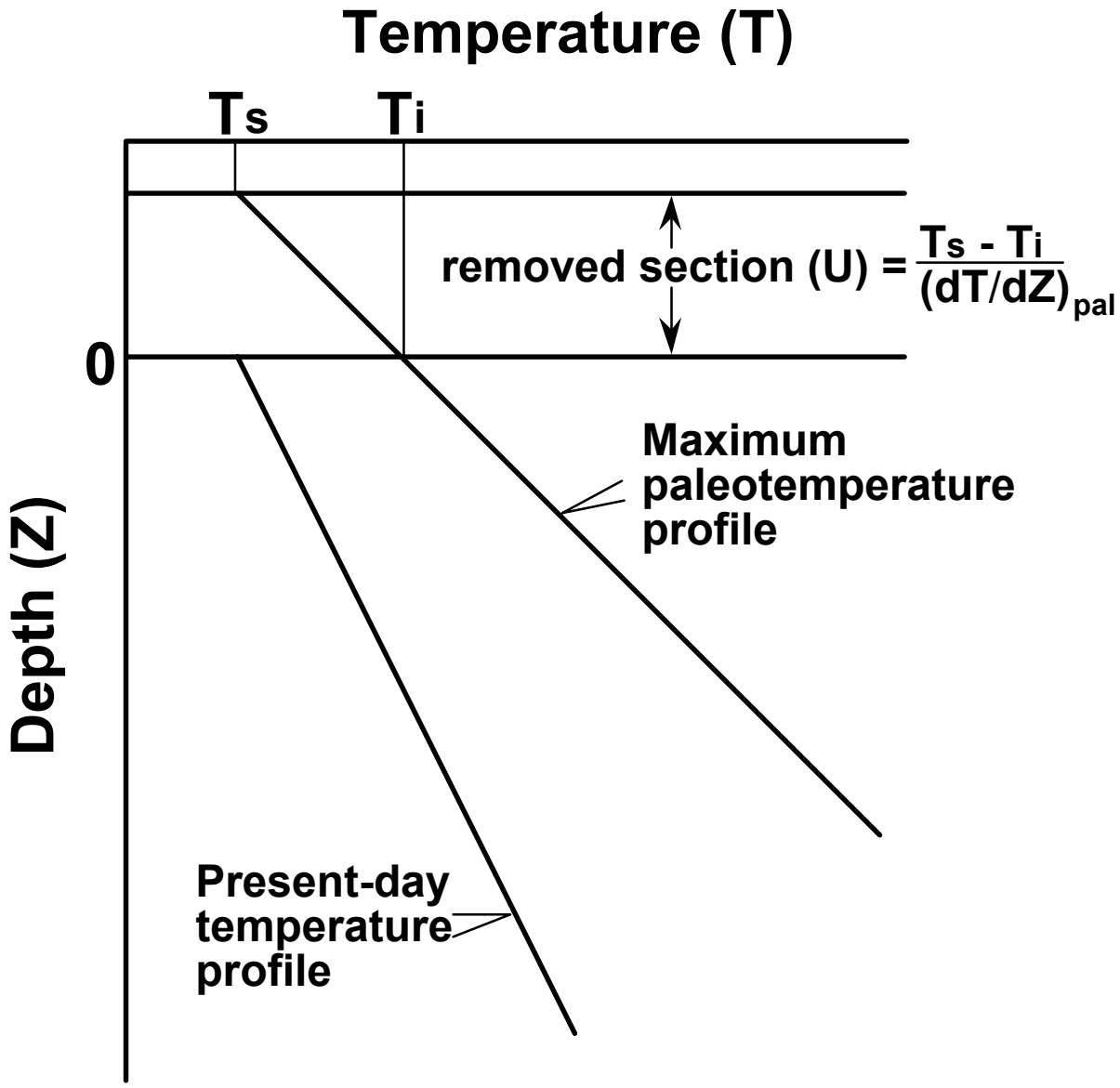

Figure C.10 If the paleogeothermal gradient can be constrained by AFTA and VR, as explained in the text, then for an assumed value of surface temperature, T_S, the amount of section removed can be estimated, as shown.

APPENDIX D

Vitrinite Reflectance Measurements

D.1 New vitrinite reflectance determinations

New vitrinite reflectance data were collected as part of this study, with details of determinations described in sections D.1 and D.2 below. In addition, further vitrinite reflectance data were supplied by the client, as summarised in section D.3.

Samples

Samples were submitted for vitrinite reflectance determination to Keiraville Konsultants, Australia. Results and sample details are summarised in Table D.2, while supporting data, including maceral descriptions and raw data sheets, are presented in the following pages.

Equipment

Leitz MPV1.1 photometer equipped with separate fluorescence illuminator, Swift point counter. Reflectance standards: spinel 0.42%, YAG 0.91%, GGG 1.72%, SiC standard for cokes and masked uranyl glass for measurement of intensity (I) in fluorescence mode. With the Keiraville Konsultants equipment, it is possible to alternate from reflectance to fluorescence mode to check for associated fluorescing liptinite, or importantly with some samples, to check for bitumen impregnation, or the presence, intensity, and source of oil-cut.

Sample preparation

Samples are normally mounted in cold setting polyester resin and polished using Cr_2O_3 and MgO polishing powders. Epoxy resins or araldite can be used if required. "Whole rock" samples are normally used but demineralisation can be undertaken. Large samples of coals and cokes can be mounted and examined.

Vitrinite Reflectance measurement

The procedure used generally follows Australian Standard (AS) 2486, but has been slightly modified for use with dispersed organic matter (DOM). For each sample, a minimum of 25 fields is measured (the number may be less if vitrinite is rare or if a limited number of particles of vitrinite is supplied, as may be the case with hand-picked

samples). If wide dispersal of vitrinite reflectances is found, the number of readings (N) is increased until a stable mean is obtained.

Vitrinite identification is made primarily on textural grounds, and this allows an independent assessment to be made of cavings and re-worked vitrinite populations. Histograms are only used for population definition when a cavings population significantly overlaps the range of the indigenous population. Where such data provides additional information, the mean maximum reflectance of inertinite and/or the mean maximum reflectance of liptinite (exinite) is reported. For each field, the maximum reflectance position is located and the reading recorded. The stage is then rotated by 180° which should give the same reading. In practice, the readings are seldom identical because of stage run-out and slight surface irregularities. If the readings are within ±5% relative, they are accepted. If not, the cause of the difference is sought and the results rejected. The usual source of differences is surface relief. The measurement of both maxima results in a total of 50 measurements being taken for the 25 fields reported. Thus, the 50 readings consist of 25 pairs of closely spaced readings which provide a check on the levelling of the surface and hence additional precision.

As the vitrinite reflectance measurements are being made, the various features of the samples are noted on a check sheet to allow a sample description to be compiled. When the reflectance measurements are complete, a thorough check is made of liptinite fluorescence characteristics. At the same time, organic matter abundance is estimated using a global estimate, a grain count method or point count method as required.

Data presentation

Individual sample results are reported in the following format:

KK No.	Depth (ft)	$\overline{R}_V$max*1	Range*2	N*3
x10324	3106	0.79	0.64 - 0.91	25

*1 Mean of all the maximum reflectance readings obtained.

*2 Lowest Rmax and highest Rmax of the population considered to represent the first generation vitrinite population.

*3 Number of fields measured (Number of measurements = 2N because 2 maximum values are recorded for each field)

Methods - Organic matter abundance and type.

After completion of vitrinite reflectance readings, the microscope is switched to fluorescence-mode and an estimate made of the abundance of each liptinite maceral. Fluorescence colours are also noted (BG 3 long UV excitation, TK400 dichroic mirror and a K490 barrier filter). The abundances are estimated using comparison charts. The categories used for liptinite (and other components) are:

Descriptor	%	Source potential
Absent	0	None
Rare	<0.1	Very poor
Sparse	0.1<x<0.5	Poor to fair
Common	0.5<x<2.0	Fair to good
Abundant	2.0<x<10.0	Good to very good
Major	10.0<x<40.0	Very good (excellent if algal)
Dominant	>40.0	Excellent

Dispersed Organic Matter (DOM) composition

At the same time as liptinite abundances are estimated, total DOM, vitrinite and inertinite abundances are estimated and reported in the categories listed above. Liptinite (exinite) fluorescence intensity and colour, lithology and a brief description of organic matter type and abundance are also recorded in a further column. Coal is described separately from dispersed organic matter (DOM). These data can be used to estimate the specific yield of the DOM and form a valuable adjunct to TOC data.

Lithological composition

The lithological abundances are ranked. For cuttings, these data can be useful in conjunction with geophysical logs in assessing the abundance and nature of cavings. For cores, it provides a record of the lithology examined and of the lithological associations of the organic matter.

Coal abundance and composition

Where coals are present, their abundance is recorded and their composition is reported as microlithotypes thus:

Coal major, **V**itrinite>**I**nertinite>**E**xinite, Clarodurite>vitrite>clarite>inertite.

These data give an approximate maceral composition and information about the organic facies of the coal. Where coal is a major or dominant component, and more precise maceral composition data are required, point count analyses should be requested. However, the precision of the original sampling is commonly a limiting factor in obtaining better quality data.

Abundance factor analysis

Especially where cuttings samples are used, abundance factor analyses are used to obtain an assessment of the maceral assemblages in the various lithologies. This can be done by a combination analysis using a point counter, but a large number of categories is required, and the precision is low if DOM is less than about 10%. For an abundance factor analysis (for core, 50 microscope fields of view) we assess the abundance of DOM, coal and shaly coal in 50 grains. The data can be used to plot DOM and coal abundance profiles.

Analyst/Advisor: Professor A.C. Cook

Prior to transmittal of final results, all samples are examined and checked by A.C. Cook who has more than 30 years' experience of work on coals, cokes, source rocks and source rock maturation.

D.2 Integration of vitrinite reflectance data with AFTA

Vitrinite reflectance is a time-temperature indicator governed by a kinetic response in a similar manner to the annealing of fission tracks in apatite as described in Appendix C. In this study, vitrinite reflectance data are interpreted on the basis of the distributed activation energy model describing the evolution of VR with temperature and time described by Burnham and Sweeney (1989), as implemented in the BasinMod™ software package of Platte River Associates. In a considerable number of wells from around the world, in which AFTA has been used to constrain the thermal history, we have found that the Burnham and Sweeney (1989) model gives good agreement between predicted and observed VR data, in a variety of settings.

As in the case of fission track annealing, it is clear from the chemical kinetic description embodied in equation 2 of Burham and Sweeney (1989) that temperature is more important than time in controlling the increase of vitrinite reflectance. If the Burham and Sweeney (1989) distributed activation energy model is expressed in the form of an Arrhenius plot (a plot of the logarithm of time versus inverse absolute temperature),

then the slopes of lines defining contours of equal vitrinite reflectance in such a plot are very similar to those describing the kinetic description of annealing of fission tracks in Durango apatite developed by Laslett et al. (1987), which is used to interpret the AFTA data in this report. This feature of the two quite independent approaches to thermal history analysis means that for a particular sample, a given degree of fission track annealing in apatite of Durango composition will be associated with the same value of vitrinite reflectance regardless of the heating rate experienced by a sample. Thus paleotemperature estimates based on either AFTA or VR data sets should be equivalent, regardless of the duration of heating. As a guide, Table D.1 gives paleotemperature estimates for various values of VR for two different heating times.

One practical consequence of this relationship between AFTA and VR is, for example, that a VR value of 0.7% is associated with total annealing of all fission tracks in apatite of Durango composition, and that total annealing of all fission tracks in apatites of more Chlorine-rich composition is accomplished between VR values of 0.7 and ~0.9%.

Furthermore, because vitrinite reflectance continues to increase progressively with increasing temperature, VR data allow direct estimation of maximum paleotemperatures in the range where fission tracks in apatite are totally annealed (generally above ~110°C) and where therefore AFTA only provides minimum estimates. Maximum paleotemperature estimates based on vitrinite reflectance data from a well in which most AFTA samples were totally annealed will allow constraints on the paleogeothermal gradient that would not be possible from AFTA alone. In such cases the AFTA data should allow tight constraints to be placed on the time of cooling and also the cooling history, since AFTA parameters will be dominated by the effects of tracks formed after cooling from maximum paleotemperatures. Even in situations where AFTA samples were not totally annealed, integration of AFTA and VR can allow paleotemperature control over a greater range of depth, e.g. by combining AFTA from sand-dominated units with VR from other parts of the section, thereby providing tighter constraint on the paleogeothermal gradient.

D.3 Client-supplied vitrinite reflectance

Vitrinite reflectance and other data (if applicable) supplied by the client is summarised in Table D.3. Unless specified, this vitrinite reflectance data has been treated at face value, as if it were collected in the same manner as described for the new data, because detailed information is usually not available.

References

Burnham, A.K. and Sweeney, J.J. (1989). A chemical kinetic model of vitrinite reflectance maturation. *Geochim. et Cosmochim. Acta,* 53, 2649-2657.

Laslett, G.M., Green, P.F., Duddy, I.R. and Gleadow, A.J.W. (1987). Thermal annealing of fission tracks in apatite 2. A quantitative analysis. *Chem. Geol. (Isot. Geosci.Sect.)*, 65, 1-13.

Table D.1: Paleotemperature - vitrinite reflectance nomogram based on Equation 2 of Burnham and Sweeney (1989)

Paleotemperature (°C / °*F*)	Vitrinite Reflectance (%) 1 Ma Duration of heating	10 Ma Duration of heating
40 / *104*	0.29	0.32
50 / *122*	0.31	0.35
60 / *140*	0.35	0.40
70 / *158*	0.39	0.45
80 / *176*	0.43	0.52
90 / *194*	0.49	0.58
100 / *212*	0.55	0.64
110 / *230*	0.61	0.70
120 / *248*	0.66	0.78
130 / *266*	0.72	0.89
140 / *284*	0.81	1.04
150 / *302*	0.92	1.20
160 / *320*	1.07	1.35
170 / *338*	1.23	1.55
180 / *356*	1.42	1.80
190 / *374*	1.63	2.05
200 / *392*	1.86	2.33
210 / *410*	2.13	2.65
220 / *428*	2.40	2.94
230 / *446*	2.70	3.23

Table D.2: Vitrinite reflectance sample details and results - well samples from Otway Basin (Geotrack Report #876)

Sample number	Depth (m)	Sample type	Stratigraphic Subdivision	Stratigraphic age (Ma)	Present temperature *1 (°C)	VR (Range) %	N
Bridgewater Bay-1							
GC876-1.1	870	cuttings	Narrawaturk Marl	40-38	38	0.42 (0.33-0.57)	5
GC876-2.1	930-940	cuttings	Dilwyn Fm	54-50	40	-	
GC876-3.1	1110	cuttings	Dilwyn Fm	54-50	45	0.39 (0.29-0.49)	25
GC876-4.1	1200	cuttings	Pember Mdst	56-54	48	-	
GC876-5.1	1560	cuttings	Timboon Sst	77-64.5	59	0.40 (0.33-0.51)	10
GC876-6.1	1995	cuttings	Paaratte Fm	83-77	72	0.48 (0.37-0.61)	25
GC876-7.1	2120	cuttings	Paaratte Fm	83-77	76	-	
GC876-8.1	2595	cuttings	Paaratte Fm	83-77	90	0.57 (0.48-0.66)	25
GC876-9.1	2795	cuttings	Belfast Mdst	89-84	97	-	
GC876-10.1	3495	cuttings	Belfast Mdst	89-84	118	0.63 (0.54-0.72)	8
GC876-11.1	3885	cuttings	Belfast Mdst	89-84	130	-	

Note: Some samples may contain both vitrinite and inertinite. Only vitrinite data is shown.

*1 See Appendix A for discussion of present temperature data.

Table D.3: Vitrinite reflectance sample details and results; open file data - Otway Basin (Geotrack Report #876)

Source number	Depth (m)	Sample type	Stratigraphic Subdivision	Stratigraphic age (Ma)	Present temperature *1 (°C)	VR (Range) %	N
Bridgewater Bay-1							
33394	934-934		Dilwyn Fm	54-50	40	0.49 (0.40-0.57)	50
33393	1185-1185		Pember Mdst	56-54	47	0.52 (0.42-0.62)	48
33392	1318-1318		Timboon Sst	77-64.5	51	0.54 (0.45-0.63)	50
64618	1400-1400		Timboon Sst	77-64.5	54	0.36 (0.26-0.52)	25
33391	1522-1522		Timboon Sst	77-64.5	58	0.56 (0.46-0.66)	50
33390	1870-1870		Paaratte Fm	83-77	68	0.58 (0.47-0.69)	50
49990	2050-2050		Paaratte Fm	83-77	74	0.43 (0.32-0.62)	26
33389	2215-2215		Paaratte Fm	83-77	79	0.57 (0.50-0.67)	50
33388	2450-2450		Paaratte Fm	83-77	86	0.65 (0.52-0.74)	48
33386	2735-2735		Belfast Mdst	89-84	95	0.64 (0.54-0.77)	50
64619	2800-2800		Belfast Mdst	89-84	97	0.62 (0.46-0.77)	11
250579	2800		Belfast Mdst	89-84	97	0.56 (0.54-0.57)	2
250582	2850		Belfast Mdst	89-84	98	0.55 (0.54-0.57)	2
33379	3015-3015		Belfast Mdst	89-84	103	0.67 (0.57-0.77)	40
250584	3200		Belfast Mdst	89-84	109	0.52 (0.50-0.56)	3
33373	3295-3295		Belfast Mdst	89-84	112	0.70 (0.58-0.82)	51
64620	3500-3500		Belfast Mdst	89-84	118	0.80 (0.60-1.08)	28
33365	3640-3640		Belfast Mdst	89-84	122	0.80 (0.71-1.00)	77
250587	3640		Belfast Mdst	89-84	122	0.86 (0.71-1.00)	77
33351	3960-3960		Belfast Mdst	89-84	132	1.07 (0.92-1.20)	57

Table D.3: Continued

Source number	Depth (m)	Sample type	Stratigraphic Subdivision	Stratigraphic age (Ma)	Present temperature *1 (°C)	VR (Range) %	N
64621	4120-4120		Waare Fm	92-90	137	1.10 (0.79-1.22)	8
33353	4175-4175		Waare Fm	92-90	139	1.29 (1.16-1.40)	52

Note: Some samples may contain both vitrinite and inertinite. Only vitrinite data is shown.

*1 See Appendix A for discussion of present temperature data.

OTWAY BASIN

GC876

BRIDGEWATER BAY-1, p1

KK # / Ref #.	Depth (m) /Type	$\overline{R}_{vmax}$	Range	N	Sample description including liptinite fluorescence, maceral abundances, mineral fluorescence
					NARRAWATURK MARL
T9148	870	0.42	0.33-0.57	5	Rare lamalginite and liptodetrinite yellow to orange. (Carbonate
1.1	$\overline{R}_{Imax}$	1.31	0.80-1.94	14	>calcareous siltstone>sandstone. Dom rare, I>L>V. All three
Ctgs					maceral groups rare. Common foraminiferal tests. Mineral fluorescence moderate orange. Glauconite rare. Iron oxides rare. Pyrite sparse.)
					DILWYN FORMATION
T9149	930-940				Relatively barren sandstone with some carbonate.
T9150	1110	0.39	0.29-0.49	25	Sparse lamalginite and rare liptodetrinite yellow to orange, rare
3.1	$\overline{R}_{Imax}$	0.99	0.86-1.14	3	sporinite yellow to orange, rare cutinite, orange. (Artificial
Ctgs					composites>argillaceous siltstone>sandstone. Dom common, V>L>I. Vitrinite and liptinite sparse, inertinite rare. sparse foraminiferal tests. Mineral fluorescence weak dull orange. . Iron oxides abundant. Pyrite common, locally abundant.)
					PEMBER MEMBER
T9051	1200				Siltstone with sparse dom, but sparse yellow oil drops and the mounting resin shows very strong fluorescence presumably due to extraction of oil-like material from the sediment.
					TIMBOON SANDSTONE
T9152	1560	0.40	0.33-0.51	10	Rare lamalginite and liptodetrinite yellow to orange, rare
5.1	$\overline{R}_{Imax}$	1.23	0.76-2.46	20	sporinite orange. (Sandstone>>argillaceous siltstone>carbonate.
Ctgs					Dom rare to sparse, I>V>L. Inertinite rare to sparse, vitrinite and liptinite rare. Mineral fluorescence mostly none, weak dull orange in fine grained sediments and in clay matrix. . Iron oxides rare. Pyrite common, locally abundant.)
					PAARATTE FORMATION
T9153	1995	0.48	0.37-0.61	25	Rare lamalginite and liptodetrinite yellow to orange, rare
6.1	$\overline{R}_{Imax}$	1.24	0.92-2.12	20	sporinite dull orange, rare cutinite orange. (Argillaceous
Ctgs					siltstone>sandstone>carbonate. Dom common, I>V>L. Inertinite common, vitrinite rare to sparse, liptinite rare. Rare greenish yellow fluorescing oil droplets in siltstone. Rare dull orange fluorescing bitumen. Mineral fluorescence weak dull orange in fine grained sediments and clay matrix, none in quartz grains. . Iron oxides abundant. Pyrite sparse.)
T9054	2120				Similar lithology to sample 9153, but more ferruginous. Organic matter sparse and mainly comprises inertinite.
T9155	2595	0.57	0.48-0.66	25	Rare lamalginite and liptodetrinite yellow to orange, rare
8.1	$\overline{R}_{Imax}$	1.40	1.02-1.78	20	sporinite orange. Claystone>argillaceous siltstone> artificial
Ctgs					composites. Dom common, I>V>L. Inertinite common, vitrinite and liptinite rare. Mineral fluorescence moderate to weak orange. Iron oxides abundant. Pyrite common.)
					BELFAST MUDSTONE
T9056	2795				Sample consists mainly of artificial composites with minor claystones and siltstones. Organic matter is sparse. Inertinite sparse and vitrinite and liptinite rare.

OTWAY BASIN

GC876

BRIDGEWATER BAY-1, p2

KK # / Ref #.	Depth (m) /Type	$\overline{R}_{v\max}$	Range	N	Sample description including liptinite fluorescence, maceral abundances, mineral fluorescence
					BELFAST MUDSTONE
T9157	3495	0.63	0.54-0.72	8	Rare lamalginite and liptodetrinite orange to dull orange.
10.1 Ctgs	$\overline{R}_{I\max}$	1.59	1.00-2.18	20	(Artificial composites>>siltstone>claystone. Dom common, I>>V>L. Inertinite common, vitrinite and liptinite rare. Artificial composites were ignored when assessing the maceral abundance. Mineral fluorescence patchy weak to moderate orange. Glauconite rare. Iron oxides rare. Pyrite sparse.)
T9058	3885				Over 90% of the sample comprise of artificial composites. Representative lithologies are rare and consists mainly of siltstones. Organic matter rare.

The alternate samples were mounted and examined briefly. Short notes are given on each alternate sample for completeness.

The upper part of the section is immature and the top of the oil window can be estimated to occur at between about 2100 m and 2200 m. The deepest sample measured indicates that the Belfast Mudstone is mid mature. The deeper sample was not examined in detail, but was unlikely to yield useful data because of the dominance of artificial composites and some of these resemble turbo-drill cuttings.

Source potential tends to be fair at best.

ACC 28 May 2003

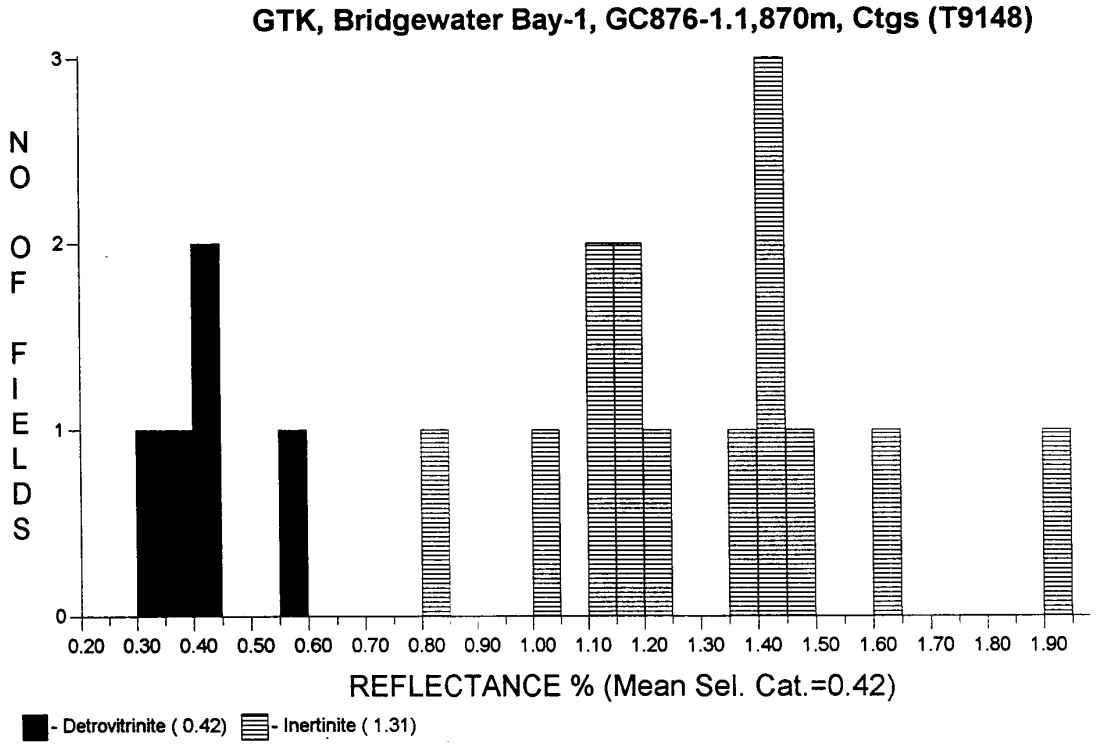
GTK, Bridgewater Bay-1, GC876-1.1,870m, Ctgs (T9148)
NO OF FIELDS
0
1
2
3
0.20 0.30 0.40 0.50 0.60 0.70 0.80 0.90 1.00 1.10 1.20 1.30 1.40 1.50 1.60 1.70 1.80 1.90
REFLECTANCE % (Mean Sel. Cat.=0.42)
- Detrovitrinite (0.42)
- Inertinite (1.31)

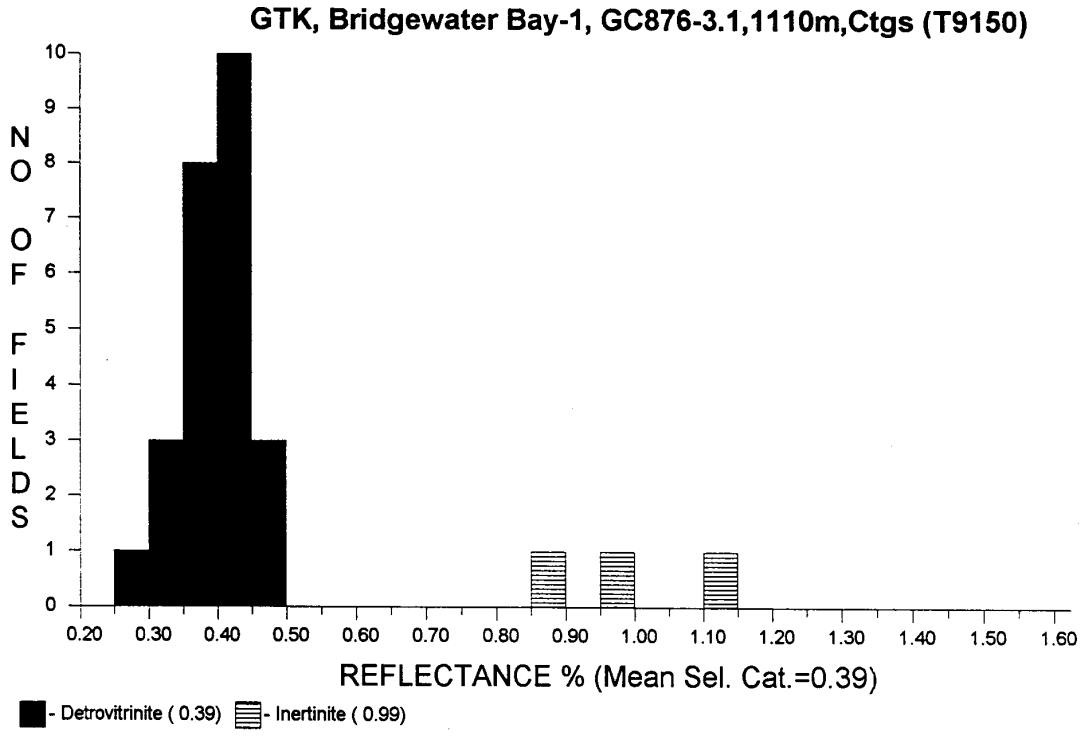
GTK, Bridgewater Bay-1, GC876-3.1,1110m,Ctgs (T9150)
NO OF FIELDS
0
1
2
3
4
5
6
7
8
9
10
0.20 0.30 0.40 0.50 0.60 0.70 0.80 0.90 1.00 1.10 1.20 1.30 1.40 1.50 1.60
REFLECTANCE % (Mean Sel. Cat.=0.39)
- Detrovitrinite (0.39)
- Inertinite (0.99)

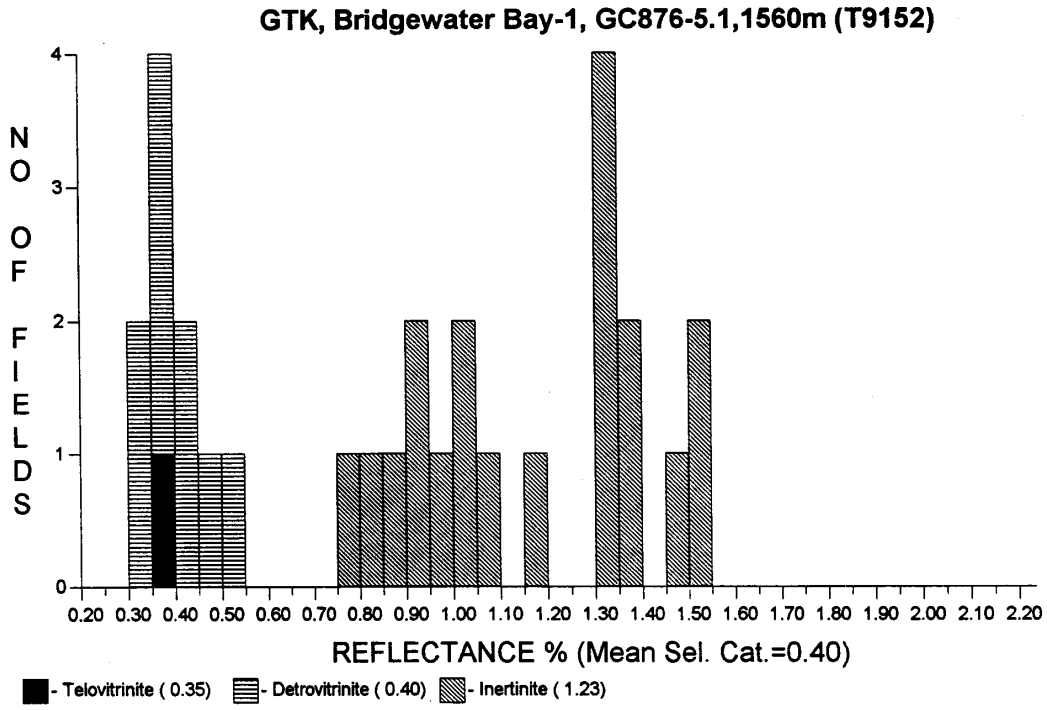
GTK, Bridgewater Bay-1, GC876-5.1,1560m (T9152)
NO OF FIELDS
0
1
2
3
4
0.20 0.30 0.40 0.50 0.60 0.70 0.80 0.90 1.00 1.10 1.20 1.30 1.40 1.50 1.60 1.70 1.80 1.90 2.00 2.10 2.20
REFLECTANCE % (Mean Sel. Cat.=0.40)
- Telovitrinite (0.35)
- Detrovitrinite (0.40)
- Inertinite (1.23)

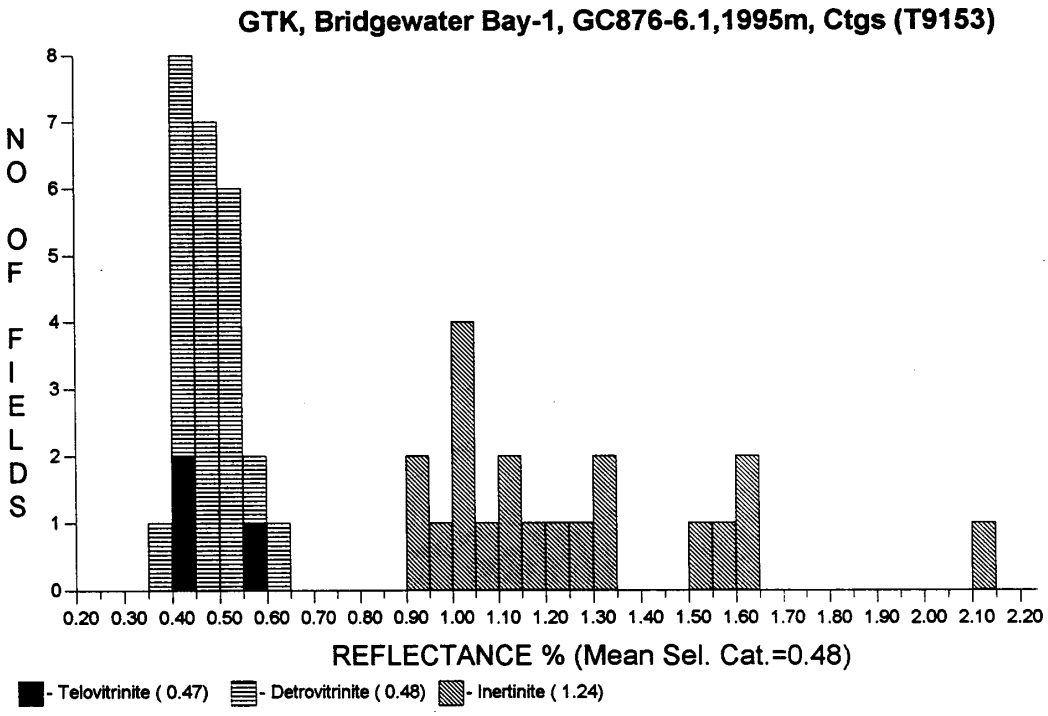
GTK, Bridgewater Bay-1, GC876-6.1,1995m, Ctgs (T9153)
NO OF FIELDS
0
1
2
3
4
5
6
7
8
0.20 0.30 0.40 0.50 0.60 0.70 0.80 0.90 1.00 1.10 1.20 1.30 1.40 1.50 1.60 1.70 1.80 1.90 2.00 2.10 2.20
REFLECTANCE % (Mean Sel. Cat.=0.48)
- Telovitrinite (0.47)
- Detrovitrinite (0.48)
- Inertinite (1.24)

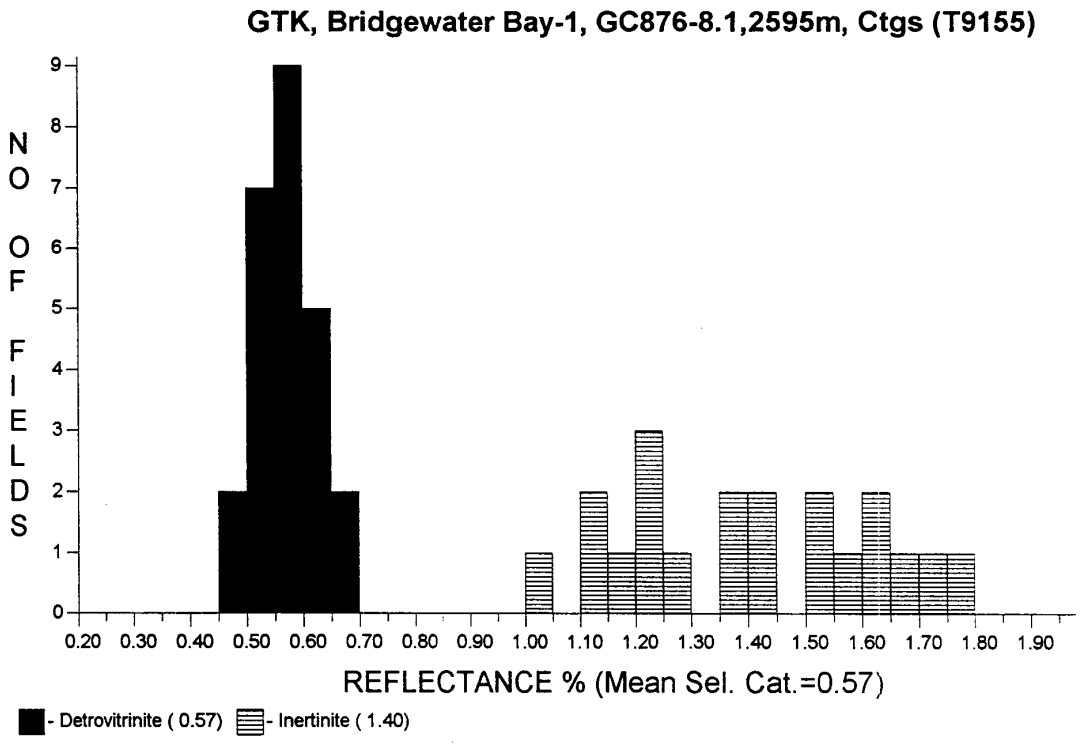
GTK, Bridgewater Bay-1, GC876-8.1,2595m, Ctgs (T9155)
NO OF FIELDS
0
1
2
3
4
5
6
7
8
9
0.20 0.30 0.40 0.50 0.60 0.70 0.80 0.90 1.00 1.10 1.20 1.30 1.40 1.50 1.60 1.70 1.80 1.90
REFLECTANCE % (Mean Sel. Cat.=0.57)
- Detrovitrinite (0.57)
- Inertinite (1.40)

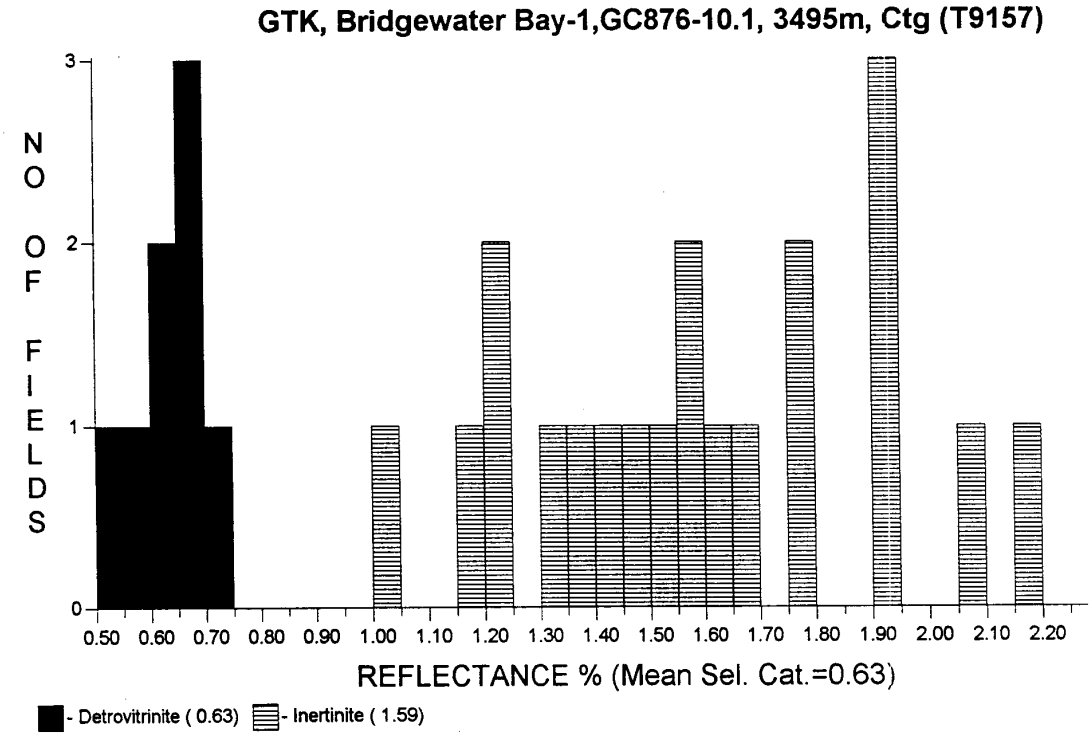
GTK, Bridgewater Bay-1,GC876-10.1, 3495m, Ctg (T9157)
NO OF FIELDS
0
1
2
3
0.50 0.60 0.70 0.80 0.90 1.00 1.10 1.20 1.30 1.40 1.50 1.60 1.70 1.80 1.90 2.00 2.10 2.20
REFLECTANCE % (Mean Sel. Cat.=0.63)
- Detrovitrinite (0.63)
- Inertinite (1.59)

R	No Read	Pop Range	R	No Read	Pop Range	R	No Read	Pop Range	R	No Read	Pop Range	R	No Read	Pop Range	R	No Read	Pop Range	R	No Read	Pop Range	R	No Read	Pop Range	R	No Read	Pop Range
0.10			0.40	1		0.70			1.00	1		1.30			1.60			1.90			2.20			2.50		
0.11			0.41	1		0.71			1.01			1.31			1.61			1.91			2.21			2.51		
0.12			0.42			0.72			1.02			1.32			1.62	1		1.92			2.22			2.52		
0.13			0.43			0.73			1.03			1.33			1.63			1.93		Inert	2.23			2.53		
0.14			0.44			0.74			1.04			1.34			1.64			1.94	1	↓	2.24			2.54		
0.15			0.45			0.75			1.05			1.35			1.65			1.95			2.25			2.55		
0.16			0.46			0.76			1.06			1.36			1.66			1.96			2.26			2.56		
0.17			0.47			0.77			1.07			1.37			1.67			1.97			2.27			2.57		
0.18			0.48			0.78			1.08			1.38	1		1.68			1.98			2.28			2.58		
0.19			0.49			0.79			1.09			1.39			1.69			1.99			2.29			2.59		
0.20			0.50			0.80	1	↑	1.10	1		1.40	1		1.70			2.00			2.30			2.60		
0.21			0.51			0.81		Inert	1.11			1.41			1.71			2.01			2.31			2.61		
0.22			0.52			0.82			1.12			1.42	2		1.72			2.02			2.32			2.62		
0.23			0.53			0.83			1.13			1.43			1.73			2.03			2.33			2.63		
0.24			0.54			0.84			1.14	1		1.44			1.74			2.04			2.34			2.64		
0.25			0.55			0.85			1.15			1.45			1.75			2.05			2.35			2.65		
0.26			0.56		FGV	0.86			1.16			1.46	1		1.76			2.06			2.36			2.66		
0.27			0.57	1	↓	0.87			1.17			1.47			1.77			2.07			2.37			2.67		
0.28			0.58			0.88			1.18	2		1.48			1.78			2.08			2.38			2.68		
0.29			0.59			0.89			1.19			1.49			1.79			2.09			2.39			2.69		
0.30			0.60			0.90			1.20			1.50			1.80			2.10			2.40			2.70		
0.31			0.61			0.91			1.21			1.51			1.81			2.11			2.41			2.71		
0.32			0.62			0.92			1.22			1.52			1.82			2.12			2.42			2.72		
0.33	1	↑	0.63			0.93			1.23			1.53			1.83			2.13			2.43			2.73		
0.34		FGV	0.64			0.94			1.24	1		1.54			1.84			2.14			2.44			2.74		
0.35			0.65			0.95			1.25			1.55			1.85			2.15			2.45			2.75		
0.36			0.66			0.96			1.26			1.56			1.86			2.16			2.46			2.76		
0.37			0.67			0.97			1.27			1.57			1.87			2.17			2.47			2.77		
0.38	1		0.68			0.98			1.28			1.58			1.88			2.18			2.48			2.78		
0.39			0.69			0.99			1.29			1.59			1.89			2.19			2.49			2.79		

VITRINITE <0.1%		INERTINITE <0.1%						LIPTINITE <0.1%								OIL DROPS	BITUMEN
TV	DV	Sfus	Scler	Fus	Macr	ID	Micr	Spor	Cut	Sub	Res	Ld <0.1	Bituminite	Telalginite	Lamalginite <0.1	Oil cut	

Sample Number..T9148....Well Name..GTK...BRIDGEWATER BAY-1, GC876-1.1.....Narrawaturk Marl..... Depth...870m..... ..... SampleType....Ctgs...
Date. ..25/.05/ 2003.. Op..SPR..... FGV - First Generation Vitrinite, RV - Reworked Vitrinite, BTT - Bituminite, B - Bitumen, Inert - Inertinite, Cav - Cavings, DA - Drilling Mud Additives MICR D:\RWORK.ms6\876VRW.doc

R	No Read	Pop Range	R	No Read	Pop Range	R	No Read	Pop Range	R	No Read	Pop Range	R	No Read	Pop Range	R	No Read	Pop Range	R	No Read	Pop Range	R	No Read	Pop Range	R	No Read	Pop Range
0.10			0.40	2		0.70			1.00			1.30			1.60			1.90			2.20			2.50		
0.11			0.41	3		0.71			1.01			1.31			1.61			1.91			2.21			2.51		
0.12			0.42	3		0.72			1.02			1.32			1.62			1.92			2.22			2.52		
0.13			0.43			0.73			1.03			1.33			1.63			1.93			2.23			2.53		
0.14			0.44	2		0.74			1.04			1.34			1.64			1.94			2.24			2.54		
0.15			0.45			0.75			1.05			1.35			1.65			1.95			2.25			2.55		
0.16			0.46	1		0.76			1.06			1.36			1.66			1.96			2.26			2.56		
0.17			0.47	1		0.77			1.07			1.37			1.67			1.97			2.27			2.57		
0.18			0.48		FGV	0.78			1.08			1.38			1.68			1.98			2.28			2.58		
0.19			0.49	1	↓	0.79			1.09			1.39			1.69			1.99			2.29			2.59		
0.20			0.50			0.80			1.10			1.40			1.70			2.00			2.30			2.60		
0.21			0.51			0.81			1.11			1.41			1.71			2.01			2.31			2.61		
0.22			0.52			0.82			1.12			1.42			1.72			2.02			2.32			2.62		
0.23			0.53			0.83			1.13		Inert	1.43			1.73			2.03			2.33			2.63		
0.24			0.54			0.84			1.14	1	↓	1.44			1.74			2.04			2.34			2.64		
0.25			0.55			0.85			1.15			1.45			1.75			2.05			2.35			2.65		
0.26			0.56			0.86	1	↑	1.16			1.46			1.76			2.06			2.36			2.66		
0.27			0.57			0.87		Inert	1.17			1.47			1.77			2.07			2.37			2.67		
0.28			0.58			0.88			1.18			1.48			1.78			2.08			2.38			2.68		
0.29	1	↑	0.59			0.89			1.19			1.49			1.79			2.09			2.39			2.69		
0.30		FGV	0.60			0.90			1.20			1.50			1.80			2.10			2.40			2.70		
0.31			0.61			0.91			1.21			1.51			1.81			2.11			2.41			2.71		
0.32			0.62			0.92			1.22			1.52			1.82			2.12			2.42			2.72		
0.33	2		0.63			0.93			1.23			1.53			1.83			2.13			2.43			2.73		
0.34	1		0.64			0.94			1.24			1.54			1.84			2.14			2.44			2.74		
0.35	2		0.65			0.95			1.25			1.55			1.85			2.15			2.45			2.75		
0.36	1		0.66			0.96	1		1.26			1.56			1.86			2.16			2.46			2.76		
0.37	2		0.67			0.97			1.27			1.57			1.87			2.17			2.47			2.77		
0.38	3		0.68			0.98			1.28			1.58			1.88			2.18			2.48			2.78		
0.39			0.69			0.99			1.29			1.59			1.89			2.19			2.49			2.79		

VITRINITE 0.4%		INERTINITE <0.1%						LIPTINITE 0.3%								OIL DROPS	BITUMEN
TV	DV	Sfus	Scler	Fus	Macr	ID	Micr	Spor <0.1	Cut	Sub	Res	Ld <0.1	Bituminite	Telalginite	Lamalginite 0.3	Oil cut	

Sample Number..T9150....Well Name..GTK...BRIDGEWATER BAY-1, GC876-3.1.....Narrawaturk Marl..... Depth...1110m..... ..... SampleType....Ctgs...
Date. ..25/.05/ 2003.. Op..SPR..... FGV - First Generation Vitrinite, RV - Reworked Vitrinite, BTT - Bituminite, B - Bitumen, Inert - Inertinite, Cav - Cavings, DA - Drilling Mud Additives MICR D:\RWORK.ms6\876VRW.doc

R	No Read	Pop Range	R	No Read	Pop Range	R	No Read	Pop Range	R	No Read	Pop Range	R	No Read	Pop Range	R	No Read	Pop Range	R	No Read	Pop Range	R	No Read	Pop Range	R	No Read	Pop Range
0.10			0.40	1		0.70			1.00	1		1.30	1		1.60			1.90			2.20			2.50		
0.11			0.41			0.71			1.01			1.31			1.61			1.91			2.21			2.51		
0.12			0.42	1		0.72			1.02	1		1.32			1.62			1.92			2.22			2.52		
0.13			0.43			0.73			1.03			1.33			1.63			1.93			2.23			2.53		
0.14			0.44			0.74			1.04			1.34	3		1.64			1.94			2.24			2.54		
0.15			0.45			0.75			1.05			1.35			1.65			1.95			2.25			2.55		
0.16			0.46			0.76	1	↑	1.06	1		1.36	1		1.66			1.96			2.26			2.56		
0.17			0.47			0.77		Inert	1.07			1.37			1.67			1.97			2.27			2.57		
0.18			0.48	1		0.78			1.08			1.38	1		1.68			1.98			2.28			2.58		
0.19			0.49			0.79			1.09			1.39			1.69			1.99			2.29			2.59		
0.20			0.50		FGV	0.80			1.10			1.40			1.70			2.00			2.30			2.60		
0.21			0.51	1	↓	0.81			1.11			1.41			1.71			2.01			2.31			2.61		
0.22			0.52			0.82	1		1.12			1.42			1.72			2.02			2.32			2.62		
0.23			0.53			0.83			1.13			1.43			1.73			2.03			2.33			2.63		
0.24			0.54			0.84			1.14			1.44			1.74			2.04			2.34			2.64		
0.25			0.55			0.85			1.15			1.45			1.75			2.05			2.35			2.65		
0.26			0.56			0.86			1.16			1.46			1.76			2.06			2.36			2.66		
0.27			0.57			0.87			1.17			1.47			1.77			2.07			2.37			2.67		
0.28			0.58			0.88	1		1.18	1		1.48	1		1.78			2.08			2.38			2.68		
0.29			0.59			0.89			1.19			1.49			1.79			2.09			2.39			2.69		
0.30			0.60			0.90	1		1.20			1.50			1.80			2.10			2.40			2.70		
0.31			0.61			0.91			1.21			1.51			1.81			2.11			2.41			2.71		
0.32			0.62			0.92	1		1.22			1.52			1.82			2.12			2.42			2.72		
0.33	1	↑	0.63			0.93			1.23			1.53			1.83			2.13			2.43			2.73		
0.34	1	FGV	0.64			0.94			1.24			1.54	2		1.84			2.14			2.44			2.74		
0.35	1		0.65			0.95			1.25			1.55			1.85			2.15			2.45		Inert	2.75		
0.36	1		0.66			0.96			1.26			1.56			1.86			2.16			2.46	1	↓	2.76		
0.37			0.67			0.97			1.27			1.57			1.87			2.17			2.47			2.77		
0.38	1		0.68			0.98	1		1.28			1.58			1.88			2.18			2.48			2.78		
0.39	1		0.69			0.99			1.29			1.59			1.89			2.19			2.49			2.79		

VITRINITE <0.1%		INERTINITE 0.1%						LIPTINITE <0.1%								OIL DROPS	BITUMEN
TV	DV	Sfus	Scler	Fus	Macr	ID	Micr	Spor <0.1	Cut	Sub	Res	Ld <0.1	Bituminite	Telalginite	Lamalginite <0.1	Oil cut	

Sample Number..T9152....Well Name..GTK...BRIDGEWATER BAY-1, GC876-5.1.....Timboon Sst..... Depth...1560m..... ..... SampleType....Ctgs...
Date. ..28/.05/ 2003.. Op..SPR..... FGV - First Generation Vitrinite, RV - Reworked Vitrinite, BTT - Bituminite, B - Bitumen, Inert - Inertinite, Cav - Cavings, DA - Drilling Mud Additives MICR D:\RWORK.ms6\876VRW.doc

R	No Read	Pop Range	R	No Read	Pop Range	R	No Read	Pop Range	R	No Read	Pop Range	R	No Read	Pop Range	R	No Read	Pop Range	R	No Read	Pop Range	R	No Read	Pop Range	R	No Read	Pop Range
0.10			0.40			0.70			1.00	2		1.30	1		1.60			1.90			2.20			2.50		
0.11			0.41	1		0.71			1.01			1.31			1.61			1.91			2.21			2.51		
0.12			0.42	2		0.72			1.02	1		1.32	1		1.62	1		1.92			2.22			2.52		
0.13			0.43	2		0.73			1.03			1.33			1.63			1.93			2.23			2.53		
0.14			0.44	3		0.74			1.04	1		1.34			1.64	1		1.94			2.24			2.54		
0.15			0.45	2		0.75			1.05			1.35			1.65			1.95			2.25			2.55		
0.16			0.46	2		0.76			1.06			1.36			1.66			1.96			2.26			2.56		
0.17			0.47			0.77			1.07			1.37			1.67			1.97			2.27			2.57		
0.18			0.48	1		0.78			1.08	1		1.38			1.68			1.98			2.28			2.58		
0.19			0.49	2		0.79			1.09			1.39			1.69			1.99			2.29			2.59		
0.20			0.50	1		0.80			1.10	2		1.40			1.70			2.00			2.30			2.60		
0.21			0.51	1		0.81			1.11			1.41			1.71			2.01			2.31			2.61		
0.22			0.52	2		0.82			1.12			1.42			1.72			2.02			2.32			2.62		
0.23			0.53	2		0.83			1.13			1.43			1.73			2.03			2.33			2.63		
0.24			0.54			0.84			1.14			1.44			1.74			2.04			2.34			2.64		
0.25			0.55			0.85			1.15			1.45			1.75			2.05			2.35			2.65		
0.26			0.56	1		0.86			1.16	1		1.46			1.76			2.06			2.36			2.66		
0.27			0.57			0.87			1.17			1.47			1.77			2.07			2.37			2.67		
0.28			0.58	1		0.88			1.18			1.48			1.78			2.08			2.38			2.68		
0.29			0.59			0.89			1.19			1.49			1.79			2.09			2.39			2.69		
0.30			0.60		FGV	0.90			1.20	1		1.50			1.80			2.10			2.40			2.70		
0.31			0.61	1	↓	0.91			1.21			1.51			1.81			2.11		Inert	2.41			2.71		
0.32			0.62			0.92	1	↑	1.22			1.52			1.82			2.12	1	↓	2.42			2.72		
0.33			0.63			0.93		Inert	1.23			1.53			1.83			2.13			2.43			2.73		
0.34			0.64			0.94	1		1.24			1.54	1		1.84			2.14			2.44			2.74		
0.35			0.65			0.95			1.25			1.55			1.85			2.15			2.45			2.75		
0.36			0.66			0.96	1		1.26	1		1.56	1		1.86			2.16			2.46			2.76		
0.37	1	↑	0.67			0.97			1.27			1.57			1.87			2.17			2.47			2.77		
0.38		FGV	0.68			0.98			1.28			1.58			1.88			2.18			2.48			2.78		
0.39			0.69			0.99			1.29			1.59			1.89			2.19			2.49			2.79		

VITRINITE 0.1%		INERTINITE 0.8%						LIPTINITE %								OIL DROPS <0.1	BITUMEN <0.1
TV	DV	Sfus	Scler	Fus	Macr	ID	Micr	Spor <0.1	Cut <0.1	Sub	Res	Ld <0.1	Bituminite	Telalginite	Lamalginite <0.1	Oil cut	

Sample Number..T9153....Well Name..GTK...BRIDGEWATER BAY-1, GC876-6.1.....Paaratte Fm..... Depth...1995m..... ..... SampleType....Ctgs...
Date. ..28/.05/ 2003.. Op..SPR..... FGV - First Generation Vitrinite, RV - Reworked Vitrinite, BTT - Bituminite, B - Bitumen, Inert - Inertinite, Cav - Cavings, DA - Drilling Mud Additives MICR D:\RWORK.ms6\876VRW.doc

R	No Read	Pop Range	R	No Read	Pop Range	R	No Read	Pop Range	R	No Read	Pop Range	R	No Read	Pop Range	R	No Read	Pop Range	R	No Read	Pop Range	R	No Read	Pop Range	R	No Read	Pop Range
0.10			0.40			0.70			1.00			1.30			1.60	1		1.90			2.20			2.50		
0.11			0.41			0.71			1.01			1.31			1.61			1.91			2.21			2.51		
0.12			0.42			0.72			1.02	1	↑	1.32			1.62	1		1.92			2.22			2.52		
0.13			0.43			0.73			1.03		Inert	1.33			1.63			1.93			2.23			2.53		
0.14			0.44			0.74			1.04			1.34			1.64			1.94			2.24			2.54		
0.15			0.45			0.75			1.05			1.35			1.65			1.95			2.25			2.55		
0.16			0.46			0.76			1.06			1.36	1		1.66			1.96			2.26			2.56		
0.17			0.47			0.77			1.07			1.37			1.67			1.97			2.27			2.57		
0.18			0.48	1	↑	0.78			1.08			1.38	1		1.68	1		1.98			2.28			2.58		
0.19			0.49	1	FGV	0.79			1.09			1.39			1.69			1.99			2.29			2.59		
0.20			0.50			0.80			1.10	1		1.40	1		1.70			2.00			2.30			2.60		
0.21			0.51	2		0.81			1.11			1.41			1.71			2.01			2.31			2.61		
0.22			0.52	1		0.82			1.12	1		1.42			1.72			2.02			2.32			2.62		
0.23			0.53	4		0.83			1.13			1.43			1.73			2.03			2.33			2.63		
0.24			0.54			0.84			1.14			1.44	1		1.74	1		2.04			2.34			2.64		
0.25			0.55	3		0.85			1.15			1.45			1.75			2.05			2.35			2.65		
0.26			0.56	1		0.86			1.16	1		1.46			1.76			2.06			2.36			2.66		
0.27			0.57			0.87			1.17			1.47			1.77		Inert	2.07			2.37			2.67		
0.28			0.58	4		0.88			1.18			1.48			1.78	1	↓	2.08			2.38			2.68		
0.29			0.59	1		0.89			1.19			1.49			1.79			2.09			2.39			2.69		
0.30			0.60	1		0.90			1.20	1		1.50			1.80			2.10			2.40			2.70		
0.31			0.61			0.91			1.21			1.51			1.81			2.11			2.41			2.71		
0.32			0.62	2		0.92			1.22	1		1.52	1		1.82			2.12			2.42			2.72		
0.33			0.63	2		0.93			1.23			1.53			1.83			2.13			2.43			2.73		
0.34			0.64			0.94			1.24	1		1.54	1		1.84			2.14			2.44			2.74		
0.35			0.65	1	FGV	0.95			1.25			1.55			1.85			2.15			2.45			2.75		
0.36			0.66	1	↓	0.96			1.26	1		1.56			1.86			2.16			2.46			2.76		
0.37			0.67			0.97			1.27			1.57			1.87			2.17			2.47			2.77		
0.38			0.68			0.98			1.28			1.58	1		1.88			2.18			2.48			2.78		
0.39			0.69			0.99			1.29			1.59			1.89			2.19			2.49			2.79		

VITRINITE <0.1%		INERTINITE 1.2%						LIPTINITE <0.1%								OIL DROPS	BITUMEN
TV	DV	Sfus	Scler	Fus	Macr	ID	Micr	Spor <0.1	Cut	Sub	Res	Ld <0.1	Bituminite	Telalginite	Lamalginite <0.1	Oil cut	

Sample Number..T9155....Well Name..GTK...BRIDGEWATER BAY-1, GC876-8.1.....Paaratte Fm..... Depth..2595m..... ..... SampleType....Ctgs...
Date. ..28/.05/ 2003.. Op..SPR..... FGV - First Generation Vitrinite, RV - Reworked Vitrinite, BTT - Bituminite, B - Bitumen, Inert - Inertinite, Cav - Cavings, DA - Drilling Mud Additives MICR D:\RWORK.ms6\876VRW.doc

R	No Read	Pop Range	R	No Read	Pop Range	R	No Read	Pop Range	R	No Read	Pop Range	R	No Read	Pop Range	R	No Read	Pop Range	R	No Read	Pop Range	R	No Read	Pop Range	R	No Read	Pop Range
0.10			0.40			0.70			1.00	1	↑	1.30			1.60			1.90	1		2.20			2.50		
0.11			0.41			0.71		FGV	1.01		Inert	1.31			1.61			1.91			2.21			2.51		
0.12			0.42			0.72	1	↓	1.02			1.32			1.62	1		1.92			2.22			2.52		
0.13			0.43			0.73			1.03			1.33			1.63			1.93			2.23			2.53		
0.14			0.44			0.74			1.04			1.34	1		1.64			1.94	2		2.24			2.54		
0.15			0.45			0.75			1.05			1.35			1.65			1.95			2.25			2.55		
0.16			0.46			0.76			1.06			1.36			1.66	1		1.96			2.26			2.56		
0.17			0.47			0.77			1.07			1.37			1.67			1.97			2.27			2.57		
0.18			0.48			0.78			1.08			1.38	1		1.68			1.98			2.28			2.58		
0.19			0.49			0.79			1.09			1.39			1.69			1.99			2.29			2.59		
0.20			0.50			0.80			1.10			1.40			1.70			2.00			2.30			2.60		
0.21			0.51			0.81			1.11			1.41			1.71			2.01			2.31			2.61		
0.22			0.52			0.82			1.12			1.42	1		1.72			2.02			2.32			2.62		
0.23			0.53			0.83			1.13			1.43			1.73			2.03			2.33			2.63		
0.24			0.54	1	↑	0.84			1.14			1.44			1.74			2.04			2.34			2.64		
0.25			0.55		FGV	0.85			1.15			1.45			1.75			2.05			2.35			2.65		
0.26			0.56			0.86			1.16			1.46			1.76	1		2.06	1		2.36			2.66		
0.27			0.57	1		0.87			1.17			1.47			1.77			2.07			2.37			2.67		
0.28			0.58			0.88			1.18	1		1.48	1		1.78	1		2.08			2.38			2.68		
0.29			0.59			0.89			1.19			1.49			1.79			2.09			2.39			2.69		
0.30			0.60	1		0.90			1.20	1		1.50	1		1.80			2.10			2.40			2.70		
0.31			0.61	1		0.91			1.21			1.51			1.81			2.11			2.41			2.71		
0.32			0.62			0.92			1.22			1.52			1.82			2.12			2.42			2.72		
0.33			0.63			0.93			1.23			1.53			1.83			2.13			2.43			2.73		
0.34			0.64			0.94			1.24	1		1.54			1.84			2.14			2.44			2.74		
0.35			0.65			0.95			1.25			1.55			1.85			2.15			2.45			2.75		
0.36			0.66			0.96			1.26			1.56			1.86			2.16			2.46			2.76		
0.37			0.67	2		0.97			1.27			1.57			1.87			2.17		Inert	2.47			2.77		
0.38			0.68			0.98			1.28			1.58	2		1.88			2.18	1	↓	2.48			2.78		
0.39			0.69	1		0.99			1.29			1.59			1.89			2.19			2.49			2.79		

VITRINITE <0.1 %		INERTINITE 0.6%						LIPTINITE <0.1%								OIL DROPS	BITUMEN
TV	DV	Sfus	Scler	Fus	Macr	ID	Micr	Spor	Cut	Sub	Res	Ld <0.1	Bituminite	Telalginite	Lamalginite <0.1	Oil cut	

Sample Number..T9157....Well Name..GTK...BRIDGEWATER BAY-1, GC876-10.1.....Belfast Mdst..... Depth..3495m..... ..... SampleType....Ctgs...
Date. ..28/.05/ 2003.. Op..SPR..... FGV - First Generation Vitrinite, RV - Reworked Vitrinite, BTT - Bituminite, B - Bitumen, Inert - Inertinite, Cav - Cavings, DA - Drilling Mud Additives MICR D:\RWORK.ms6\876VRW.doc

APPENDIX E

(U-Th)/He dating of apatite: Technical and analytical details

E.1 Sample details

Three samples from the Bridgewater Bay-1 well, Otway Basin, offshore Victoria (Figure 1.1) were processed for apatite to carry out (U-Th)/He dating. All samples contained sufficient apatite for analysis, as summarised in Table E.1. Full results of all (U-Th)/He age determinations are provided in Tables E.2 and E.3. The (U-Th)/He age determinations were carried out under the auspices of Dr. Peter Crowhurst, CSIRO Division of Petroleum Geosciences, Sydney, where all analyses were carried out.

E.2 Instrumentation

The CSIRO He extraction and analysis facility comprises an all-metal He extraction and gas-handling line connected to a dedicated on-line Balzers Prisma™ 200 quadrupole mass spectrometer. Gas extraction is performed by using a Nd-YAG laser system at ~1 to 2 watts of power applied to the sample for ~10 minutes, heating the sample to a temperature of ~1000°C. With the lower blanks afforded by the laser-based system, single grains can be analysed, although in some cases multiple grains are combined in a single run.

The laser heating procedure is essentially the same as that described by House et al. (2000). Individual grains (or occasionally two or three grains) selected on the basis of clarity and absence of inclusions (see Section E.3) were packaged into 1mm x 1mm platinum tubing which was crimped at each end sufficient to hold the grain(s) but still allow gas to escape. Up to 25 platinum tubing packages are placed in individual pits drilled into a copper base plate inside a 10^{-8} Torr vacuum chamber, enabling each sample package to be heated sequentially. Blanks are analysed between each unknown sample.

The line and laser (or furnace) are evacuated via ion, turbo and backing pumps. Active gases, particularly hydrogen, are removed using SAES getters. The analysis procedure is operated by LabVIEW™ automation software supplied by Prof. Ken Farley, Caltech.

E.3 Sample selection and measurement of grain radii

Apatite grains are carefully handpicked in order to avoid U- and Th-rich mineral inclusions (e.g. zircon, monazite), that may produce excess He. Images of selected grains are captured by a CCD video camera mounted on the microscope and measured using image analysis techniques for the purposes of alpha ejection correction calculation. This correction is mathematically calculated using the estimated dimensions of each grain and is applied directly to the final age (discussed in more detail below).

E.4 Helium measurement

Abundances of ^{4}He are determined by isotope dilution using a pure ^{3}He spike, which is calibrated on a regular basis against an independent ^{4}He standard tank. Line and laser blank analyses are performed before lasing each of the samples. Each sample is lased twice in order to ascertain if there is any re-extracts ("^{4}He hot blanks"). Acceptable ^{4}He standard and blank levels are <0.05ncc ^{4}He. After the heating and purification procedures, the extracted gas is handled and measured via the fully automated computer controlled system.

E.5 Uranium and thorium Concentration

The U and Th content of degassed apatite samples are determined on a Perkin Elmer Sciex 5000a ICP-MS using the Isotope Ratio application. A quantity of 100µl of each ^{235}U and ^{230}Th spike solution (about 5ng and 6ng U and Th respectively) and 200µl of concentrated nitric acid are added to a vial containing the capsule and degassed apatite. Similarly, 100µl of 0.25 ppm U and Th standard solutions (Johnson Matthey) are spiked and acidified. Our determination of the ^{235}U/^{238}U ratio of the Johnson Matthey U-standard solution is 135, close to the natural value of 138.

Blanks are prepared by adding an equivalent amount of nitric acid to washed, empty capsules. The blanks, standards and samples are all diluted to 5% nitric solution with Alpha Q water prior to analysis. Based on replicate analysis of spiked standard solutions, precision for ^{235}U/^{238}U and ^{230}Th/^{232}Th determination is 0.77% and 0.41%, respectively.

E.6 Age determination

The basic equation governing the production of Helium in apatite is as follows:

$$^{4}He = 8\,[^{238}U]\,(e^{l_{238}\,t} - 1) + 7\,[^{235}U]\,(e^{l_{235}\,t} - 1) + 6\,[^{232}Th]\,(e^{l_{232}\,t} - 1)$$

where ^{4}He, $[^{238}U]$, $[^{235}U]$ and $[^{232}Th]$ are the measured concentration of the respective isotopes, the numeral before each term refers to the number of alpha particles produced in the appropriate decay chain, each l represents the alpha-decay constants for the respective isotopes and t is the time over which He has accumulated. The three isotopes represented in the equation represent the only significant contributors of helium in natural samples. By measurement of the amounts of each isotope, the time t can be evaluated by solving this equation iteratively. The resulting number is known as a (U-Th)/He age.

As with the case of fission track ages, in the absence of other factors, this would provide a measure of the time over which helium has accumulated in the apatite lattice. However, due to a number of factors, outlined in the following Sections, a (U-Th)/He age must be interpreted carefully before the true meaning of the measured age can be evaluated.

E.7 Grain size correction

The ranges of alpha particles produced by decay of uranium and thorium isotopes are typically between 12 and 34 µm (Farley et al., 1996). Since these "stopping distances" are a significant fraction of the radius of typical accessory or detrital apatite grains (between 30 and 100 µm), a significant proportion of alpha particles produced with an apatite grain may be emitted from the grain, resulting in loss of radiogenic helium. Farley et al. (1996) showed how this effect can be corrected for, by calculation of a correction factor (known as F_T) for a particular grain size.

E.8 Thermal sensitivity

Calculations of Helium retention over geological timescales, based on laboratory diffusion measurements, suggest that Helium is progressively lost at temperatures between 40 and 90°C (for timescales of tens of millions of years), with this temperature range constituting a Helium "Partial Retention Zone" or He PRZ.

More recently, measurements of (U-Th)/He ages in samples from hydrocarbon exploration boreholes in the Otway Basin of S.E. Australia (House et al., 1999) have confirmed this general pattern of behaviour. Their results also suggest that, in general, helium diffusion systematics derived from laboratory measurements can be extrapolated to geological conditions with confidence, although the exact details remain to be quantitatively assessed.

Again analogous to the case of fission track ages in apatite, the progressive reduction of (U-Th)/He ages with increasing temperature means that a measured (U-Th)/He age from a sample of detrital apatite from a sediment cannot be interpreted as representing the timing of a specific cooling episode (with the exception of the situation where a sample cools very rapidly from above 90°C to less than 40°C). Instead, the measured age must be interpreted in terms of the interplay between production of Helium by alpha decay and loss due to thermally controlled diffusion (as described below).

E.9 Effect of grain size on sensitivity

Detailed experimental measurements at Caltech have led to further refinements in understanding the diffusion systematics of Helium in apatite (Farley, 2000). This work, focussed on the much-studied Durango apatite, has suggested that the diffusion systematics are controlled by the physical grain size. This key observation implies that for any specified thermal history, modelled (U-Th)/He ages can be produced for a particular sample using the measured mean grain size together with single values of the key diffusion parameters E_a and log (D_o), using best estimates of E_a = 33 ± 0.5 kcal/mol and log (D_o) = 1.5 ± 0.6 cm^2/s. These values have been used in modelling (U-Th)/He ages for this report.

Because of the greater diffusive loss expected from smaller grains compared to larger grains, the helium closure temperatures in apatite will also vary with grain radius. The overall variation in closure temperature for samples with grain radii of

50-150 microns is predicted to be only 5°C (Farley, 2000). However, effects related to grain size may be significant in the interpretation of apatites from sediments which have been heated to paleotemperatures within the He PRZ, as grains of different radii will give different ages for a particular thermal history. While this has yet to be demonstrated in natural samples, this holds considerable promise for obtaining more precise thermal history control in sedimentary basins.

E.10 Compositional effects

Several studies suggest that the composition of the apatite does not appear to affect the sensitivity of the He closure temperature (Wolf et al., 1996; House et al., 1999), in contrast to the effect of Cl contents on AFTA annealing kinetics. Further studies of possible variation in diffusion rates between different apatite species are currently being carried out at Caltech.

References

Farley, K.A. 2000. Helium diffusion from apatite: general behaviour as illustrated by Durango fluorapatite. Journal of Geophysical Research, 105 (B2), 2903-2914.

Farley, K.A., Wolf, R.A. and Silver, L.T. 1996. The effects of long alpha-stopping distances on (U-Th)/He ages. *Geochimica et Cosmochimica Acta*, **60**, 4223-4229.

House, M.A., Wernicke, B.P., Farley, K.A. and Dumitru, T.A. 1997. Cenozoic thermal evolution of the central Sierra Nevada, California, from (U-Th)/He thermochronometry. *Earth and Planetary Science Letters*, **151**, 167-179.

House, M.A., Farley, K.A. and Kohn, B.P. 1999. An empirical test of helium diffusion in apatite: borehole data from the Otway Basin, Australia. *Earth and Planetary Science Letters*, **170**, 463-474.

House, M.A. Farley, K.A. and D. Stockli, D. 2000. Helium chronometry of apatite and titanite using Nd-YAG laser heating. Earth and Planetary Science Letters, 183, pp. 365-368.

Lippolt, H.J., Leitz, M., Wernicke, R.S. and Hagedorn, B. 1994. (Uranium + thorium)/helium dating of apatite: experience with samples from different geochemical environments. *Chemical Geology (Isotope Geoscience Section)*, **112**, 179-191.

Warnock, A.C., Zeitler, P.K., Wolf, R.A. and Bergman, S.C. 1997. An evaluation of low-temperature apatite U-Th/He thermochronometry. *Geochimica et Cosmochimica Acta*, **61**, 5371-5377.

Wolf, R.A., Farley, K.A. and Kass, D.M. 1998. Modeling of the temperature sensitivity of the apatite (U-Th)/He thermochronometer. *Chemical Geology*, **148**, 105-114.

Wolf, R.A., Farley, K.A. and Silver, L.T. 1996. Helium diffusion and low-temperature thermochronometry of apatite. *Geochimica et Cosmochimica Acta*, **60**, 4231-4240.

Wolf, R.A., Farley, K.A. and Silver, L.T. 1997. Assessment of (U-Th)/He thermochronometry: the low temperature history of the San Jacinto mountains, California. *Geology*, **25**, 65-68.

Table E.1: Samples selected for (U/Th)/He dating - Otway Basin wells offshore South Australia and Victoria (Geotrack Report #876)

Sample number	Depth	Stratigraphic	Stratigraphic age (Ma)	Present temperature*1 (°C)
Bridgewater Bay-1				
GC876-5	1600-1750	Paaratte Fm	83-77	62
GC876-6	1890-2020	Paaratte Fm	83-77	71
GC876-7	2115-2215	Paaratte Fm	83-77	77

*1See Appendix A for discussion of present temperature data.

Note: All depths quoted are TVD with respect to KB.

Table E.2: Apatite (U-Th)/He determinations Otway Basin wells offshore South Australia and Victoria (Geotrack Report #876)

Sample number	He4 (ncc)	Uranium (ppm)	Thorium (ppm)	Uncorrected He age[*1] (Ma)
Bridgewater Bay-1				
GC876-5a	3.115 – 0.004	3.92E11 – 1.63E10	5.81E10 – 2.89E09	158.73
GC876-5b	0.919 – 0.003	9.63E10 – 4.09E09	2.04E11 – 9.64E09	132.83
GC876-5c	1.903 – 0.004	3.70E11 – 1.55E10	4.72E11 – 2.19E10	82.68
GC876-5d	0.876 – 0.003	1.17E11 – 4.99E09	2.02E11 – 9.49E09	111.36
GC876-5e	0.760 – 0.003	1.26E11 – 5.27E09	6.02E10 – 2.94E09	112.62
GC876-6d	0.743 – 0.003	2.13E11 – 9.07E09	5.61E11 – 2.68E10	45.29
GC876-6e	0.048 – 0.003	7.22E10 – 3.13E09	1.95E12 – 9.24E10	1.92
GC876-7a	0.153 – 0.003	7.22E11 – 3.02E10	5.80E11 – 2.70E10	3.74
GC876-7b	0.418 – 0.003	9.43E10 – 3.97E09	1.65E11 – 7.94E09	65.84
GC876-7c	0.045 – 0.003	1.65E11 – 6.97E09	2.48E11 – 1.17E10	4.24

*1 Not corrected for grain-size effects – see Table E.3.

Table E.3: Apatite (U-Th)/He age alpha particle ejection corrections - samples from the Otway Basin, offshore South Australia and Victoria (Geotrack Report #876)

Sample number	Uranium (ppm)	Thorium (ppm)	Th/U ratio	Mean grain radii (µm)	Number of grains	F_T*1	Corrected He age (Ma)
Bridgewater Bay-1							
GC876-5a	82.08	11.78	0.150	25.00	3	0.47	337.73 – 13.31
GC876-5b	16.67	34.22	2.120	32.50	2	0.61	217.75 – 6.96
GC876-5c	47.53	58.61	1.270	35.83	3	0.59	140.14 – 4.65
GC876-5d	14.52	24.33	1.730	31.67	3	0.56	198.86 – 6.51
GC876-5e	16.19	7.48	0.480	33.33	3	0.57	197.58 – 7.31
GC876-6d	47.09	120.07	0.800	30.00	2	0.55	82.34 ± 2.59
GC876-6e	7.57	198.08	1.750	50.00	1	0.72	2.66 ± 0.18
GC876-7a	68.44	53.19	1.500	37.50	3	0.63	5.94 ± 0.23
GC876-7b	16.32	27.60	2.630	30.00	3	0.53	124.22 ± 4.07
GC876-7c	24.37	35.33	27.05	25.63	4	0.49	8.64 ± 0.56

*1 Grain-size dependent correction factor to allow for ejection of alpha particles from grain periphery.